Danksagung/Acknowledgments

Diese Arbeit wurde an der Technischen Universität Darmstadt angefertigt. Ich danke Herrn Prof. Dr. Paul G. Layer für die Überlassung des Themas und die Bereitstellung des Arbeitsplatzes. Außerdem für das hohe Maß an Toleranz und Freiheit, das mir Herr Layer bei der Durchführung und Zeitplanung ermöglicht hat.
Danken möchte ich auch Herrn Prof. Gerhard Thiel für die Übernahme des Korreferates und die Teilnahme an der Prüfungskommission, sowie Herrn Prof. Wolfgang Ellermeier und Herrn PD Dr. Mark Maraun für Ihre Teilnahme an der Prüfungskommission.
Ich danke Herrn Dr. Peter Andermann für die Betreuung dieser Arbeit und Diskussionsbereitschaft.
Des weiteren danke ich Wolfgang und Ulrike für die Fischpflege. Ein zusätzlicher Dank gilt Ulrike für die Anfertigung so mancher Querschnittspräparate. Ich danke Michaela, deren Hilfestellung und wertvolle Tipps mir bei der Lösung molekularbiologischer Fragen weitergeholfen haben. Ein besonderer Dank geht an Jutta, die sämtliche Bestellung für mich übernommen hat. Außerdem danke ich allen Mitgliedern der Arbeitsgruppe für die freundschaftliche Arbeitsatmosphäre im Labor.
Ich danke auch ganz besonders Monika Medina, die mir mit allen bürokratischen, finanziellen und organisatorischen Schwierigkeiten geholfen hat.

I am also grateful for the hospitality of the Laboratory of Peter Currie in Sydney, where I spent several weeks during my post-graduate studies. Especially I thank PhD Robert Bryson-Richardson, who patiently introduced me to the technique of optical tomography. Additionally, I thank him for his scientific and mental support while writing this thesis.

Ein ganz besonderer Dank gilt meinen Freunden Jan, Cita, Marit, Jochen und Tanja, die mich nach dem Studium nun auch durch meine Doktorarbeitszeit begleitet haben. Mit Ihnen habe ich viele erlebnisreiche und fröhliche Stunden verbracht, von denen hoffentlich noch viele folgen werden.

Von ganzem Herzen danke ich meinen Eltern, die immer an mich geglaubt haben und deren Unterstützung mir über so manche Durststrecke hinweg helfen konnte.

Last but not least i thank Ben Martin, who changed my life and perspective. He has shown me that there is a life “outside” of the institute.

Preface

Developmental Genetics –

or what can genetics tell us about evolution, development, human birth defects, and disease?

The idea of a genetic basis of development began in the mid-19th century at the intersection of descriptive embryology and cytology. Modern histological techniques afforded WILHELM HIS (1831-1904) to visualise the cell nucleus, chromosomes, and distinct steps of mitosis. By improving these techniques THEODOR BOVERI (1862-1915) could demonstrate that each parent contributes equivalent chromosomes to the zygote, and each chromosome is an independently inherited unit. He revealed that an incorrect number or improper combination of chromosomes in the embryo causes abnormal development of the organism. Finally, THOMAS H. MORGAN (1866-1945) founded the field of *Drosophila* genetics and was able to demonstrate that genes are carried on chromosomes and that the latter represent the mechanical basis of heredity [KOHLER, 1994; GARLAND, 2000; MOODY, 2007]. Thenceforward the main interest was to determine the fundamental principles of genetics. New technologies in molecular biology and cloning were developed to reveal gene inheritance, regulation of expression, and discovering the genetic code. Mutagenising the entire genome and screening for developmental abnormalities in *Drosophila* revealed important regulatory genes in invertebrates. Following homology cloning in various animals discovered counterparts of many of these genes in other invertebrates and vertebrates. The existence of genes, which are important for developmental processes, found in various organisms, demonstrate that developmental programs and molecular genetic processes are highly conserved during development [MOODY, 2007]. Indeed, the Human Genome Project could identify homologues in humans and demonstrate that many of these regulatory genes underlie human developmental disorders. The conservation between genomes of different species allows the utilization of animal models to gain important insights of clinical relevance.

Hearing and Deafness

The senses of hearing and balance rely on the function of specialised mechanoreceptor cells called “hair cells”, which are vital to perceive sound as well as motion. Sound frequencies and intensities are detected by hair cells in the cochlear, while those in the semicircular canals and otolith organs sense changes in gravity and acceleration. In the past it has been difficult to study the biology of hair cells because they are housed within the inner ear, which itself is located in the temporal bone of the skull, a less accessible region in model organisms like mouse or chicken [BISSONNETTE, 1996]. However, since the establishment of the zebrafish as genetic model organism, the understanding of structure and function of hair cells has been improved because of the embryonic zebrafish’s transparency and better accessibility. Hair cells are extremely sensitive to mechanical irritations and damages are irreversible and can lead to hearing impairment or even to the complete loss of the ability to hear. Deafness might caused by complications at birth, certain infectious diseases, use of ototoxic drugs, exposure to excessive noise, advanced age or may be inherited.

Deafness is the most common inherited sensory defect. Studies have attributed about 50% of childhood sensorineural hearing impairment to genetic factors. More than 62 human deafness genes, including mitochondrial genes, have been identified yet [VAN CAMP & SMITH, 2007]. Heritable forms of hearing loss can be congenital or delayed onset; conductive, sensorineural, or mixed type; mild to profound in degree; progressive or non-progressive; unilateral or bilateral and symmetrical or asymmetrical in severity and configuration [CORDES & FRIEDMAN, 2000]. Mutations giving rise to anatomical defects in the inner ear have been isolated in a large-scale screen for mutations causing visible abnormalities in the zebrafish embryo [MULLINS, 1994; HAFFTER, 1996; WHITFIELD, 1996; VAN EEDEN, 1999]. 58 mutants have been classified as having a primary ear phenotype; these fall into several phenotypic classes, affecting presence or size of the otoliths, size and shape of the otic vesicle and formation of the semicircular canals. Many of the ear and otolith mutants show an expected behavioural phenotype: embryos fail to balance correctly, and may swim on their sides, upside down, or in circles [GRANATO, 1996].

Hereditary hearing impairment is classified into nonsyndromic (or isolated) or syndromic (i.e., hearing loss associated with other anomalies) forms [PETIT, 1996]. Nonsyndromic hearing impairment is almost exclusively caused by mutations within a single gene and are not associated with any other abnormalities or defects. Up to 30% of deafness in children can be attributed to syndromic forms.

To date several hundred such syndromes have been described, a number of these can be classified as early developmental defects [GORLIN, 1995]. Progress in localization and identification of genes, which are responsible for sensorineural hearing loss, provide new subclassification of the diseases associated with appropriated genes. 75% to 80% of genetic deafness is attributed to autosomal recessive gene disorders and 18% to 20% to autosomal dominant gene disorders. The identification of autosomal dominant disorders is facilitated by a positive family history reflecting a classical dominant inheritance pattern and recognizable phenotype. In reality, the variation in expressivities of dominant genes leads to different phenotypic characteristics being present in various affected members of the same family.

Inherited Deafness Disorders

One example for such an autosomal dominant disorder is the Branchio-Oto-Renal syndrome, caused by a mutation in the *EYA1* gene, which has a counterpart in the zebrafish *dog-eared* mutation, characterised by defective formation of the inner ear, less responsiveness to vibrational stimuli and failure to balance when swimming [WHITFIELD, 1996]. Branchio-Oto-Renal syndrome is a disorder with otologic, branchial and renal manifestations, that shows a highly variable expressivity. The Branchio-Oto-Renal syndrome occurs in 2% of children with congenital hearing impairment. Seventy-five percent of patients with Branchio-Oto-Renal syndrome have significant hearing loss. Of these, 30% are conductive, 20% are sensorineural, and 50% demonstrate mixed forms.

Another example gives the Usher syndrome (USH), the most common condition that involves both hearing and vision problems. The major features are hearing impairment and retinitis pigmentosa. Some people with Usher syndrome also have balance problems. Approximately three to six percent of all deaf or hard-hearing children have Usher syndrome. The three types of Usher syndrome are Usher

syndrome type 1 (USH1), Usher syndrome type 2 (USH2), and Usher syndrome type 3 (USH3). USH1 is the most severe form and together with USH2 are the most common types. Together, they account for approximately 90-95 percent of all children come down with the Usher syndrome. Persons with USH1 are profoundly deaf from birth, correlated with severe balance problems. Usually these children start to develop vision problems by the age ten, most often beginning with difficulty seeing at night. In general the progression is rapidly until the patient is completely blind. Among others the Usher syndrome has been linked to the *MYO7A* gene, the *USH1C* gene and the *CDH23* gene [KEATS & COREY, 1999; AHMED, 2003]. Recently, the zebrafish mutation *sputnik* [SÖLLNER, 2004], which shows defects in hearing and balance, could be linked to mutations in the *cadherin-23* gene, the homologue of the human *CDH23* gene. The zebrafish *mariner* mutation [ERNEST, 2000], is due to mutations in the gene encoding myosin VIIA, homologous to the human *MYO7A* gene.

These are just a few examples for inherited hearing diseases and their correlated mutations found in zebrafish. They should illustrate that the investigation of these genes in zebrafish can help to get a better understanding of inherited deafness diseases in human.

1 Introduction

Within the last 25 years the zebrafish have become a very popular vertebrate model organism to study cellular, molecular and genetic mechanisms of development [STREISINGER, 1981]. Zebrafish embryos are transparent and simply organised. In contrast to other vertebrate model organisms, zebrafish embryos develop rapidly, the generation interval takes two to three months, and each female produces approximately 200 eggs per week. Because mutations are easy to induce, large-scale screens allow the identification of mutations causing defects in particular biological processes [TWYMAN 2002].

1.1 Ontogenetic development of the zebrafish

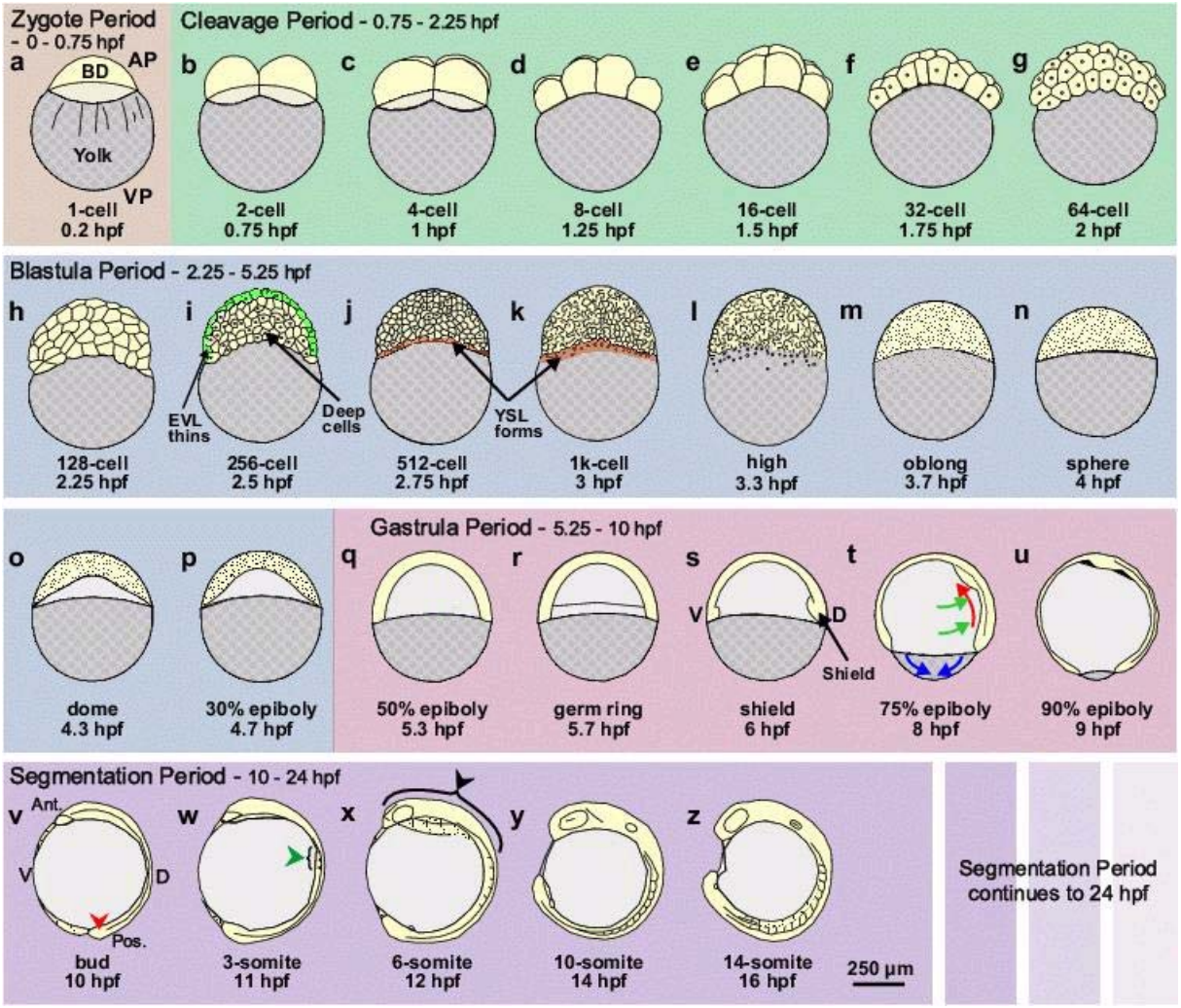

Figure 1 Schematic representation of zebrafish development from the zygote period to the mid-segmentation period. Following the brief zygote period (a), when the embryo is at the one-cell stage, the cleavage (b-g) runs from the 2-cell to 64-cell stage. The blastula-phase (h-p) follows, and runs from the 128-cell stage to the 50% epiboly stage. The formation of the enveloping layer (EVL) and yolk syncytial layer (YSL) starts (l-k). The gastrulation sets off at 50% epiboly and is completed with the bud stage. Then, the process of segmentation begins. Main events during the gastrulation-period: 1. Dorso-ventral axis becomes visible morphologically at Shield stage (s); 2. Simultaneous cell movements of epiboly (blue arrows), convergence (green arrows) and involution (red arrows) (t); Tail bud, somites and brain anlage are indicated by red, green and black arrowheads, respectively (v-x). AP animal pole; VP vegetal pole; BD blastodisc [modified from WEBB & MILLER, 2007].

The externally fertilized zebrafish egg is telolecithal, i.e. a large amount of yolk accumulates at the vegetal pole of the egg (Fig. 1a). Following fertilisation, at the one-cell-stage (0-¾ hours post fertilisation/hpf), the chorion swells and lifts from the egg. Non-yolk cytoplasm streams towards the animal pole of the zygote, segregating the blastodisc from the yolk-rich vegetal pole. The following six cleavages (¾-2¼ hpf) of the cytoplasm pass through are meroblastic, i.e. they intersect the blastodisc incompletely so that the resulting blastomeres remain interconnected by cytoplasmatic bridges (Fig. 1b-g). Following the cleavage-stage, the embryo enters a period referred to as blastula-stage (2¼-5¼ hpf), even though there is no blastocoel present. Rather, small irregular extracellular spaces are formed between the deep cells of the blastodisc. The blastomeres at the boundary of the blastoderm (still cytoplasmically connected) collapse and release their cellular content, including nuclei, into the underlying cytoplasm of the yolk cells, forming a teleost-specific extraembryonic structure, known as the yolk syncytial layer (YSL). When the late blastula stage epiboly starts, both YSL and blastodisc move and spread over the yolk cells in an animal-to-vegetal direction (Fig. 1h-p). At 50% epiboly, when the spread reaches the equator, there is a transient pause and the process of gastrulation (5¼-10 hpf) begins. The morphogenetic cell movements of involution, convergence, and extension occur, developing the primary germ layers (ectoderm and endoderm). Involuting cells shape the germ ring (5.7 hpf) by folding the blastoderm back upon itself and moving in a vegetal-to-animal direction. At the same time, convergence movements start to accumulate cells at a position along the germ ring, the future dorsal margin of the embryo, termed the shield (6 hpf). Epiboly continues after shield formation. Due to the process of involution there are two layers within the germ ring. The upper epiblast and the lower hypoblast (Fig. 1q-u). The epiblast keeps moving and forms a second layer, the mesoderm. When gastrulation is completed, cells of the epiblast correspond to the definitive ectoderm and gives rise to neuroectodermal structures, such as the central nervous system and sensory placodes. The hypoblast gives rise to derivates, ascribed to both mesoderm and endoderm. At the end of gastrulation, when epiboly is completed, the concerted movements have established the dorsal-ventral as well as the anterior-posterior body axis. During the period of segmentation (10-24 hpf), the first rudiments of the primary organs become visible, the somites develop, and the tailbud extends away from the yolk to develop the embryonic tail region (Fig. 1v-z). By 1 day post fertilisation (dpf) the embryos body axis straightens, heartbeat, circulation and pigmentation appear and the fins extend. After 2 dpf the embryo hatches from the chorion and has completed most of its organ formation with heart, brain, etc. detectable. [KIMMEL, 1995; MÜLLER & HASSEL, 2006].

1.2 Neural cell fate determination

During the developmental period of multicellular organisms a diverse range of cell types are manifest showing variances in anatomy, physiological function, neurochemsitry and connectivity. The fate of a cell describes what type of cell a certain precursor will become in the course of normal development. With the formation of the three germ layers, the ectoderm, endoderm, and mesoderm, embryonic cells, previously undifferentiated, take on a specific developmental character. Accordingly endodermal cells form the stomach, liver, pancreas, and lungs. Cells arise from the mesoderm form the skeletal

muscle, skeleton, urogenital system, heart, and blood. The ectoderm forms the neural crest, central nervous system, cranial and sensory, ganglia and nerves, pigment cells, and epidermis. How distinct cell fates are generated from initially homogeneous cell populations is a driving question in developmental biology. The ectoderm is such a cell population that is capable of producing an array of derivatives, cells as different in function and form as the sensory neurons or the pigment cells in the skin. The final specification of a cell depends on its competence, the potential to adopt a particular fate. Specification can involve both cell-autonomous mechanisms (intrinsic signals) and inductive signals from a cell's surroundings (extrinsic signals). The migrating ectodermal cells become exposed to these instructive environments and respond to these factors. While cells migrating particular pathways, they segregated into several classes of more specialised progenitors with limited potential. This first specification is not a permanent stage and cells can be reversed based upon different cues. In contrast, during the later determination cells become irreversibly committed to a particular fate ("cell fate determination"), the ultimate differentiated state to which a cell turns into like a sensory neuron or a pigment cell. This final determination is promoted by a distinct set of extracellular signal molecules [BAKER & BRONNER-FRASER, 2001; CHISHOLM, 2001].

1.3 Pre-placodal ectoderm and cranial sensory placodes

The formation of the vertebrate cranial sensory nervous system depends mainly on the cranial sensory placodes, transient thickened ectodermal regions with neurogenic potential, that expand in the vertebrate head next to the neural tube. These ectodermal placodes comprise the adenohypophyseal, olfactory, lens, trigeminal, and profundal placodes, as well as the otic placode, a series of epibranchial placodes, and a series of lateral line placodes (Fig. 2A). Each of them make vital contributions to the paired sense organs associated with hearing, balance, olfaction and vision by giving rise to a multitude of different cell types, including the neurons of the cranial sensory ganglia [BAKER & BRONNER-FRASER, 2001; MAZET & SHIMMELD, 2005].

Despite the structural and functional diversity of sensory organs and cranal ganglia in the adult, earlier studies led to the assumption that all placodes are initiated through a common cellular and molecular mechanism, which involves a common placodal field [JACOBSON, 1963] – named the "pre-placodal region" comprising the ectodermal precursor cells of all cranial placodes [NIEUWKOOP, 1985; GALLAGHER, 1996; GRAINER, 1992; BAKER & BRONNER-FRASER, 2001]. By late gastrulation (90% epiboly onward), the ectoderm surrounding the anterior neural plate becomes specified. The medial part, which includes the edge of the neural plate, gives rise to the neural crest. In contrast, the lateral section increases to become the pre-placodal ectodermal field (Fig. 4A). Fate-mapping studies in the chicken and zebrafish have mapped the precursors for the olfactory, lens, otic and epibranchial placodes to overlapping regions within this pre-placodal ectodermal field [STREIT, 2002].The hypothesis of a common placodal region implies that all placodal precursors arise from a continuous domain of the embryonic ectoderm. Additionally this region should be characterised by unique properties like the expression of specific molecular markers, which are expressed in this pre-placodal domain but not in other ectodermal regions. Members of several gene families are expressed in this area, like *Fgf*, *Dlx*,

Pax, *Six*, and *Eya*. However, most of these genes are not uniquely found in placodal cells but also at later stages of development in other ectodermal and even mesodermal derivates [AKIMENKO, 1994; WHITFIELD, 2002].

During the period of neurulation, extrinsic signals from the underlying mesoderm cause the pre-placodal ectoderm to split into discrete placodes, with a wide variety of distinct developmental cell fates [MOODY, 2007], including sensory receptor cells, sensory neurons, neuroendocrine and endocrine cells, glia, and other supporting cells, depending on their placode of origin. Cranial placodes have been subdivided into two categories. Firstly, the sensory placodes, which give rise to cranial sense organs. They can be further subdivided into non-neurogenic placodes (adenohypophyseal, lens) and complex placodes (otic, olfactory, lateral line). Secondly, the neurogenic placodes (trigeminal, branchial, profundal) whose derivates are crucial elements of several cranial ganglia [BHATTACHARYYA & BRONNER-FRASER, 2004]. Neurons in the cranial sensory ganglia do not solely derive from the neurogenic placodes but also from the neural crest, which forms the rest of the peripheral nervous system [BAKER & BRONNER-FRASER, 2001; BAKER & BRONNER-FRASER, 2002]. Extensive cell and tissue rearrangements are necessary to modify placodal precursor cells to highly specified neurons, involving processes of delamination or invagination (Fig. 2B). In a number of placodes, the underlying basement membrane of thickened epithelium becomes fragmented, thereby allowing cells to delaminate from the epithelium (e.g. lateral line) and migrating within the ectoderm to form patches of sensory organs or moving away from the ectodermal surface to become part of the sensory ganglia (e.g. trigeminal). Other placodes invaginate as cup-shaped structures (e.g. adenhypophyseal, lens) and delaminate from the ectodermal surface to form a vesicle first, which differentiates into a highly specialised structure at later stages [MOODY, 2007; SCHLOSSER, 2005]. Except for the lens placode, the cranial placodes differentiate into neuronal or endocrine cells, which comprise the respective sensory and endocrine organs of the peripheral nervous system. The trigeminal, epibranchial and otic placodes provide mitotic neuroblasts, which delaminate from the ectoderm to form the sensory ganglia for the trigeminal (V), the glossopharyngeal (IX), vagus (X), facial (VII), and the statoacoustic (VIII) nerves [WEBB & NODEN, 1993].

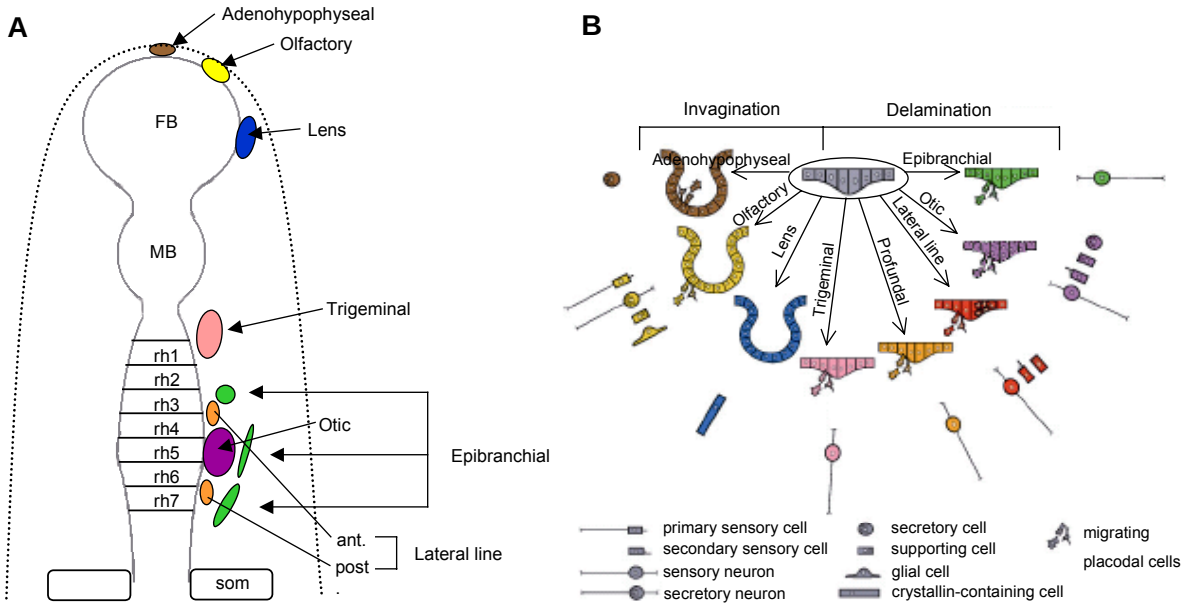

Figure 2 Ectodermal placodes in zebrafish. (A) Schematic overview of the different types of ectodermal placodes as distributed at the 10 somite stage. (B) Schematic summary of morphogenesis and cellular derivates of various ectodermal placodes in zebrafish [B, modified from SCHLOSSER, 2005]. Adenohypophyseal, olfactory, and lens placodes invaginate, trigeminal, lateral line, and epibranchial placodes delaminate from the ectodermal surface. In contrast with higher vertebrates the otic development in zebrafish is different. Instead of placodal cells invaginating to form a cup, ectodermal cells appear basically to thicken and arrange themselves into a solid ball just beneath the surface. All placodal precursor cells (except for the lens) leave the placodal epithelium as mesenchymal cells to migrate and become specialised. In the lateral line placodes, a subset of cells forms the lateral line primordial cell clusters, which migrate as a compact group along the basement membrane. FB, forebrain; MB, midbrain; rh, rhombomere; som, somites.

1.4 Placode subset summary[1]

Olfactory placodes

The olfactory placode is the only placode known to produce glia cells which otherwise originate from neural crest. Derivates from the olfactory placodes are the ciliated sensory receptor cells of the olfactory (odorant-sensing) and vomeronasal (pheromone-sensing) epithelia, whose axons project into the brain to form the olfactory, vomeronasal, and terminal nerves.

Trigeminal placodes

The trigeminal placode forms the trigeminal ganglial complex of two separat ganglia, the ophthalmic and the maxillomandibular ganglion. In vertebrates, the trigeminal neurons are born very early. These primary sensory neurons transmit somatosensory stimuli like touch, pain, and temperature from the skin of the face (ophthalmic branch) and the jaws and teeth (maxillomandibular branch). In anamniotes, like zebrafish, they become part of the primary nervous system that mediates the swimming reflexes.

Lateral line placodes

In fish and aquatic amphibians a variable number of pre- and post-otic lateral line placodes give rise to receptors and sensory neurons of the mechanosensory lateral line system. These placodes undergo remarkable migrations to deposit clusters of cells as precursors of lateral line receptor organs, the neuromasts, in lines over the head and along the entire body axis. Besides the mechanoreceptive lateral line organs that respond to disturbances in the water, some fish (but not the zebrafish) also possess a line system of electroreceptive ampullary organs that respond to weak electrical fields.

Otic placodes

The entire inner ear arises from the otic placode. The cell types deriving from otic placodes include the mechanosensory hair cells (balance and auditory information), supporting cells as well as endolymph secreting cells. Additionally, the otic placodes gives rise to the neurons of the statoacoustic ganglion of the cranial nerve VIII, which provide afferent innervation for the inner ear hair cells.

1.5 Inner ear development in zebrafish

The vertebrate inner ear is a highly developed auditory (cochlea) and vestibular (membranous labyrinth and semicircular canals) system, accountable for the detection of sound waves and accelerations enabling the organism to maintain balance. In the adult it forms a complex three-dimensional construction with several sensory patches, thickened regions of epithelium containing two major cell types, hair cells and supporting cells, arranged in remarkably organised patterns [TORRES & GIRALDEZ, 1998; NORAMLY & GRAINER, 2002].

[1] For review see BAKER & BRONNER-FRASER 2001

Although the mature structure is found only in jawed vertebrates, some urochordates possess mechanoreceptor cells with remarkable similarities to vertebrate otic hair cells, molecules and morphogenesis [FRITZSCH, 2002; 2006; 2007]. Based on fossil records it is known that the early cyclostomes had a well developed labyrinth with up to seven semicircular canals. Throughout evolution of higher vertebrates these canals have undergone several reductions. Today's living vertebrates commonly obtain three semicircular canals [WEVER, 1974]. Across the vertebrates the dorsal part of the inner ear is highly similar and contains the utricle with the gravity-sensing macula, and the semicircular canals with their rotating-sensing cristea. The ventral part of the ear is more different within the vertebrates, but it typically consists the saccular and lagenar maculae with vestibular and auditory functions (Fig. 3)[BEVER & FEKETE, 2002].

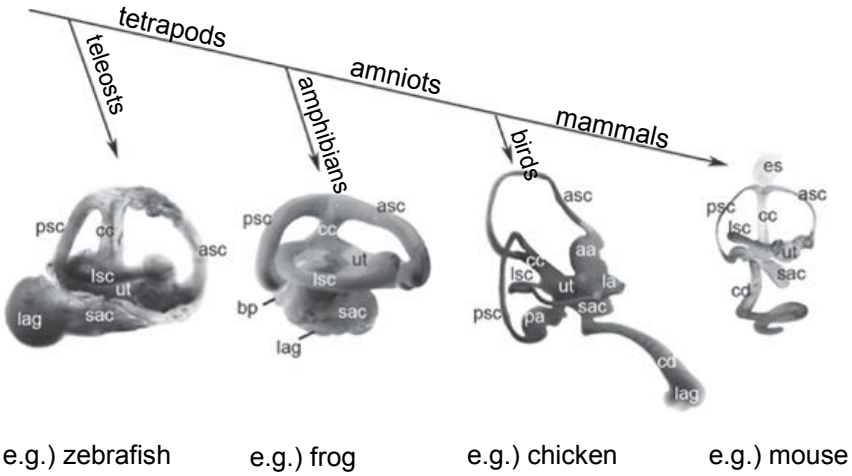

Figure 3 Phylogeny of the vertebrate inner ear. Zebrafish (20 days), Xenopus (stage 49), chicken (embryonic day 9) and mouse (embryonic day 15) are shown from lateral. The three semicircular canals and both utricular and saccular recess in all four representatives of different chordates during development. The lagenar chamber is rather conserved, and it may be elongated into the cochlear duct. The location of the hearing organs of birds and mammals supports the assumption it may have originated from the saccular macula, which is the hearing organ in most fish and some amphibians. aa, anterior ampulla; asc, anterior semicircular canal; bp, basilar papilla; cc, common crus; es, endolymphic sac; lag, lagena; la, lateral ampulla; lsc, lateral semicirclar canal; pa, posterior ampulla; psc, posterior semicircular canal; sac, saccule; ut, utricle [MOODY, 2007].

In zebrafish the inner ear develops, like in other vertebrates, on either side of the hindbrain. The earliest rudiment, the otic placode, becomes visible at around 16 hpf and extends from the posterior end of rhombomere 4 down to rhombomere 6 (Fig. 4B; Fig. 5A). Recent genetic studies have shown that both mesoderm and hindbrain are involved in otic placode induction. The initial signal to start the process of induction comes from the mesoderm and is maintained by signals from the hindbrain. During later gastrulation members of the *Fgf* gene family appear to be the primary transcription factors involved in otic induction. The response to these early otic induction events involves expression of a variety of transcription factors, many of which are already expressed in the pre-placodal ectodermal field before overt otic morphogenisis (Tab. 1). By the 10 somites stage cells express a wide range of transcription factors and signalling molecules (Fig. 4B). The otic placode-forming competence is initially widespread but becomes restricted to the hindbrain-area as well as the vagal ectoderm at midneural stage. Transplantation of otic placode cells have shown a tendency to develop

autonomously to a certain extent. However, the final otic fate determination occurs in later stages of formation [FEKETE, 1996; BAKER & BRONNER-FRASER, 2001; STREIT, 2001; STREIT 2004; WHITFIELD, 2002].

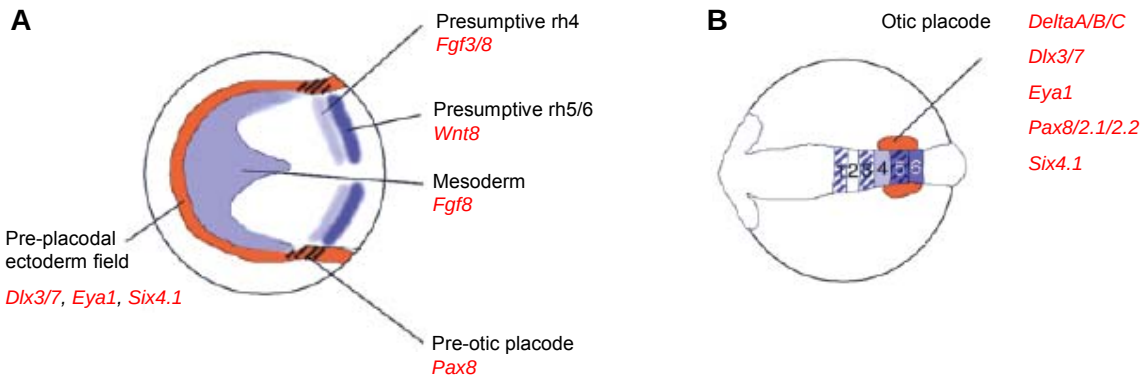

Figure 4 Signalling interactions influencing otic induction. Schematic drawings, dorsal view: (A) The pre-placodal ectodermal field at the late epiboly (9-10 hpf) stage. (B) Developing otic placode at 10 somite (14 hpf) stage. A variety of transcription factors genes is involved in the induction of the otic vesicle, e.g. *six* and *eya* genes [modified from WHITFIELD, 2002].

Table 1 Molecular markers and early events in otic placode development [modified from BAKER & BRONNER-FRASER, 2001].

8 hpf	Late gastrula	*Dlx3; Dlx7*	Transcription factors	AKIMENKO 1994; ELLIES 1997
8.5 hpf	Late gastrula	*Pax8*	Transcription factor	PFEFFER 1998
10 pfh	End of gastrulation	*eya1*	Transcription cofactor	SAHLY 1999
10 hpf	End of gastrulation	*six4.1*	Transcription factor	KOBAYASCHI 2000
11 hpf	3 somites	*Pax2.1*	Transcription factors	KRAUSS 1991
12 hpf	6 somites	*Pax2.2*	Transcription factor	PFEFFER 1998
13 hpf	8 somites	*Islet-1*	Transcription factor	KORZH 1993
14 hpf	10 somites	Placodes visible		HADDON & LEWIS 1996
14 hpf	10 somites	*deltaA, deltaB, deltaC*	Notch ligands	HADDON 1998
18.5 hpf	19 somites	*Fgf8*	Transcription factor	REIFERS 1998
19 hpf	21 somites	Otoliths form		HADDON & LEWIS 1996
22 hpf	26 somites	Neuroblast delaminate		HADDON & LEWIS 1996
24 hpf	30 somites	Hair cells differentiate		HADDON & LEWIS 1996

The otic placode (Fig. 5B) hollows rapidly into the otic vesicle, but unlike in higher vertebrates, such as the chicken, it do not invaginate to form a cup, which pinches off the ectodermal surface to become a closed vesicle. Instead, it appears that the otocyst forms by cavitation. An initially oval group of cells in the ectoderm thickens and models itself into a solid ball without any lumen beneath the surface. The

apical part of the cells, the site where the lumen is about to open up, is already polarised. With increasing polarisation, the nuclei migrate to the basal end and cause the loss of cell-cell contacts at the apical side. Thus, a small slit-like lumen appears and extends into the otic vesicle (Fig. 5D). The vesicle in turn undergoes a series of shape changing events, before it converts into an elaborate three-dimensional array of chambers and ducts filled with endolymphatic fluid [HADDON & LEWIS, 1996]. From 22 hpf onward individual neuroblasts start to delaminate from the otic epithelium passing through an epithelial to mesenchymal transition to leave the otic vesicle. They accumulate beneath the rostral half of the otic vesicle and differentiate into neurons of the statoacustic ganglion. The ganglion becomes more compact and extends underneath the sensory maculae. Neurons of the statoacoustic ganglion will send projections back to the ear's sensory patches. At around 42 hpf the process of delamination is completed. While the neuronal precursor cells are delaminating, some of the cells remaining in the otic epithelium differentiate into a variety of sensory patches. All sensory structures of the inner ear contain specialised receptor cells called hair cells. These mechanosensory cells with their characteristic staircased bundle of stereocilia and a kinocilium lie apically in the epithelium to couple endolymphatic vibration with motion of the hair cell bundles (Fig. 5F) [WHITFIELD, 2002].

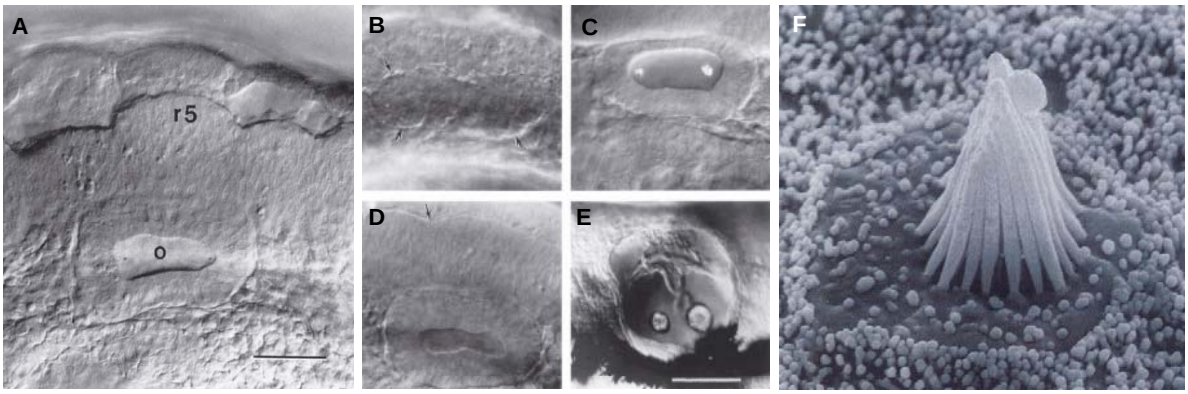

Figure 5 The inner ear development in zebrafish. (A) The hollow otic vesicle at 18 hpf, expands from rhombomere 4 up to rhambomere 6. (B-E) Morphogenesis of the otic vesicle. (B) The early otic placode (outlined by arrows) at 13,5 hpf; (C) At 18,5 hpf the placode has hollowed into the otic vesicle, arrow indicates the boundary between rhombomere 4 and 5; (D) Otoliths prominent in the otic vesicle by the stage of 25 hpf; (E) Protrusions of the semicircular canals grow out from the vesicle walls (48 hpf) and meet and fuse at 60-72 hpf. (F) Characteristic bundle of stereocilia of the neuromast. ov, otic vesicle; r, rhombomeres. Scale bar, 50µm [KIMMEL, 1995].

The first indication of the future sensory patches, at about 19 hpf, is the appearance of the otoliths in the otic lumen, two tiny crystalline deposits of calcium carbonate and protein. By 24 hpf the first differentiated hair cells become visible, grouped in two separate clusters beneath each otolith. These early hair cells referred to as tether cells are uncharacteristic in several ways. Both the utricular and the saccular otoliths are formed originally at the anterior and posterior ends of the vesicle (Fig. 5C). By a process termed otolith seeding the first real sensory patches develop. Free otolith precursor particles move through the lumen and to the opposite ends of the vesicle where they bind to the stationary kinocilia of the tether cells. In the adult zebrafish four otoliths are present, one associated with the maculae in the utricle (anterior), one with the macula in the saccula (posterior), and two with the maculae in the lagena (lateral), which arises later during larval development (Fig. 6B). The second

sensory structure, the semicircular canal system, appears between 42 and 48 hpf. It features two main modules, the canals themselves, which are endolymph-filled and bounded by nonsensory epithelium, and their associated sensory patches, the cristea (Fig. 6B). The first sign of canal formation is the inward protrusion of the vesicle epithelium. These thin layers of epithelium covers a hub of acellular matrix, which increases and generates continuous pillars, the developing semicircular canal pirmordia. All together, four such bulges project into the lumen, from the anterior, posterior, ventral, and lateral walls. By 60 hpf the lateral bulge forms three more lumps, pointing in anterior, posterior and ventral direction. These lumps fuse with the anterior, posterior and ventral protrusions, defining the three semicircular canals. The anterior and the posterior canals meet in the middle of the ear at a duct called common crust (Fig. 6A). At this point three canals are present, and each of them ends in an enlarged ampullary sac that houses the sensory cristae. The cristea do not become visible before 60 hpf and their hair cells differ from those of the maculae, presenting exceptionally long kinocilia [HADDON & LEWIS, 1996; WHITFIELD, 2002; MOODY, 2007]. Fish do not possess a cochlea, the specialised hearing organ of amniotes, nor are their inner ears linked to a middle and outer ear system. Instead the macula organs of the sacculus, utricle and lagena detect sound waves, and the swimbladder is used to enhance auditory stimulation of the inner ear [POPPER & FAY, 1993]

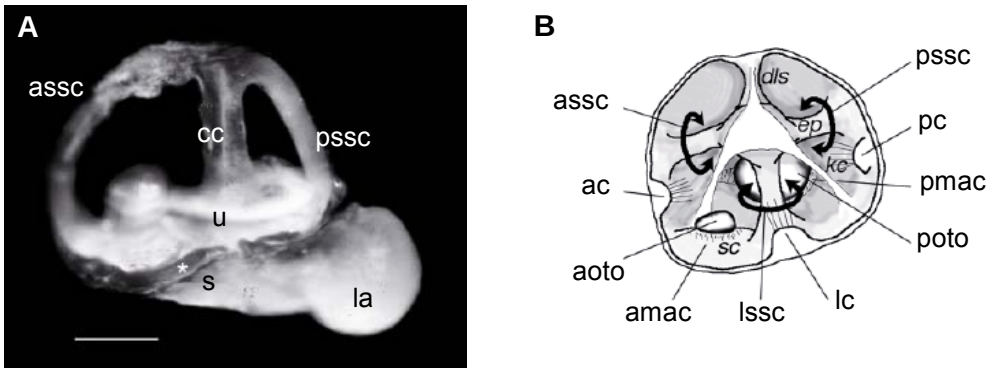

Figure 6 (A) Three-dimensional morphology of the adult zebrafish inner ear. Dorsal to the top, anterior to the left [modified from BEVER & FEKETE, 2002]. (B) Drawing of a zebrafish ear at four days post fertilisation, the three-dimensional structure within the vesicle [WHITFIELD, 2002]. ac, anterior crista; amac, anterior macula; aoto, anterior otolith; assc, anterior semicircular canal; cc, crus commune; la, lagena; lc, lareral crista; lssc, lateral semicircular canal; pc, posterior crista; pmac, posterior macula; poto, posterior otolith; pssc, posterior semicircular canal; s, saccula; u, utricle. Scale bar, 500µm.

1.6 Lateral line development in zebrafish

The vertebrate lateral line is a primitive mechanosensory system, like the inner ear, that is present in fish, and larval and adult aquatic amphibians. The neuromasts, the sensory receptors, respond to water movements and allow detection of unidirectional or oscillatory flows. A large number of these neuromasts form a line along the flanks of the animal, extending from the ear to the tail. The neuromasts are arranged on the body surface in a species-specific pattern [GHYSEN & DAMBLY-CHAUDIÈRE, 2004]. The prominent similarity of hair cells in both lateral line and inner ear led to two different theories about the origin of the otic placode. The first was established by VAN BERGEIJK

[1967], who assumed the inner ear to be a derivate of the lateral line. The other theory, postulated by WEVER [1974], states, that both the lateral line and the otic placode evolved independently. Even though the otic placode is situated very close to the pre- and postotic lateral line placodes in the embryo, the distinct differences in ectodermal competence as well as the timing and distribution of signalling support WEVER'S hypothesis. Furthermore, unlike the inner ear the lateral line has disappeared in the terrestrial tetrapods [WEBB & SHIREY, 2003; STREIT, 2001]

The lateral line system is composed of two major modules, the anterior lateral line encompass all head neuromasts, and the posterior lateral line all neuromast in the trunk and tail. The sensory neurons of the anterior lateral lines are located in the anterior lateral line ganglia, which are found rostral to the ear. The cell bodies of posterior lateral line neurons reside in the posterior lateral line ganglia, located caudal to the ear [WINKELBAUER, 1989; WEBB & NODEN, 1993; NORTHCUTT, 1994]. Both types of ganglia receive contributions from the neural crest [COLLAZO, 1994]. A characteristic structure of the developing posterior lateral line is the primordium, which originates from the posterior lateral line placode (just posterior to the otic placode), and begins to migrate posteriorly along the horizontal myoseptum at about 20 hpf. During this migration, the primordium deposits clusters of cells at regular intervals of five to six somites. Each cluster will develop into a neuromast. At about 42 hpf, the primordium has reached the tail tip and the migration process is completed [GOMPEL, 2001]. The first fully differentiated neuromasts are those of the anterior lateral line and appear during the second day of development at around 36 hpf, closely followed by the posterior neuromasts (Fig. 7A). The differentiation process of the posterior lateral line is completed by the end of developmental day two. Six to eight neuromasts are spread along the myoseptum, the first five evenly distributed, while the last two to three are grouped near the tip of the tail. Soon after the establishment of the posterior line by these primary neuromasts, new neuromasts, termed secondary neuromasts, differentiate along the myoseptum and intersperse between the primary neuromasts in a head-to-tail direction, generally with two somites between each (Fig. 7B) [LENDENT, 2001].

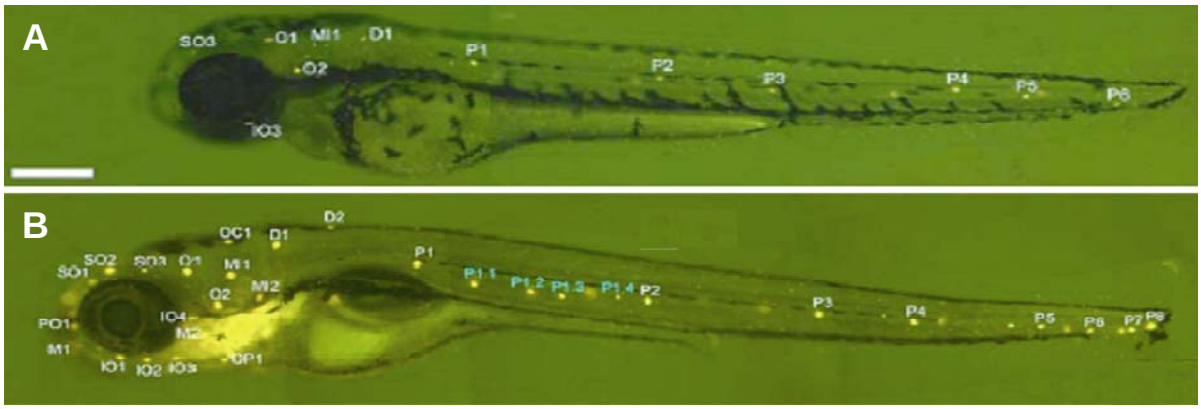

Figure 7 Live staining of lateral line hair cells with DASPEI at 2 dpf (A) and 5 dpf (B). Neuromast designation is according to Raible et al.,(2000) and Harris et al. (2003). Scale bar,0,5 mm (Hartmut Cuny, 2004, Regeneration von Haarzellen und Rolle des Transkriptionsfaktors AP-2α2 im Seitenlinienorgan des Zebrafischs (*Danio rerio*).

1.7 Cell type development – cell proliferation, cell death, and cell differentiation

During embryonic development cells undergo a variety of specification processes like cell proliferation, programmed cell death (apoptosis), cell migration and differentiation. Combination and coordination of these processes is essential for accurate shape, size, and cellular composition in the developing tissues. A cell death programme, which selects appropriate sets of cells and eliminates inappropriate ones, is important for many developing tissues. In vertebrates for instance, massive numbers of neurons are generated during early development many of which are eliminated at later developmental stages [HAMBURGER & LEVI-MONTALCINI, 1949; FESUS 1991; OPPENHEIM, 1991]. Particularly during critical differentiation events, like sensory organ development, programmed cell death seems to be a seriously important specification factor in multicellular organisms [GLÜCKSMANN, 1951; JACOBSON, 1997]. During apoptosis cells die in response to a range of stimuli in a controlled, regulated way. In this way, cells play an active role in their own death (which is why apoptosis is often referred to as cell suicide) [MOODY, 2007]. In an extrinsic apoptosis pathway, death inducing signalling molecules, bind as ligands to transmembrane death receptors on the target cell. These receptors transmit the information whereupon caspase protein cascades get triggered and activate DNases[2], inhibiting DNA repair enzymes and breaking down structural proteins in the nucleus. The caspase protein family is one of the main executors of the apoptotic process. After a cell receives the signal to undergo programmed cell death, a series of apoptotic events occur. Actin filaments in the cytoskeleton are disrupted, the cell shrinks and the cytoplasm fragmented. The main apoptotic characteristic is the cleavage of chromosomal DNA into nucleosomal units. Both nucleus and cytoplasm fragments form membrane-bound apoptotic bodies which can be engulfed by phagocytes [DASH, 2007]. Many of the signalling pathways that regulate organ formation are initiated by growth factors that bind on the cell surface of precursor cells. Information transfer from the cell surface to the nucleus regularly pass throughout receptor mediated signal molecules. These cell-signal molecule interactions trigger the activation of transcription factors, which in turn can activate or repress a cascade of events inside the cell. Several different signal transduction pathways can be linked together and can increase or inhibit each others activity. Transcriptional activation or repression of target genes control essential cellular function including cell proliferation, differentiation, and apoptosis during organogenesis. The posttranslational modification of proteins, including those that regulate gene expression, such as transcription factors, provides sensitive and flexible mechanism to dynamically modulate protein function in response to specific signalling input. The alteration occurs either through the addition of phosphate groups (phosphorylation) via the transfer of the terminal phosphate form ATP to an amino acid residue or their removal (dephosphorylation). In cases of transcription factors, changes in phosphorylation state can influence protein stability, conformation, subcellular localisation, cofactor interactions, transactivation potential and transcriptional output. Enzymes catalyse the addition (kinases) or removal (phosphatases) of phosphate groups from proteins [HUNTER, 2000].

[2] Enzymes capable of cleaving the phosphodiester bonds between the nucleotide subunits of nucleic acids.

1.8 The *eyes absent* (*eya*) gene family

The *eyes absent* gene was first identified in *Drosophila* [BONINI, 1993] as a nuclear protein, being essential for appropriate eye formation during early embryonic development, where it participates synergistically with *eyeless* (Pax family), *sine oculis* (Six family), and *dachshund* (Dach family) [PIGNONI, 1997; CHEN, 1997; BONINI, 1997, HALDER, 1998; NIIMI, 1999]. Identified in many species, *Eya* family genes are expressed in a complex manner in various embryonic and adult tissues and play important roles in the processes of morphogenesis, organogenesis, and cell differentiation. Vertebrate homologues of *eya* have been isolated from mouse (*Eya1-Eya4*), human (*EYA1-EYA4*) and chicken (*Eya2, Eya3*). All of these *eya* genes are widely expressed in sensory organs like the eye, ear, lateral line (teleosts), but also in muscle and kidney. Many members of the zebrafish *six (1-6)*, *pax (6)* and *dach (1-2)* gene families show a similar range of expression [KOBAYASHI, 2000; PFEFFER, 1998; RILEY, 1999; HAMMOND, 2001].

Vertebrate *Eya* genes seem to be components of regulatory networks similar to the one acting during eye development in *Drosophila*. [HEANUE, 1999; XU, 1999; XU, 2003]. In *eyes absent* mutations in *Drosophila*, eye progenitor cells display an increased incidence of programmed cell death prior to the first differentiation events. Transcript variations in different *eya* alleles show variable severity of the eye phenotype, which ranges from rough and only slightly smaller eyes, to rough and much reduced eyes, frequently absent eyes on one side of the head and finally complete absence of eyes. Nevertheless, even with increasing allele severity, there are no specific cell types missing. Therefore, mutations in the *eya* gene do not seem to affect differentiation of the precursor cells, but the switch between the differentiation pathway and the pathway of apoptosis [BONINI, 1993; LEISERSON, 1994].

1.8.1 Structure and function of the *eya* gene

While there is only a single *eyes absent* gene in *Drosophila*, at least four homologues of this gene (*Eya1-4*) are present in vertebrates. cDNA cloning of the *Drosophila eyes absent* gene revealed a conceptual protein sequence with two domains: a divergent proline-serine-threonine rich N-terminus, which functions as transcriptional activation domain, and a highly conserved 271-274 amino acid C-terminus, that has been referred to as eya homologous region (eyaHR), eya domain or Eya homology domain 1 (ED1), which is required for protein-protein interactions [ABDELHAK, 1997; XU, 1997; ZIMMERMAN, 1997; BORSANI, 1999]. In addition, a short region of weak homology, named Eya homology domain 2 (ED2), occurs between the fly and the mammalian sequences in the N-terminal region (Fig. 8C). In this domain a large number of tyrosine (Y) residues are conserved [BONINI, 1993; ZIMMERMAN, 1997]. The *eyes absent* gene is part of a regulatory gene network, together with the DNA-binding homeodomain factor *sine oculi*s (*six*) and the *dachshund* (*dach*) nuclear cofactor. This network is characterised by transcriptional feedback loops and complex protein-protein interactions [CHEN, 1997]. Because *eya* genes do not encode a nuclear localization signal or an apparent DNA-binding domain, an interaction with a Six protein, mediated by the eya domain, is required to get the Eyes absent

protein from the cytoplasm to the nucleus and allow for transcriptional regulation of downstream genes (Fig. 8A) [OHIO, 1999; FAN, 2000].

In addition to a function as transcriptional co-factor, Eyes absent can function as an enzyme. Analysis of Eya amino acid sequences reveals that the eya domain contains sequence motifs equivalent to the haloacid dehalogenase (HAD) superfamily of phosphohydrolases. The HAD family, which includes several types of enzymes, including phosphatases, is characterised by a conserved α/β-hydrolase fold that unites three short sequence motifs to form the catalytic core of the enzyme. Motif I at the N-terminal end of the domain is a conserved quintet consisting of two aspartic acid (D), and one threonine (T) residues as well as two variable amino acids (x) in the order of DxDxT. The second aspartic acid distinguishes the phosphatase/phosphohydrolase subgroup from other branches of the HAD suprafamily. Motif II contains an essential serine (S)/threonine (T) at the end of the β-strand. Motif III contains two glycine (G), one aspartic acid (D) and one glutamic acid (E) residue, furthermore two changeable amino acids (x) in the order of GDGxxE at the C-terminal end of the domain (Fig. 8B). The HAD-related region of the eya domain is highly conserved and indicates that Eyes absent might have intrinsic protein tyrosine phosphatase activity and can autocatalytically dephosphorylate itself. Indeed, experiments have shown that the eya domain dephosphorylates various artificial substrates. Mutations in key amino acids within the eya domain can decrease or eliminate catalytic activity. The gene-specific recruitment of a co-activator with intrinsic phosphatase activity provides a molecular mechanism for activation of specific gene targets, including those regulating precursor cell proliferation and survival [LI, 2003; RAYAPUREDDI, 2003; TOOTLE, 2003; REBAY, 2005].

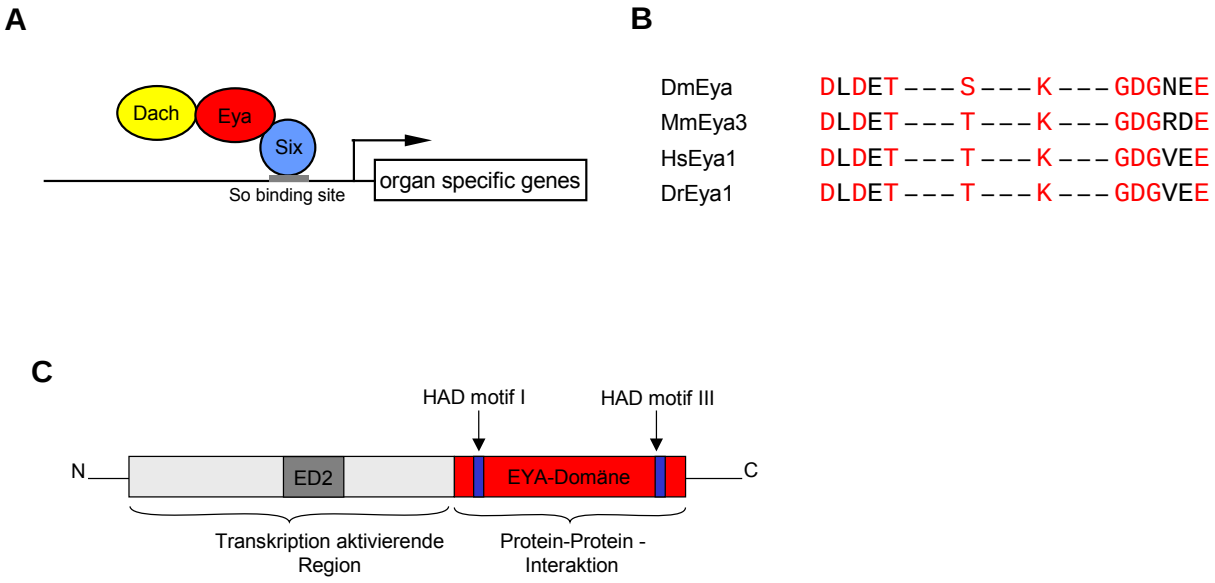

Figure 8 (A) Biochemical interactions in a model of a proposed activation of potential downstream targets through Eya, Six, and Dach. Because Eya proteins have no DNA-binding motif, its activation is mediated through interactions with a DNA-binding Six protein [modified from BRODBECK & ENGLERT, 2004]. (B) Eya is a member of the phosphatase subgroup of the HAD superfamily. Eya domain sequences contain the three characteristic HAD motifs (I - III), which are highly conserved in all eya homologues (red residues). Dm, *Drosophila melanogaster*; Mm, *Mus musculus*; Hs, *Homo sapiens*; Dr, *Danio rerio* [TOOTLE, 2003]. (C) Domain structure of EYA.

1.8.2 Expression sites of *eya1* in zebrafish

In the zebrafish embryo, major expression sites of *eya1* are several cranial sensory placodes, the branchial arches, and the developing somites (Fig. 9B). Initially, *eya1* is expressed in the whole band of the pre-placodal field at the end of gastrulation (Fig. 9A). At around 12 hpf, expression becomes restricted to an anterior and a posterior part, which in later stages of development give rise to the olfactory, otic and lateral line placodes. In the otocyst, *eya1* is solely expressed in the ventral part, including the nascent neurons of the statoacoustic ganglion and the sensory patches. While *eya1* is expressed in delaminating ganglionic precursor neurons, expression appears to cease from differentiated neurons and is entirely absent from the mature ganglion at the end of the second developmental day. In the anterior and posterior lateral line placode, *eya1* is expressed even before condensation of these placodes, as indicated by diffuse *eya1* expression in the preotic and postotic areas at 16 hpf. A further expression site of *eya1* is the migrating posterior lateral line primordium and the neuromasts generated by the primordium. The neuromasts present the only structures, in which *eya1* is expressed in both undifferentiated precursor cells and differentiated cell types. In contrast, *eya1* expression in the somites appears only after they have formed from the presomitic mesoderm [SAHLY, 1999].

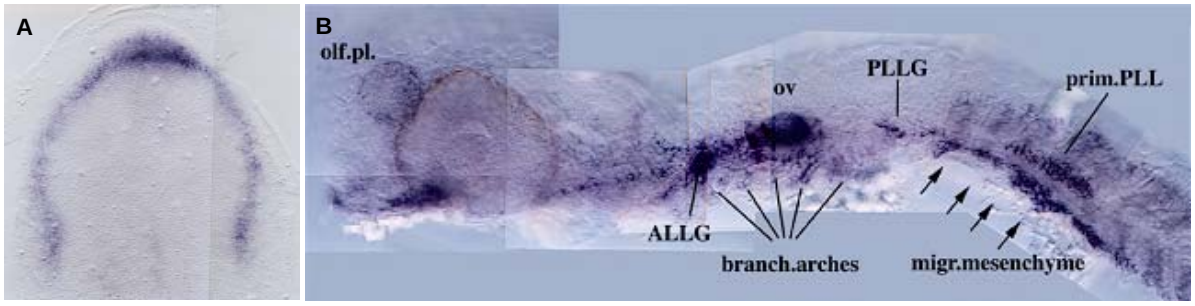

Figure 9 (A) Early *eya1* expression in the pre-placodal ectodermal field at 10hph (dorsal view; anterior to the top) [ANDERMANN]. (B) Expression of *eya1* at 24 hpf. ALLG, anterior lateral line ganglion; olf.pl. olfactory placode; ov, otic vesicle; PLLG, posterior lateral line placode [SAHLY, 1999].

1.9 Mutations in *eyes absent* affect vertebrate inner ear development

Mutations of vertebrate *Eya* genes and *Eya* knock-down experiments have shown negative effects on the developing auditory system. The *eya1*/*dog-eared* (*dog*) mutation in zebrafish was identified in a large-scale mutagenesis screen by abnormal morphology of the inner ear [WHITFIELD; 1996]. Homozygous *dog-eared* embryos show serious defects of both sensory and nonsensory tissues. While the hair cells of the cristea do not differentiate during development, those in the maculae are reduced and misarranged. The otoliths are decreased and the epithelial protrusions of the developing semicircular canals are present, but disorganised (Fig. 10C,D). The mutation also affects the lateral line, where the number of the posterior lateral line neuromasts is reduced, those at the tail tip are absent in almost all *dog-eared* larvae (Fig. 10A,B). Furthermore, the embryos show ectopic and an

increased level of apoptosis in the developing otic vesicle as well as the lateral line primordium [WHITFIELD, 1996]. The *dog-eard* phenotype is recessive and caused by a point mutation, found in three independent *dog* alleles, with various severity. Morphologically, the *dog-eared* phenotype becomes visible at around 48 - 72 hpf, but this also varies with the different *dog* alleles. Sequence analysis of *eya1* cDNA from each allele revealed, that the mutations result in a truncation of the the *eyes absent* homology domain. The *dog* phenotype can be phenocopied by *eya1* gene knock-down experiments using morpholino antisense oligonucleotides [KOZLOWSKI, 2005].

Xu et al. [1999] generated a *Eya1* knockout mouse, which shows several developmental defects, including abnormal inner ear development. *Eya1* heterozygotes ($Eya^{+/-}$) have conductive hearing loss and renal anomalies similar to those found in human Branchio-Oto-Renal (BOR) syndrome. The hearing loss is associated with middle and inner ear aberrations, whereas the anomalous sound conduction through the middle ear is the main reason for the hearing loss. In contrast *Eya1* homozygote ($Eya^{-/-}$) mice die at birth. The size of the mutant embryos heads is reduced and they lack ears and kidneys completely. In addition, the mutants are characterised by open eyelids, and craniofacial and skeletal defects in the skull, neck, and ripcage (Fig. 10E,F). Otic anomalies involve the outer, middle and inner ear. Outer anomalies include absent or malformed auricles, atresis of the external auditory canal as well as malformed eardrums. The mutant middle ears reveal a present but malformed incus, whereas the maleus and the stapes are absent. Additionally the tympanic cavity is not formed. In contrast, the otic vesicle of the inner ear initially formed is terminated in later development, the inner ear structures are not differentiated at all. The deficiency of otic development is associated with an abnormal induction of apoptosis. Also affected are the facioacoustic ganglia (gVII-VIII) and the endolymphatic duct [XU, 1999].

The Laboratory of PETIT (1996) identified *eyes absent* as the gene underlying the BOR syndrome, an autosomal dominant inherited birth defect that causes human deafness with variable degrees of severity [ABDELHAK, 1997]. Sequence analysis of the eya coding region in unrelated patients affected by BOR syndrome result in six novel mutations[3], all of which are different. However all mutants are located within or in the immediately vicinity of the eya-domain. The clinical phenotype in persons with BOR syndrome is characterised by numerous congenital anomalies involving the branchial arch system, inner and middle ears, as well as kidneys. The most common features are hearing loss (98.5% affected individuals, and approximately 2% of profoundly deaf children), which can be conductive (i.e., due to outer and/or middle ear anomalies), sensorineural (i.e., due to inner ear anomalies), or a mix of both [GRIMSING & DYRMOSE, 1986]. Further features are preauricula pits (83.6%), branchial anomalies (68.5%), renal anomalies (38.2%), and external ear abnormalities (31.5%). Furthermore, there is a higher rate of miscarriage and infant mortality in BOR families. The syndrome has an estimated prevalence of 1 in 40.000 and the penetrance of the syndrome is highly variable both between and within families [CHEN, 1995].

The association of branchial arch anomalies and hearing impairment has been recognised since the nineteenth century. The name branchio-oto (BO) syndrome has been used to describe a combination of both branchial and otic anomalies, without association of renal abnormalities. The description and addition of the renal anomalies to complete the whole spectrum of the branchio-oto-renal (BOR)

[3] To date 14 mutations have been detected in BOR patients.

syndrome is credited to the work of MELNICK [1978] and FRASER [1978]. Positional cloning has been shown that the *EYA1* gene on chromosom 8q13.3, homologous to the *Drosophila eyes absent* gene, underlies these syndromes, and that both BOR and BO are allelic phenotypes of mutations in this gene [ABDELHAK, 1997].

Hereditary hearing impairment (HHI) is a heterogeneous class of disorders that shows various patterns of inheritance and involves a multitude of different genes. Mutations that affect the EyaHR domain of the Eyes absent 4 (EYA4) protein were identified to cause late-onset hearing impairment at the DFNA10 locus on chromosome 6q22-23. This nonsyndromic autosomal dominant sensorineural hearing loss (SNHL) was described in two Australian families [WAYNE, 2001; DE LEENHEER, 2001]. PFISTER et al. (2002) reported about a Hungarian family comprising four generations with 11 SNHL affected and eight unaffected members. Mutation analysis of the EYA4 gene revealed an insertion of 4 base pairs, which results in an inaccurate stop codon nearly the eyaHR in all affected family members. Recently screening of the EYA4 gene of an Australian family with nonsyndromic SNHL showed a point mutation in EYA4 that is hypothesized to lead to aberrant pre-mRNA splicing and human disease [HILDEBRAND, 2007].

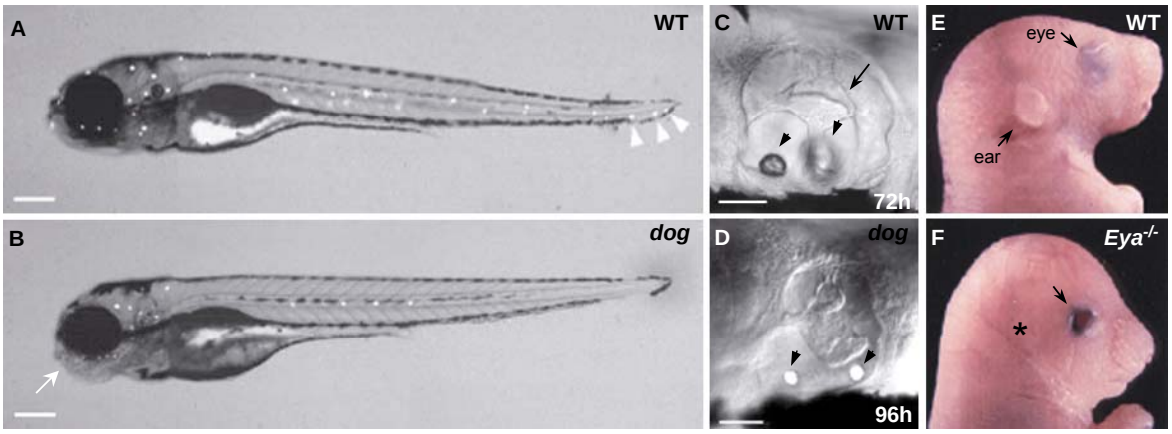

Figure 10 (A, B) DASPEI stain of lateral line neuromasts at 120 hpf. (A) Wild-type (WT) and *dog* embryo. Neuromasts appear as bright dots. *Dogs* lack the set of three neuromasts at the tail tip (arrowheads in WT) and show an abnormal jaw morphology (arrow) [WHITFIELD, 1996]. (C, D) Lateral view of the ear in WT (72 hpf) and in dog (96 hpf); arrowheads indicate the otoliths, arrows mark epithelial protrusions in the ear [WHITFIELD, 1996]. (E, F) WT mouse embryo and $Eya^{-/-}$ embryo. At E10.5 *Eya1* homozygous mice show severe craniofacial anomalies like open eyelids, an absent or malformed (asterisk) outer ear and neck [XU, 1999]. Scale bar, (A, B) 200µm; (C, D) 50µm.

2 Aim of thesis

The morphological abnormalies described for the zebrafish *dog-eared* embryos are, in comparison to the widespread embryonic expression of the *eya1* gene, rather partial and restricted to specific embryonic structures. This comparatively mild phenotype is likely the consequences of functional redundancy between various Eya family members. To date four *Eya* genes have been identified in mice and human (*Eya1-Eya4*).

The aim of this thesis is to analyse three novel zebrafish *eyes absent* genes, *eya2*, *eya3*, and *eya4*. In order to elucidate the role of *Eya* genes during early embryonic development, with a focus on the inner ear, sequences and temporal expression pattern sites of the three genes were compared to reveal conservation as well as unique and/or overlapping expression sites of these genes. This is due to the fact that functional redundancy most likely can be found between duplicated and/or co-expressed genes. An additional important step to resolve both unique and redundant functions of *eyes absent* genes during vertebrate organogenesis is the knockdown as well as overexpression of eya gene function.
KOZLOWSKI et al. (2004) have shown that a premature apoptosis in precursors in the otic vesicle is a primary consequence of loss of *eya1* function in the zebrafish embryo. As apoptosis has also resulted from loss of *eya* gene function in *Drosophila* and mouse [BONINI, 1993; XU, 1999], these may reflect a general mechanism of suppression of apoptosis by Eya proteins. Therefore, to clarify if *eya* genes regulate precursor cell survival, *eya* gene function manipulated embryos were investigated for inappropriated programmed cell death.

3 Results – Part I

Based on sequence similarities to the *Drosophila eyes absent* gene, the vertebrate *Eya* gene family was identified by BONINI (1993). To date four *Eya* homologous genes (*Eya1-4*) have been identified and described in mammalia [XU, 1997; ZIMMERMANN, 1997], one in chicken (*Eya2*) [MISHIMA, 1998], two in *Xenopus* (*Eya1; Eya3*) [DAVID, 2001; KRIEBEL, 2007], and one in zebrafish (*eya1*) [SAHLY, 1999]. However, function of the various *Eya* genes are largely unknown yet. To further understanding of the *Eya* genes during vertebrate development, the zebrafish homologues of *eya2*, *eya3*, and *eya*4 were identified and characterised by sequence analysis, expression pattern observation and functional assays in this thesis.

3.1 Structural analysis of zebrafish *eya2, eya3 and eya4* cDNA

To confirm that the isolated clones are indeed three different homologs of the *Drosophila eyes absent* gene, they were sequenced from their 5'- and 3'- ends (Fig.11). Sequence analysis and alignments of the deduced amino acid sequences by using the computer programs BLAST (Basic Local Alignment and Search Tool) and CLUSTAL W found significant homologies with other members of the vertebrate Eya family, as well with the *Drosophila* eya protein.

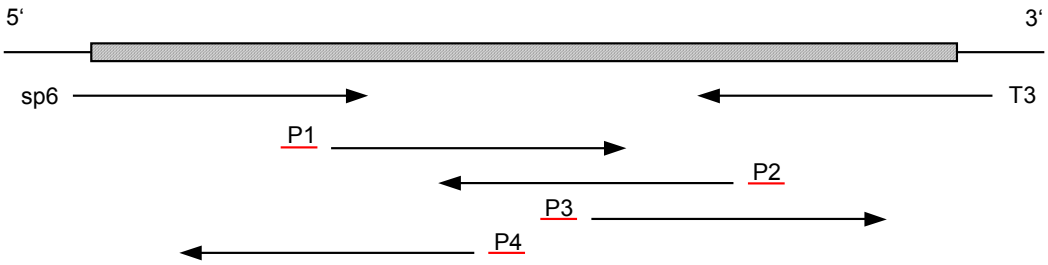

Figure 11 Sequencing strategy. The shaded bar represents the respective insert. Arrows indicate orientation of sequenced sections. Sp6 and T3 were used as sequencing primers, P1-P4 are internal primers used for sequencing the full-size clones

Based on pairwise comparison of 12 vertebrate eya proteins, amino acid identities and similarities could be determined by using the BLAST non-redundant protein database. As would be expected, closest affinity was found for each member of the zebrafish eya family in comparison with the respective mammalian homologues. The highest degree of relationship was found between zebrafish eya4 and the murine and human Eya4 proteins with 74% identity (83% similarity) and 73% (83%), respectively. Zebrafish eya2 protein is 60% identical (73%) with mouse Eya2 and 62% (72%) with human Eya2, while zebrafish eya3 shows an identity of 48% (60%) to mouse Eya3 and 58% (72%) to human Eya3. Comparison of the zebrafish eya1 protein with the other zebrafish eya proteins reveals

an identity (similarity) of 60% (73%) to eya2, 47% (63%) to eya3, and 63% (75%) to eya4. All comparisons between the various eya proteins are presented in Tab. 3.

Analysis of *eya2* cDNA (Fig. 12) led to the definition of 1766 bp, containing a coding region of 1431 bp, the ORF (open reading frame). This ORF has the first in-frame initiation codon (ATG) at nucleotide 329 and a stop codon (TAG) at nucleotide 1760, resulting in a predicted protein product of 477 amino acids. The cDNA comprises at least part of the 5'UTR (untranslated region) of 328 bp, but lacks the 3'UTR as well as the poly(A) tail. However, this *eya2* cDNA contains two insertions, which are absent in the mouse as well as human protein. The first six bp fragment is located in the N-terminal domain (nucleotides 557-562, predicted amino acids 77-78), the second fragment of nine bp is found in the highly conserved C-terminal (nucleotides 1352-1360, predicted amino acids 342-344). This insertion of three amino acids within the eyaHR (eya homology region) leads to an eyaHR of 274 residues instead of the common 271 residues. In addition, the zebrafish eya2 protein lacks a serine (S) residue in the N-terminus at amino acid position 190. Comparison of the deduced *eya2* sequence with those of mouse and human reveals an identity of 64% and 62% respectively for the entire cDNA. The eyaHRs are 79% identical between the zebrafish and the mammalian protein product. The ED2 (eya domain 2) runs from amino acid 100 to 129 and shows an identity of 48% (13/27) to the mouse and 40% (11/27) to the human predicted Eya2 protein.

Sequencing of the *eya3* cDNA (Fig. 14) determined a length of 1910 bp for this transcript, including only 96 bp of the 5'UTR. The non-sense stop codon and the 3'UTR with the poly(A) tail are missing. Therefore, the analysed *eya3* cDNA lacks the last five assumed amino acids at the 3' end of the ORF, presumably as a result of the subcloning processes. This partial ORF consists of 1814. The deduced cDNA is 48% and 58% identical to mouse and human, whereas the, 266 amino acid eyaHR shows 79% and 80% of identity to the murine Eya3 and the human Eya3 protein. In the ED2 region, from amino acids 229 to 245, the identity with the proteins of both mouse and human Eya3 is 35% (8/23*).* The predicted zebrafish eya3 protein has 12 amino acid insertions of differing lengths, which are absent in the homologus mammalian proteins. Localisation and length of these amino acid insertions are listed in Tab. 2. However, it is worth noting that all insertions are three or a multiple of three bp long and therefore do not alter the overall reading frame. All insertions are exclusively in the N-terminal region, except for one amino acid, a valine (V), which is inserted into the ED2 region.

The cDNA encoding the zebrafish *eya4* homologue is 2895 bp long, and has an ORF of 1833 bp (Fig. 16). The start codon at nucleotide 426 and a stop codon (TAA) at nucleotide 2259 encompass a predicted protein product of 611 amino acids. Besides the ORF, the sequence contains a 425 bp 5' UTR as well as a 637 bp 3' UTR (poly(A) tail not included). Additionally, one insertion and six gaps are present in the N-terminal region compared with respective mouse and human proteins. The insertion of 9 bp spans nucleotides 1287-1295 (predicted amino acids 288-300). Five of the gaps represent a single missing amino acid, one of which is found within the ED2 region, while the sixth gap encompasses a stretch of 28 amino acids. As shown for the zebrafish eya2 and eya3 proteins, there is also a high amino acid identity between the predicted eya4 protein in zebrafish and those in mouse

(74%) and human (73%). In the eyaHR this identity even rises up to 90% in mouse and 93% in human. The ED2 of the predicted zebrafish eya4 protein displays the strongest conservation of the Eya ED2 of all three Eya proteins. It is 72% (26/36) identical to both mouse and human Eya4 protein.

As previously described for Eya proteins in chicken, mouse and human [XU, 1997; MISHIMA; 1998 RAYAPUREDDI, 2003], alignments of the zebrafish deduced amino acid sequences (Fig. 13; 15; 17) have shown, that the N-terminal domains of eya2, eya3 and eya4 are less identical than the C-termini, and noticeably proline-serine-threonine-rich. These N-terminal regions consist of 39% (eya2), 34% (eya3) and 36% (eya4) proline, serine and threonine residues in total. In addition, the eyaHR of eya2, eya3 and eya4 proteins contain both motif I and motif III of the conserved halocid dehalogenase hydrolases (HAD) [LI, 2003; RAYAPUREDDI, 2003; TOOTLE, 2003; REBAY, 2005]. Motif I (DxDxT) is absolutely identical in the zebrafish, mouse and human deduced proteins of the three *eya* genes, as is motif III (GDGxxE) in the *eya3* gene. In contrast motif III reveals slight differences in the deduced proteins of both compared mammalian Eya4 proteins (Fig. 13; 15; 17).

For the phylogenetic analysis the aligned amino acid sequences shown in Fig 12, 14 and 16 as well as the *Drosophila* eyes absent protein, which serves as outgroup, were used to construct a phylogenetic tree by the neighbour-joining method [SAITOU & NEI, 1987]. This evolutionary tree approves the close relationship among the different Eya proteins and reveals four distinct groups of relatives: the zebrafish eya1, eya2, eya3 and eya4 proteins with their corresponding murine and human counterparts (Fig. 18). In all protein groups the affinity between mouse and human is higher than in comparison to the zebrafish proteins. Based on the phylogenetic tree two gene duplications must have happened during evolution. Firstly *Eya1* and *Eya3* duplicated from the original *Drosophila eyes absent* gene. A second duplication event led to the genes of *Eya2* and *Eya4*. Whereas *Eya2* is a duplicate of *Eya3* while *Eya4* is a duplicate of *Eya1*.

```
CTACTTGTTCTTTTTGCAGGATCCCATCGATTCGAATTCAAGGCCTCTCGAGAGCACACT     60
GCGATACACGCAAACACTTCGCTTTTAATAGTCGAATATAACATTATGATGCGACATTAA    120
ACTCGTCTGTCGGCGCTTTGAAGAACCCGCGTCACGCTAGGATGGACAAACTTTTCTGAA    180
CTTATTCGCTGATTTTTCGCTTGCTTTGCTTCGGATATGGAGAGCTGACAGCTGAACGTG    240
CGCAAGAGGAAGTACATAACAGACAGTGACAGGAGCCACTAGACGCACACTTCAGGAAAC    300
ACACATTTAGGCTACTCCAGCTGTGCTCATGGCAGCTTACGGACAGACGCAGTACAGCCC    360
                           M  A  A  Y  G  Q  T  Q  Y  S  P      11
GGCGTTACAGCCAGCGGGTCCTTACACACCATACACACATCACACACAGGGATACAGCAT    420
 A  L  Q  P  A  G  P  Y  T  P  Y  T  H  H  T  Q  G  Y  S  M      31
GACGTCCTACAATATTAAAACAGAAGATGGTTTGAGCCATTCACCTGGTCAGAGCAGTTT    480
 T  S  Y  N  I  K  T  E  D  G  L  S  H  S  P  G  Q  S  S  L      51
ACTGGGATACACACCAAACTTCAGCGGGACGCCCCCCGGACAGACGCTCTACAGCTACTC    540
 L  G  Y  T  P  N  F  S  G  T  P  P  G  Q  T  L  Y  S  Y  S      71
ACACGGCGGCAGCATTTCTTCTGGAATTTTCCAGGGTGCGAACAGCATCACAAGCTCAAC    600
 H  G  G  S  I  S  S  G  I  F  Q  G  A  N  S  I  T  S  S  T      91
GCCGTTCAGTCCAGCGCAGCAGGACTTCTCAACATATTCAAGCTACAGCCAAAGTCAATA    660
 P  F  S  P  A  Q  Q  D  F  S  T  Y  S  S  Y  S  Q  S  Q  Y     111
TTCTCCATACTACAACACACACTACAACAGCCCGTACATCACAGCCAGCAATATCACGCC    720
 S  P  Y  Y  N  T  H  Y  N  S  P  Y  I  T  A  S  N  I  T  P     131
ATCGGCCATCACAACGGCGATACCCTATCAGCACACAGATCACCCCGCTGTATCGACCAA    780
S  A  I  T  T  A  I  P  Y  Q  H  T  D  H  P  A  V  S  T  N      151
TCACAGCCCAGAATCACACACAGAGTACCAGGCTCCCACGAGTCCTCCAACTCCAGGAAA    840
 H  S  P  E  S  H  T  E  Y  Q  A  P  T  S  P  P  T  P  G  K     171
GGATCAGGACGGAGCTCCACCGAGACGCAGTGCGGATGGGAAGCTGAGAGGCCGGAAGCG    900
 D  Q  D  G  A  P  P  R  R  S  A  D  G  K  L  R  G  R  K  R     191
GGCCAGTGACCCCGTCCCTCTGCTGGACTCGGACATTGAGAGGGTGTTTGTTTGGGATCT    960
 A  S  D  P  V  P  L  L  D  S  D  I  E  R  V  F  V  W  D  L     211
GGATGAGACCATCATCATTTTCCACTCACTGCTTACCGGGACATTTTCCACACGCTTCGG   1020
 D  E  T  I  I  I  F  H  S  L  L  T  G  T  F  S  T  R  F  G     231
CAAGGACTCCGGGAAGGCTGTTTCTCTGGGTTTGTGGATGGAGGAGATGATCTTCAACTT   1080
 K  D  S  G  K  A  V  S  L  G  L  W  M  E  E  M  I  F  N  L     251
GGCTGATTCACGGCTGTTTTTCAATGACCTGGAGGAATGTGACCAGGTTCATATCGATGA   1140
 A  D  S  R  L  F  F  N  D  L  E  E  C  D  Q  V  H  I  D  D     271
CGTTGCTTCGGATGACAACGGTCAAGATCTCAGTACATATAACTTCGGCACAGATGGTTT   1200
 V  A  S  D  D  N  G  Q  D  L  S  T  Y  N  F  G  T  D  G  F     291
CCAGACACCAGCAGGTGGAGGTTCGCTCTGCCTGGGTTCAGGTGTTCACGGCGGGGTCGA   1260
 Q  T  P  A  G  G  G  S  L  C  L  G  S  G  V  H  G  G  V  D     311
CTGGATGAGAAAACTAGCCTTCCGCTACCGTCGGGTTAAAGAGATCTACAACACATACAA   1320
 W  M  R  K  L  A  F  R  Y  R  R  V  K  E  I  Y  N  T  Y  K     331
GAACAATGTTGGAGGTTTGTTGGGCAGCCCAAAAGCGCAAAAGCGGGAGGAGTGGCTTCA   1380
 N  N  V  G  G  L  L  G  S  P  K  A  Q  K  R  E  E  W  L  Q     351
GCTGCGGCGAGAGATGGAGGTTTTGACGGATCTGTGGCTGACGCAGGCTCTCAAAGCCCT   1440
 L  R  R  E  M  E  V  L  T  D  L  W  L  T  Q  A  L  K  A  L     371
CGCACTCATTAACTCCAGACCAAACTGTGTGAATGTGTTGGTCACGACCACGCAGCTGAT   1500
 A  L  I  N  S  R  P  N  C  V  N  V  L  V  T  T  T  Q  L  I     391
TCCAGCTCTGTCTAAAGTGCTTCTGTATGGTCTCGGAGGAGCGTTTCCCATCGAGAACAT   1560
 P  A  L  S  K  V  L  L  Y  G  L  G  G  A  F  P  I  E  N  I     411
CTACAGCGCCACCAAAACAGGTAAAGAAAGCTGTTTTGAGCGTGTGACGCAGAGGTTCGG   1620
 Y  S  A  T  K  T  G  K  E  S  C  F  E  R  V  T  Q  R  F  G     431
CAGGAGAGCCGTGTATGTGGTCGTAGGAGACGGTATTGAAGAGGAGACCGTCGCAAAGAA   1680
 R  R  A  V  Y  V  V  V  G  D  G  I  E  E  E  T  V  A  K  K     451
```

```
GAAGAACATGCCGTTCTGGCGAGTGACGTGTCGAGCGGATCTGGAGGCTTTGAGTCATGC   1740
 K  N  M  P  F  W  R  V  T  C  R  A  D  L  E  A  L  S  H  A     471
ACTAGAGCTGGATTACCTCTAGATCT                                     1766
 L  E  L  D  Y  L  *                                           477
```

Figure 12 Nucleotide and predicted amino acid sequences of the zebrafish *eya2* gene encoding EST, translated from the furthermost upstream in-frame methionine (M). The conserved *eya* homology region (eyaHR) is indicated in bold. An asterisk indicates the stop codon terminating the open reading frame. Bold letters in red indicate HAD motif I and III characteristic for a subgroup of protein tyrosine phosphatases superfamily [TOOTLE, 2003]. The eya homology domain 2 (ED2) is indicated in bold and blue.

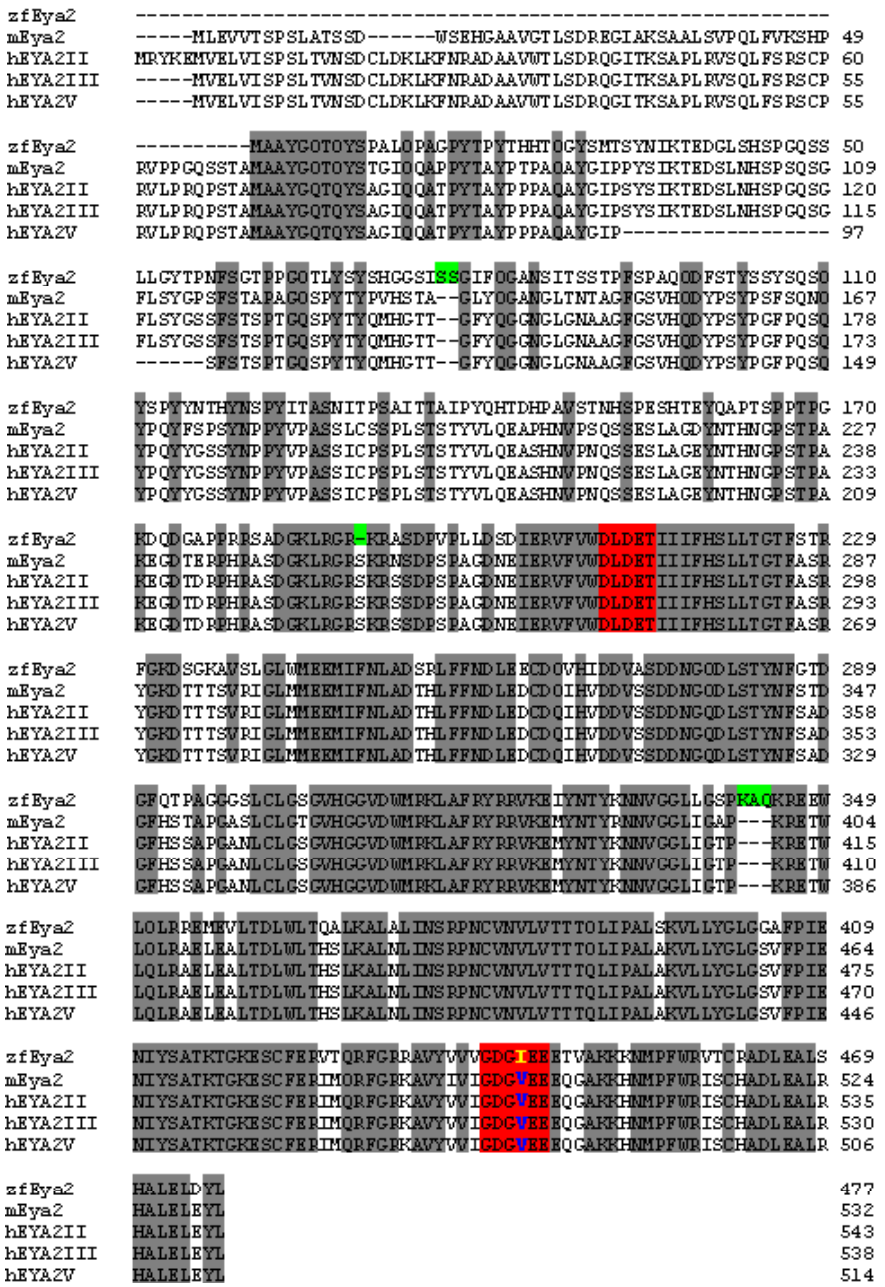

Figure 13 Amino acid sequence comparison of zebrafish, mouse and human Eya2. Alignment of the deduced amino acid sequences for zebrafish eya2 (zfeya2), murine Eya2 (mEya2), and three human EYA2 transcripts (hEya2) generated by using the MegAlign program (DNASTAR) with the Clustal method. Grey shading indicates identical residues, green shading insertions and gaps, and red shading the HAD motifs. Bolt letters in yellow and blue point out residues variation within motif III. (Gene Bank accession numbers: m*Eya2*, NM010165; h*EYA2*II, NM172113; h*EYA2*III, NM172111; h*EYA2*V, NM172110)

```
AGAGGACTTGAATGAAATGGAGAGCTTGGGCGACCTCACCATGGAGCAAAAGCTCATTTC      60
TGAAGAGGACTTGAATTCAAGGCCTCTCTCAACGGCATGGACGAATCACAAGAGGTGCCC     120
                                        M  D  E  S  Q  E  V  P       8
GAGTTACCTACAAAAAAAGCTCGGCATGATCCAGAAGTGAGTCAGGAGGGTGATTCACGT     180
E  L  P  T  K  K  A  R  H  D  P  E  V  S  Q  E  G  D  S  R        28
AGCGTCGTTGCTAATGACAGCAGTGACTCCCCAAACCAGGATGAATCCTCAACACAGTCA     240
S  V  V  A  N  D  S  S  D  S  P  N  Q  D  E  S  S  T  Q  S        48
AACGTCAACTCCTACCCTCCATCCTCTGTCACACACTTGCACTCAATTCCTGGGGCTCCA     300
N  V  N  S  Y  P  P  S  S  V  T  H  L  H  S  I  P  G  A  P        68
GACCAGTCTAATCAAGAGACGATATCAAGATCCCAGGGCTGCGTCACAGAAAATGCATAT     360
D  Q  S  N  Q  E  T  I  S  R  S  Q  G  C  V  T  E  N  A  Y        88
ACTCACAACGCAGTGACATGTAAAGACCTCGCCACAACCACATCAACTGAATATACCTCA     420
T  H  N  A  V  T  C  K  D  L  A  T  T  T  S  T  E  Y  T  S       108
CAGATCTACCAAGGAAGCAACACCGCTGTCACCGCATATGCCAGTCAAGTGGCTTTCCCC     480
Q  I  Y  Q  G  S  N  T  A  V  T  A  Y  A  S  Q  V  A  F  P       128
TCCCTGGGCCAGTCATCAATGTACAGCGCCTTTCCTCAGTCCGGCCAGACATACGGACTG     540
S  L  G  Q  S  S  M  Y  S  A  F  P  Q  S  G  Q  T  Y  G  L       148
CCACCATTTGGCGCCATGTGGCCAGGCTTAAAGACCGAGCTGCCCGAGGCGCCCTCTGTT     600
P  P  F  G  A  M  W  P  G  L  K  T  E  L  P  E  A  P  S  V       168
GGTCAGACGGGATTTCTCAGCTTCAGCTCAGCCTATACCTCAACCCAACCCAACCAGATC     660
G  Q  T  G  F  L  S  F  S  S  A  Y  T  S  T  Q  P  N  Q  I       188
CACTACTCCTACCCCAGCCAAGGTTCCTGTTTTACTACATCCAGTGTGTACACTAACATC     720
H  Y  S  Y  P  S  Q  G  S  C  F  T  T  S  S  V  Y  T  N  I       208
CCCCCATCAACCGCAGTGACCACAGCTGCTGGCACACATCAGGAGTTTACAAGTTACAAC     780
P  P  S  T  A  V  T  T  A  A  G  T  H  Q  E  F  T  S  Y  N       228
TCTGTTGGTCAGAATCAGTTTTCCCAGTACTACGTTCCTCCTCCCAGTTACATGTCTGCT     840
S  V  G  Q  N  Q  F  S  Q  Y  Y  V  P  P  P  S  Y  M  S  A       248
GGGCTGCCTAGCACTGATAGAGATGGAGCAGGGGTGGTGGCACCTGGATATCCTGCCATT     900
G  L  P  S  T  D  R  D  G  A  G  V  V  A  P  G  Y  P  A  I       268
AAGACAGAAGGCAGTGCCTCTGCAAACCTGCCCAACACTACAGATGCTTCCCCAGGTGTG     960
K  T  E  G  S  A  S  A  N  L  P  N  T  T  D  A  S  P  G  V       288
ACGCTCCCAACCGGTGTGGCTCTGCCCGCTGGCATGGCCCTTCCCaACGGAGCACGAGAC    1020
T  L  P  T  G  V  A  L  P  A  G  M  A  L  P  N  G  A  R  D       308
CAAGACGAGCAAAACCGCAAAACCCCTGCTGGCAAAGCTAAAGGCAAAGCCAAAAAATCA    1080
Q  D  E  Q  N  R  K  T  P  A  G  K  A  K  G  K  A  K  K  S       328
GACGGTTCCCAGTCTACAGACAATGACCTTGAGCGTGTCTTCTTGTGGGATCTGGATGAA    1140
D  G  S  Q  S  T  D  N  D  L  E  R  V  F  L  W  D  L  D  E       348
ACCATCATCATTTTCCACTCGCTTCTCACTGGCTCATTTGCACAGAAGTTTGGAAAGGAC    1200
T  I  I  I  F  H  S  L  L  T  G  S  F  A  Q  K  F  G  K  D       368
CCAGCAACAGTTCTCAATTTGGGTCTTCAGATGGAGGAGTTGATCTTTGAGCTTGCAGAC    1260
P  A  T  V  L  N  L  G  L  Q  M  E  E  L  I  F  E  L  A  D       388
ACGCATCTCTTCTTCAATGATCTGGAGGAATGCGATCAAGTCCATGTTGATGATGTTGCC    1320
T  H  L  F  F  N  D  L  E  E  C  D  Q  V  H  V  D  D  V  A       408
TCGGATGACAATGGACAGGATTTGAGCAACTACAACTTCTCCAGCGATGGATTCAGTGGA    1380
S  D  D  N  G  Q  D  L  S  N  Y  N  F  S  S  D  G  F  S  G       428
CCTAGTGCAGGTAGTGGTCCGGGTTCAACTGCAGCGGTACAGGGAGGAGTGGAGTGGATG    1440
P  S  A  G  S  G  P  G  S  T  A  A  V  Q  G  G  V  E  W  M       448
CGGAAACTGGCTTTCAGATATCGCAGACTTAAAGAGATCTACAATGGATACAAAGGGAAC    1500
R  K  L  A  F  R  Y  R  R  L  K  E  I  Y  N  G  Y  K  G  N       468
GTAGGAGGTCTGTTGAGTCCAATGAAGAGAGATCTGCTGCTCAGACTGCGTTCAGAGATC    1560
V  G  G  L  L  S  P  M  K  R  D  L  L  L  R  L  R  S  E  I       488
GAGACAGTCACAGATGCCTGGCTGAGCACCGCTCTCAAATCTCTATTGCTTATTCAGTCA    1620
E  T  V  T  D  A  W  L  S  T  A  L  K  S  L  L  L  I  Q  S       508
AGGGGCAGATGTATGAATGTTTTGGTCACCACCACTCAGTTGGTTCCTGCTTTAGCTAAA    1680
```

```
R  G  R  C  M  N  V  L  V  T  T  T  Q  L  V  P  A  L  A  K        528
GTGCTTCTATATGGCCTGGGTGACGTTTTTCCCATCGAGAACATCTACAGCGCCACTAAA    1740
V  L  L  Y  G  L  G  D  V  F  P  I  E  N  I  Y  S  A  T  K        548
ATAGGAAAAGAGAGCTGTTTTGAACGCATCATCTCTCGCTTTGGGAAGAAAGTAACCTAT    1800
I  G  K  E  S  C  F  E  R  I  I  S  R  F  G  K  K  V  T  Y        568
GTTGTTATAGGCGACGGCCGTGATGAAGAGTTTGCAGCAAAACAGCACAACATGCCATTT    1860
V  V  I  G  D  G  R  D  E  E  F  A  A  K  Q  H  N  M  P  F        588
TGGCGAATCTCTTCTCATGGAGACCTGATTTCTCTACATCAAGCTCTGGA              1920
W  R  I  S  S  H  G  D  L  I  S  L  H  Q  A  L                  604
```

Figure 14 (A) Nucleotide and predicted amino acid sequences of the zebrafish *eya3* gene encoding EST, translated from the furthermost upstream in-frame methionine (M). The conserved *eya* homology region (eyaHR) is indicated in bold. Bold letters in red indicate HAD motif I and III characteristic for a subgroup of protein tyrosine phosphatases superfamily [TOOTLE, 2003]. The eya homology domain 2 (ED2) is indicated in bold and blue.

Table 2 N-terminal insertions in the *eya3* sequence: nucleotide position within the cDNA, length in base pairs (bp) and predicted amino acids (aa).

Nucleotid	bp	aa
166	9	24-26
247	3	51
291	36	66-67
337	15	81-85
418	30	108-117
550	72	152-175
645	51	184-200
724	9	210-212
814	3	240
959	3	285
972	21	293-299
1075	3	327

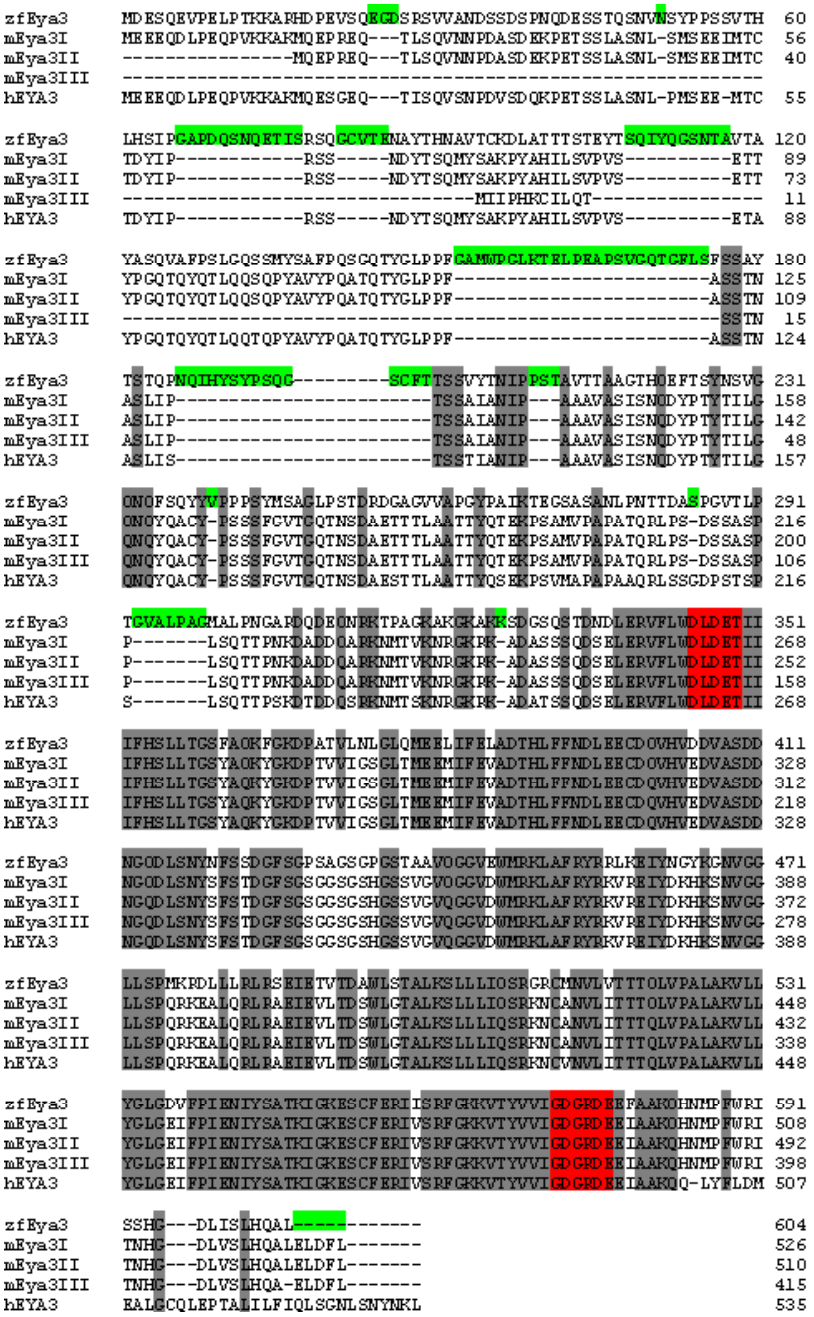

Figure 15 Amino acid sequence comparison of zebrafish, mouse and human Eya3. Alignment of the deduced amino acid sequences for zebrafish eya3 (zfeya3), three murine Eya3 transcripts (mEya3), and human EYA3 (hEya3) generated by using the MegAlign program (DNASTAR) with the Clustal method. Grey shading indicates identical residues, green shading insertions and gaps, and red shading the HAD motifs. (Gene Bank accession numbers: m*Eya3*I, NM0210071; m*Eya3*II, NM010166; m*Eya3*III, NM211357; h*EYA3*, NM001990)

```
TATTAGCTGGAGCTCCACCGCGGTGGCGGCCGCTCTAGAACTAGTGGATCCCCCGGGCTG      60
CAGGAATTCGGCACGAGGTGTGCTCACGTTAACTTCAGGATCAGCAGTTAAAGCGGAAAA     120
CACGGCTAGTGCAAGACCGCGCTCCTCGGAGTTTGGCTATAGTGCGGATCTGTTGGTTGG     180
AGCGTTCCGCTCCGGTGCGGCCAGTGCAGCTCTCATGAACTTAGGGAGGACTTCACTGAC     240
AGCGCGTGCACTGACTGGCGCGAGCTGTTCCTCGCGCTTCACGCAGCTAGACCACTTGAA     300
TATTTTTGGATGAGCATGTCAACACAGTGAAAGGGAACGGACCTTCTGGAGAGTTTGAAA     360
ATCGTTGCAACGCACAACTCATAAGAGTGTCTGGACTGTAGCTTTGTGGAGTGGAAATTC     420
AACTGATGGAGAATACACAGGATCTGAATGAACAGAGCGTGAAGAAATCCACCACTGATT     480
     M  E  N  T  Q  D  L  N  E  Q  S  V  K  K  S  T  T  D  S      19
CTCATGCTCCAGACCCAGTAGACAACAGGGCTTTGGAGATGCAGGAACTTACAGATGTCC     550
  H  A  P  D  P  V  D  N  R  A  L  E  M  Q  E  L  T  D  V  Q      39
AGCACTCTGTTAACAGTGGCAGTGACGGCACTTCCAAACTGGACAAAAACATCCTCAGCA     600
  H  S  V  N  S  G  S  D  G  T  S  K  L  D  K  N  I  L  S  N      59
ACAACATCACGACCAATGGAACCGGAGTTAAGTCTGAGCCTCTGAACAGCAGTGAAGCCG     660
  N  I  T  T  N  G  T  G  V  K  S  E  P  L  N  S  S  E  A  V      79
TGAGTTCAGCAGGAGACTCTGGGCTGGACACTTACACTGGGTCAGTCATAAGCAGCAGTG     720
  S  S  A  G  D  S  G  L  D  T  Y  T  G  S  V  I  S  S  S  G      99
GATTCAGTCCCCGGCCGGCACACCAGTATTCACCTCCTCTCTACCCTTCAAAGCCTTACC     780
  F  S  P  R  P  A  H  Q  Y  S  P  P  L  Y  P  S  K  P  Y  P     119
CTCACATCCTCACTACCCCTGTGGCTCCGCCCATGTCAGCCTACACAGGCCAATCACAGT     840
  H  I  L  T  T  P  V  A  P  P  M  S  A  Y  T  G  Q  S  Q  F     139
TCAGCAGCATGCAGCAGTCAACAGTTTACACGCCCTATTCGCAAACGACTCCACCCTACG     900
  S  S  M  Q  Q  S  T  V  Y  T  P  Y  S  Q  T  T  P  P  Y  G     159
GCCTCTCCACCTATGATTTGGGGGTGATGTTGCCAGGGATAAAGACAGAAGGAGGGCTTA     960
  L  S  T  Y  D  L  G  V  M  L  P  G  I  K  T  E  G  G  L  T     179
CACAGACCCAATCAACCCTGCAGTCAGGGCTCAGCTACAGTCCTGGATTTACCACCCCTC    1020
  Q  T  Q  S  T  L  Q  S  G  L  S  Y  S  P  G  F  T  T  P  Q     199
AGCCCGGACAGACAGCCTACTCACCCTATCAGATGCCAGCAGGTTCAGGTTTTACAACCT    1080
  P  G  Q  T  A  Y  S  P  Y  Q  M  P  A  G  S  G  F  T  T  S     219
CTCCTGGTCTCTACACTTCCAACAACTCCAACCCAGGAAATTTCACCACACAACAGCAGG    1140
  P  G  L  Y  T  S  N  N  S  N  P  G  N  F  T  T  Q  Q  Q  E     239
AATATCCCTCTTACACAACTTTTGGGCAGAATCAGTATGCTCAGTATTACTCAACCTCCT    1200
  Y  P  S  Y  T  T  F  G  Q  N  Q  Y  A  Q  Y  Y  S  T  S  S     259
CCTACGGCTCCTATATGACATCTAACAGCTCATTGGATGGCACAGGTTCAGTCTCCACCT    1260
  Y  G  S  Y  M  T  S  N  S  S  L  D  G  T  G  S  V  S  T  Y     279
ATCAGCTGCAGGACCCCATCATGACAGGGCAAGCAGCTGACCTGAATCCAGGTGAGTTTG    1320
  Q  L  Q  D  P  I  M  T  G  Q  A  A  D  L  N  P  G  E  F  E     299
AGGCGGGGCAGAGTCCATCTACACCCATCAAGGAGATGGAGGACCGGGCCTGCAGAGGGG    1380
  A  G  Q  S  P  S  T  P  I  K  E  M  E  D  R  A  C  R  G  G     319
GTGGGGCTAAAGCAAGAGGGCGGGGCAGAAAGAACAACCCCTCCCCACCACCTGACAGTG    1440
  G  A  K  A  R  G  R  G  R  K  N  N  P  S  P  P  P  D  S  D     339
ACCTTGAGAGGGTGTTTGTTTGGGATCTGGATGAGACGATCATTGTGTTTCACTCACTCC    1500
  L  E  R  V  F  V  W  D  L  D  E  T  I  I  V  F  H  S  L  L     359
TCACTGGCTCCTATGCACAGAAGTATGGCAAGGACCCTCCGTTGGCTGTAACTCTTGGGT    1560
  T  G  S  Y  A  Q  K  Y  G  K  D  P  P  L  A  V  T  L  G  L     379
TAAGGATGGAGGAGATGATCTTCAATCTTGCAGACACACATCTTTTTTTCAATGACTTAG    1620
  R  M  E  E  M  I  F  N  L  A  D  T  H  L  F  F  N  D  L  E     399
```

```
AGGAGTGCGACCAGGTGCACATCGATGACGCTTCTTCCGATGATAACGGACAAGACCTCG    1680
  E  C  D  Q  V  H  I  D  D  A  S  S  D  D  N  G  Q  D  L  G     419
GTACTTACAGTTTTGCCACTGATGGCTTCCATGCAGCTGCAACAAGCGCTAGCCTCTGCC    1740
  T  Y  S  F  A  T  D  G  F  H  A  A  A  T  S  A  S  L  C  L     439
TCGCCACAGGTGTTCGTGGTGGAGTCGACTGGATGAGGAAACTAGCCTTCAGATACAGAC    1800
  A  T  G  V  R  G  G  V  D  W  M  R  K  L  A  F  R  Y  R  R     459
GAGTCAAGGAGTTGTACTGCACCTACAAAAACAACGTGGGAGGGTTGCTTGGTCCGGCTA    1860
  V  K  E  L  Y  C  T  Y  K  N  N  V  G  G  L  L  G  P  A  K     479
AGAGAGAGGCGTGGCTTCAGCTCAGGGCAGAGGTTGAGGCACTCACGGACTCATGGTTGA    1920
  R  E  A  W  L  Q  L  R  A  E  V  E  A  L  T  D  S  W  L  T     499
CCAGTGCGCTCAAGTCCCTGTCAATCATCAGCTCCAGGAGTAACTGTGTTAATGTGTTGG    1980
  S  A  L  K  S  L  S  I  I  S  S  R  S  N  C  V  N  V  L  V     519
TGACAACGACACAATTAATACCTGCTCTTGCTAAGGTGCTGTTGTACAGCCTGGGCTCTG    2040
  T  T  T  Q  L  I  P  A  L  A  K  V  L  L  Y  S  L  G  S  A     539
CGTTTCCCATTGAAAACATTTACAGCGCAACCAAAATAGGTAAAGAGAGCTGTTTTGAGC    2100
  F  P  I  E  N  I  Y  S  A  T  K  I  G  K  E  S  C  F  E  R     559
GTATAGTATCCAGGTTTGGCACTAACATAACGTATGTTGTGATTGGTGATGGGCGCGATG    2160
  I  V  S  R  F  G  T  N  I  T  Y  V  V  I  G  D  G  R  D  E     579
AGGAAAATGCAGCCAGCCAGCACAACATGCCCTTCTGGCGAATATCCAGCCACTCTGACC    2220
  E  N  A  A  S  Q  H  N  M  P  F  W  R  I  S  S  H  S  D  L     599
TGCTTGCCCTTCATCAAGCACTGGAGTTCGAGTACCTGTAACACTCGACACCTGTATAAT    2280
  L  A  L  H  Q  A  L  E  F  E  Y  L  *                         611
AGGCCTTTTTTGTACAACTATTTAAGAACAAGAGTACACTGCGATCTCTTTTTATGTTGT    2340
TGTTGTTGTCGTCGTCTCTTTGATTATTTTAAAGAAATCTCTGGCTTTTACGATAACTCT    2400
GCACTGTCTTAAGAAGACTAGGACAGACTAGGAAGTGGAGAAAATGGGATTATTATGCTG    2460
AAACCAGGCTTGTAAAGAGCTAACTAAGGTCTTACGTCACACACACTGCATTTCACGTCT    2520
GAAGGAGGTGAGTTCTTGGGTCTTGAAAACTGCATATATCCTCACCCTCATCTACAGGAA    2580
CATTATTCTCTGTCTATATTGTAGACTTCATCTCCTCTTAAACAACTCGAACGCTGTACT    2640
CTAAACCCGGAGCATTTAGAGTAGACATAACAACTCATGTAAATTATTTTACAGGTACTG    2700
GATTAAACACTAAAGAACGCTGTGTGGTTTCACCATGGTATCGTTTTGATTTTTCCTGTT    2760
TTTTTTTGTTTTTTTTTTGTAAGTTTTTGGCAAAAAAAGGAAGTCTGTGTATAATTTGTT    2820
GTGCCTTATAAGATGTTTTGTGTGTCAGTTTTTATTTTGAGAATGTATGTAGATAAAAAT    2880
ATGTAAACATTAAAA                                                 2895
```

Figure 16 (A) Nucleotide and predicted amino acid sequences of the zebrafish *eya4* gene encoding EST, translated from the furthermost upstream in-frame methionine (M). The conserved *eya* homology region (eyaHR) is indicated in bold. An asterisk indicates the stop codon terminating the open reading frame.Bold letters in red indicate HAD motif I and III characteristic for a subgroup of protein tyrosine phosphatases superfamily [TOOTLE, 2003]. The eya homology domain 2 (ED2) is indicated in bold and blue.

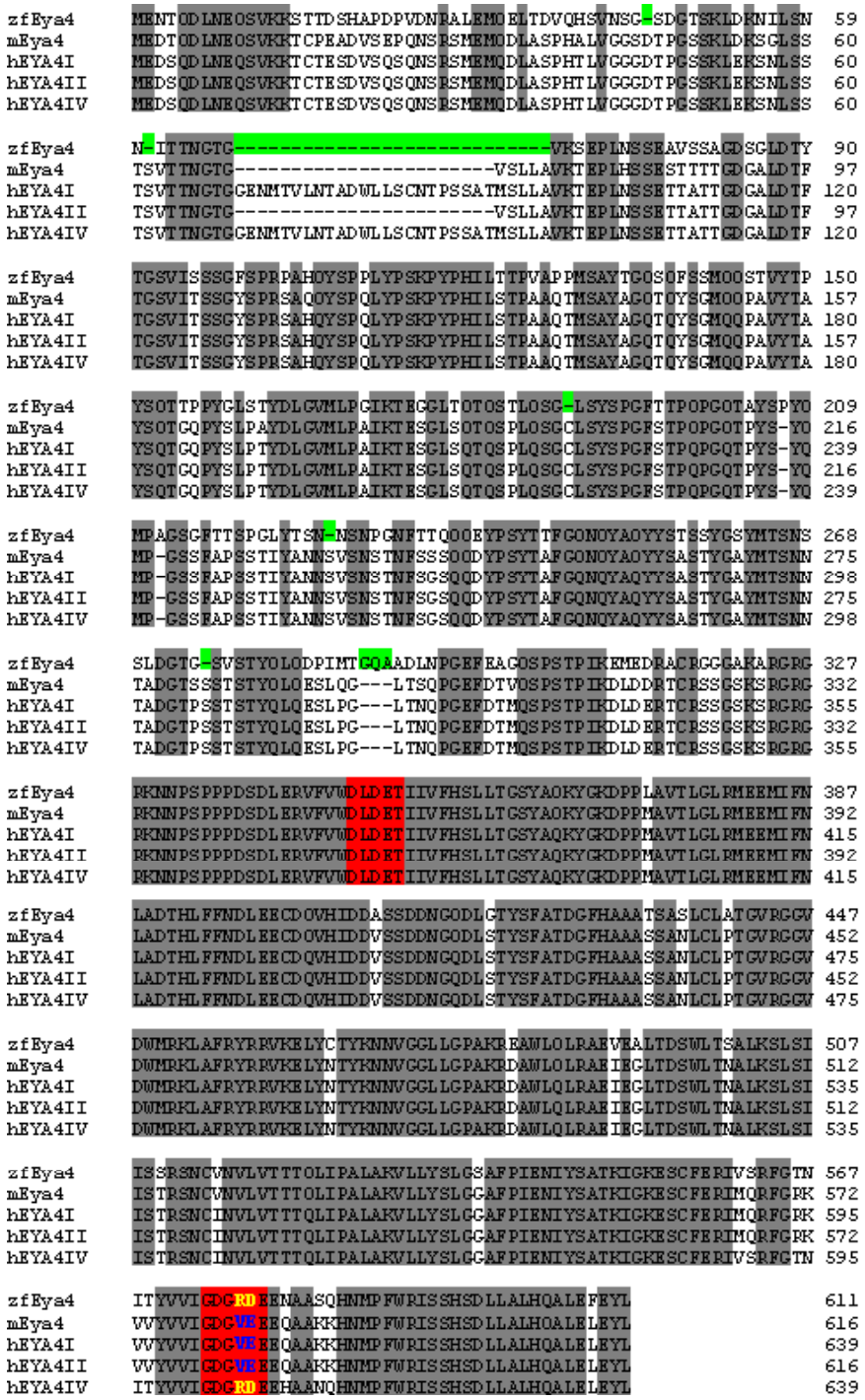

Figure 17 Amino acid sequence comparison of zebrafish, mouse and human Eya4. Alignment of the deduced amino acid sequences for zebrafish eya4 (zfeya4), murine Eya4 (mEya4), and three human EYA4 transcripts (hEya4) generated by using the MegAlign program (DNASTAR) with the Clustal method. Grey shading indicates identical residues, green shading insertions and gaps, and red shading the HAD motifs. Bolt letters in yellow and blue point out residues variation within motif III (Gene Bank accession numbers: m*Eya4*, NM010167; h*EYA4*I, NM004100; hEYA4II; NM172103; hEYA4IV, NM172105).

Table 3 Percentages of amino acid identity and similarity* of zebrafish (zf), murine (m), and human (h) Eya proteins. Highest identity/similarity between the zebrafish gene and the mammalian homologs are marked in bold. (Gene Bank accession numbers: z*feya1*, NM131193; m*Eya1*, NM010164; h*EYA1*I, NM172060; hEYA1II, NM172058; hEYA1IV, m*Eya2*, NM010165; h*EYA2*II, NM172113; h*EYA2*III, NM172111; h*EYA2*V, NM172110; m*Eya3*II NM0210071; m*Eya3*II, NM010165; m*Eya3*III, NM211357; h*EYA3*, NM001990) m*Eya4*, NM010167; h*EYA4*I, NM004100; hEYA4II; NM172103; hEYA4IV, NM172105).

	zfeya2		***zfeya3***		***zfeya4***	
zfeya1	73%	60%*	63%	47%*	75%	63%*
mEya1	73%	60%*	60%	46%*	74%	64%*
mEya2	**78%**	**64%***	60%	48%*	68%	57%*
mEya3	59%	48%*	**63%**	**48%***	62%	47%*
mEya4	76%	64%*	63%	45%*	**83%**	**74%***
hEya1	70%	58%*	69%	54%*	77%	66%*
hEya2	**72%**	**62%***	64%	50%*	69%	56%*
hEya3	72%	58%*	**72%**	**58%***	62%	47%*
hEya4	69%	57%*	62%	45%*	**82%**	**73%***

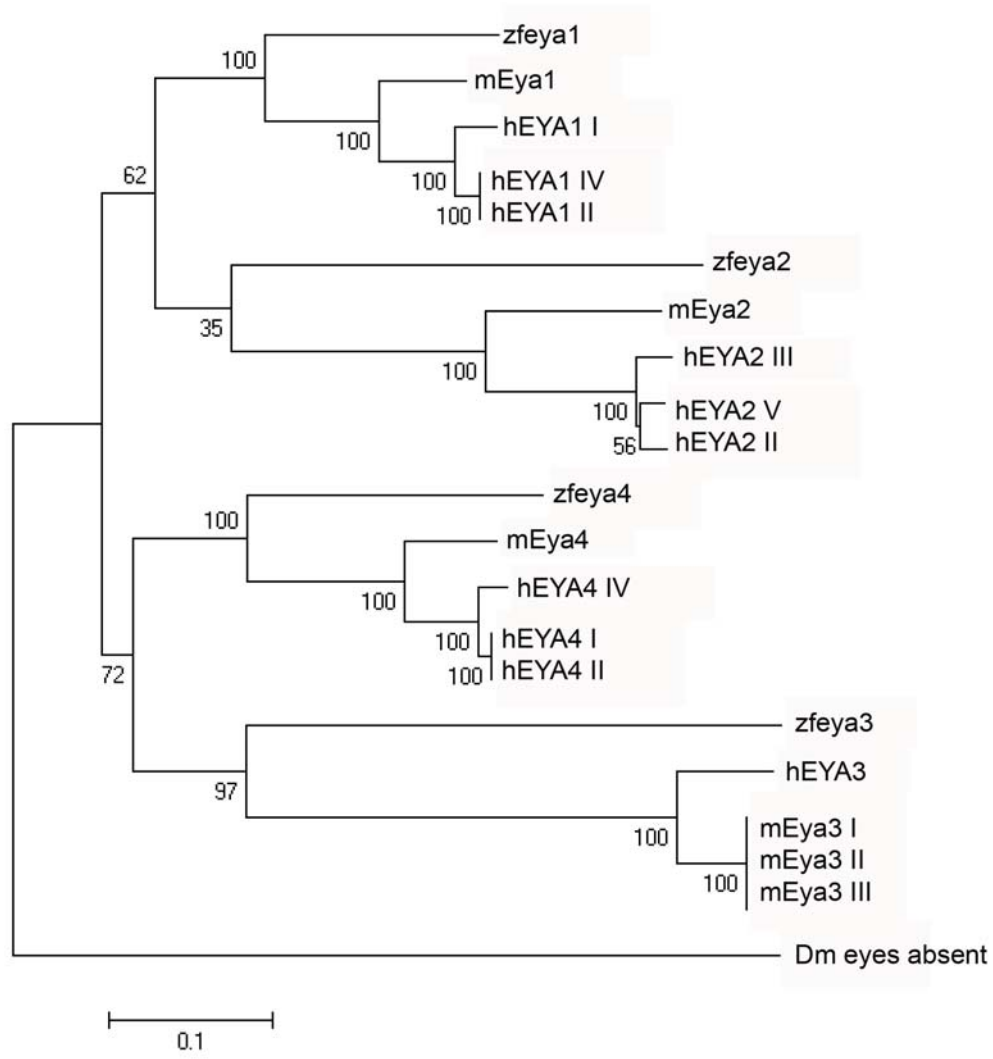

Figure 18 Phylogenetic analysis. Comparison of zebrafish and mammalian deduced Eya protein sequences: Phylogram of the Eya protein family. The amino acid sequences of the Eya proteins shown in Fig. 13, 15, 17 and of the *Drosophila* eyes absent protein (Dmeya) were used to construct a phylogenetic tree by the neighbour-joining algorithm. The *Drosophila* sequence served as outgroup. (Gene Bank accession numbers: z*feya1*, NM131193; m*Eya1*, NM010164; h*EYA1*I, NM172060; hEYA1II, NM172058; hEYA1IV, NM172059; m*Eya2*, NM010165; h*EYA2*II, NM172113; h*EYA2*III, NM172111; h*EYA2*V, NM172110; m*Eya3*II NM0210071; m*Eya3*II, NM010166; m*Eya3*III, NM211357; h*EYA3*, NM001990; m*Eya4*, NM010167; h*EYA4*I, NM004100; hEYA4II; NM172103; hEYA4IV, 172105; Dm, AC008043).

3.2 Expression pattern analysis of three *eya* genes in the zebrafish

To investigate the expression patterns of the newly identified *eya* genes during embryonic and early larval zebrafish development, whole-mount *in situ* hybridisation experiments were performed. In addition to the standard technique using non-fluorescent staining such as BM-purple or NBT/BCIP, *in situ* hybridisations were carried out using the TSA Alexa488 fluorescent amplification. This technique has been used successfully in sections earlier but only recently first results could be obtaind in zebrafish whole mount *in situ* hybridisations [CLAY & RAMAKRISHNAN, 2005]. In this work the TSA methode were used, because it affords a higher resolution of expression sites, although it is more difficult to detect signals of low-level expressed genes, as *eya2*, *eya3* and *eya4*. Nevertheless fluorescent *in situ* signals were successfully detected with the TSA Alexa488 amplification in 24 hpf embryos, hybridised with labelled *eya2* and *eya4* antisense riboprobes.

Using *in situ* hybridisation allows to obtain detailed information on the timing and localisation of the transcribed mRNA in the embryo. Embryos at the stages from 12 hpf to 72 hpf were hybridised with labelled *eya2* and *eya4* antisense riboprobes. Both genes are widely expressed in distinct but overlapping patterns and show significant similarity to mammalian *Eya2* and *Eya4* expression. Because *eya3* antisense riboprobes repeatedly did not yield any distinct *in situ* labellings, description of expression patterns is restricted to *eya2* and *eya4*.

3.2.1 Temporal patterns of *eya2* expression during sensory organ development

Shortly after the tail bud stage, at 12 hpf, *eya2* expression is detected in the developing otic epithelium in two cell clusters at opposite ends of the forming otic placode, in the region of the developing olfactory placode, as well as in a preotic (anterior) and postotic (posterior) placodal domain, the prospective anterior and posterior lateral line placodes. (Fig. 19A,B). In the course of development, expression in the olfactory placode becomes increasingly confined to its periphery. Additionally to the anterior placodal expression, *eya2* also becomes visible in the anterior lateral line ganglion and migrating primordium of the posterior lateral line at the end of the first day of development (Fig. 19C,D).

By 24 hpf, *eya2* is expressed in the ventral edge of the otic epithelium (Fig. 20A,C), where the maculae are formed. *Eya2* positive cells can be identified in delaminating neuronal precursor cells passing from the otic vesicle to the forming statoacoustic ganglion (Fig. 20C). However, there is no *eya2* expression detectable in the ganglion itself at any stage of development (Fig. 20C-E). At this time *eya2* expression in sensory structures is very similar to the zebrafish *eya1* expression, except for the otic vesicle, where *eya1* positive cells are more widespread throughout the ventral domain of the vesicle. Furthermore, contrary to *eya2*, the nascent statoacoustic ganglion expresses *eya1* [SAHLY, 1999].

At 48 hpf, *eya2* is merely detectable in the dorsal and ventral edges of the posterior macula (Fig. 20D) and can not be detected anymore at 60 hpf (Fig. 20F,G). At the same stage, *eya2* is no longer expressed in the lateral line sensory ganglia. However, cells in the olfactory placode are still expressing *eya2* in the apical surface, in which the olfactory receptors and sensory neurons exist (Fig. 19G; 20B) [WHITLOCK & WESTERFIELD, 1998]. These cells remain *eya2* positive at least until 72 hpf.

In addition, *eya2* becomes expressed in the anterior and posterior neuromasts of the lateral line system at 30 to 36 hpf and continues until at least 72 hpf (Fig. 19E-I). Expression can be observed in both the primary and secondary neuromasts.

There is no e*ya2* expression in non-neural tissues like the mesodermal somites, which are a prominent expression site of *eya1* [SAHLY, 1999]. One exception is the pectoral fin, which is a derivate of the paraxial mesoderm. Here *eya2* becomes expressed at around 36 hpf. This expression continues until at least 48 hpf, but can no longer be distinguished at 60 hpf (Fig. 19E-G).

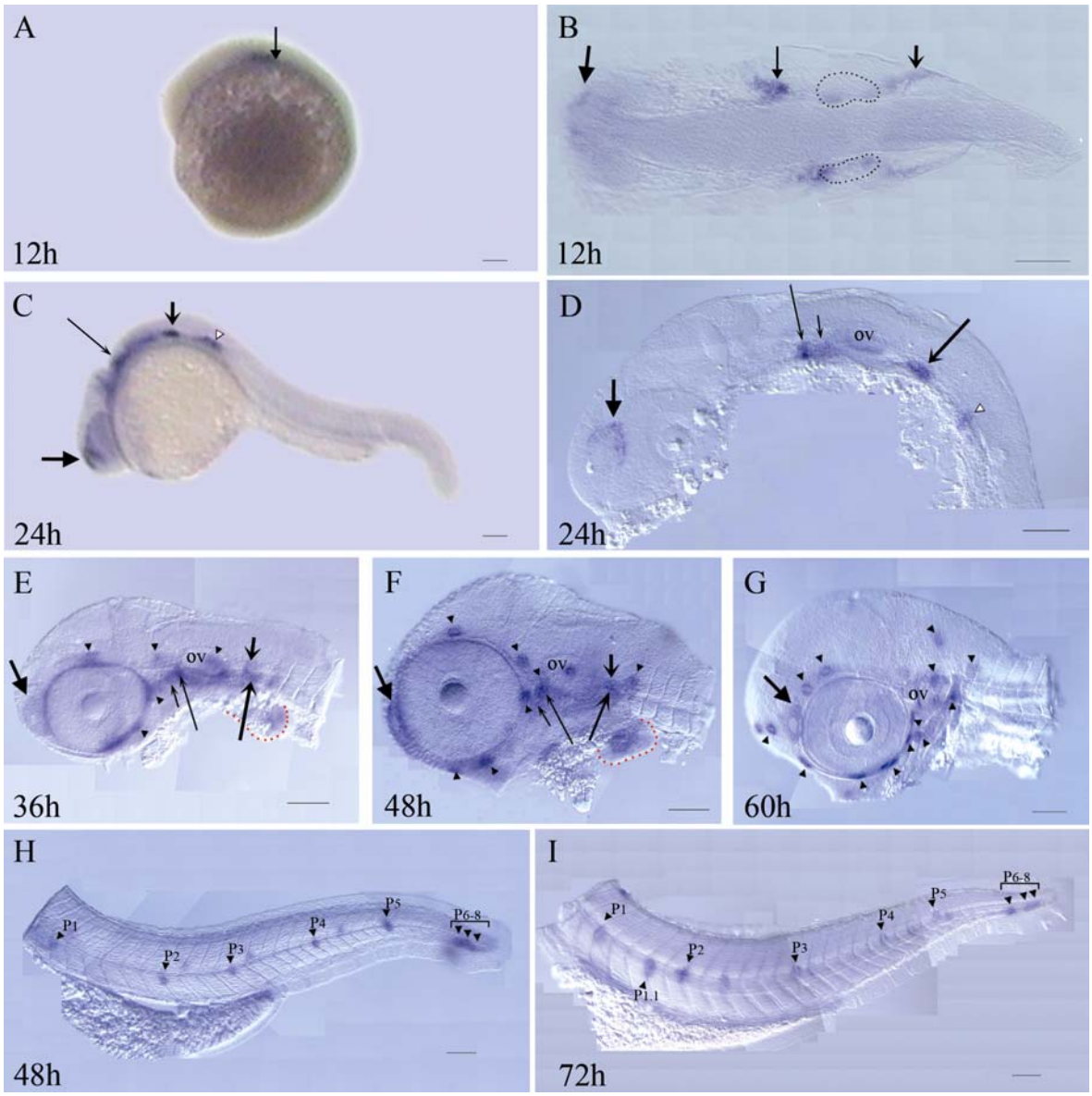

Figure 19 Expression pattern of *eya2* during the first 3 days of development. Whole mounted (A, C) and dissected (B, D-I) embryos hybridised *in situ* with *eya2* antisense riboprobe are shown in lateral views with anterior to the left and dorsal to the top (A, C-I), B shows a dorsal view with anterior left. The stages are indicated in hours post fertilization (h) on each panel. *Short arrows* indicate the various placodal regions, with *closed arrowheads* denoting trigeminal placodes, *thin open arrowheads* pointing to the anterior lateral line placodes and *thick open arrowheads* indicating posterior lateral line placodes. Longer arrows of the respective version indicate the cranial ganglia deriving from these placodes. The otic placode is outlined with a *black dotted line* (B). *Short thick arrows with closed arrowheads* indicate olfactory placodes. *Black arrowheads* point to lateral line neuromasts, $P_{(1-8)}$, primary neuromasts; $P_{1.1}$, first secondary neuromast; *white arrowheads* to lateral line primordia. The pectoral fin bud is outlined with a *red dotted line* (E, F); ov, otic vesicle. Scale bar, 100µm.

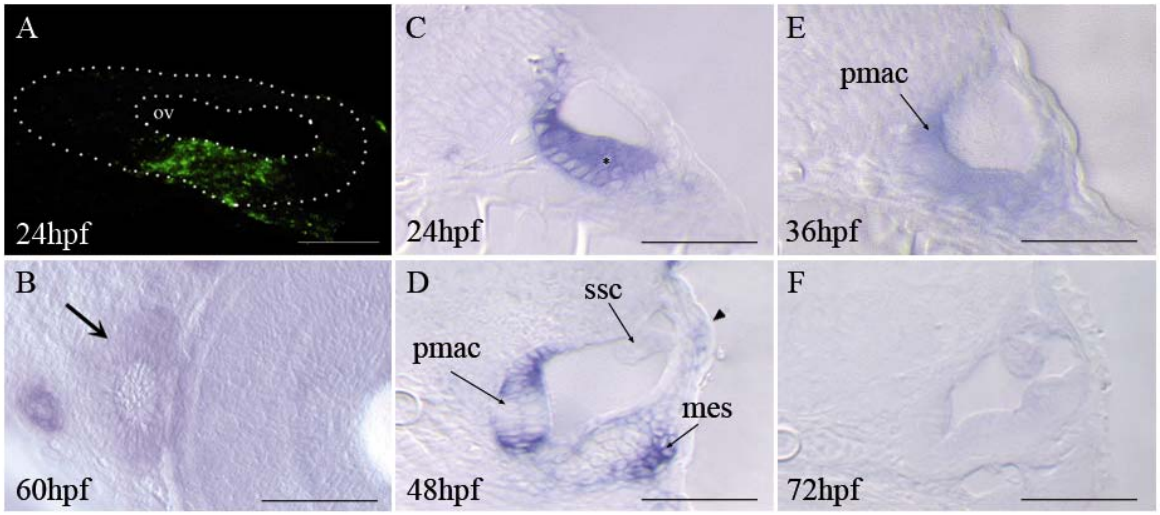

Figure 20 *eya2* expression in the developing otic vesicle. Shown are (A) Whole mounted embryo (anterior to the left, dorsal to the top), (B) dissected (anterior to the left, dorsal to the top) and (C-F) cross-sectional (dorsal to the top) views of *eya2* antisense riboprobe *in situ* hybridised embryos. The stages are indicated in hours post fertilization (hpf) on each panel. ov, otic vesicle; mes, mesenchym, pmac, posterior macula; ssc, semicircular canal primordium; * delaminating cell; arrow, pheripheric expression in the olfactory epithelium; arrowhead, neuromast. Scale bar, (A, B) 100µm; (C-F) 25µm.

3.2.2 Temporal patterns of *eya4* expression during sensory organ development

Eya4 expression is first seen in tail bud embryos at 12 hpf. Like *eya2*, it becomes visible in two cell clusters at opposite ends of the forming otic placode (Fig. 21A,B). Shortly afterwards *eya4* expression is observed in the primordium of the posterior lateral line as well as in the otic vesicle, particularly in the anteroventral domain (Fig. 21C,D; Fig. 22A,C).

By 24 hpf the expression of *eya4* is restricted to the differentiated anterior and posterior lateral line ganglion as well as the statoacoustic ganglion, excluding the respective placodes. This expression continues until at least 60 hpf (Fig. 21C-G), whereas the statoacustic ganglion is a major expression site of this transcription factor (Fig. 22D; Fig. 25H).

In addition *eya4* is abundant expressed in the inner ear. By 24 hpf *eya4* transcripts can solely be detected in the ventral part of the otic epithelium, notably strong in the anterior region (Fig. 22A,C-E), where the anterior macula is formed. Shortly afterwards, around 36 hpf, *eya4* expression becomes visible in the haircells of the anterior macula (Fig. 22E). At 48 hpf, *eya4* is, in addition to the anterior macula, also expressed in the semicircular canal primordia (Fig. 22D). By 60 hpf expression is found in four sensory patches of the inner ear, the anterior macula and three cristea, as well as in the semicircular canals (Fig, 21G; 22F) where it lasts until at least 72 hpf (Fig. 22B). *Eya4* expression in the neuromasts of the anterior and posterior lateral line system starts around 30 to 36 hpf, and becomes particularly intense by 48 hpf (Fig. 21F,H). This expression continues at least until 72 hpf (Fig. 21G,I). Expression can be observed in both, the primary and secondary neuromasts. In the non-neural tissues, *eya4* is first observed in the somites at 20 hpf and persists until around 27 hpf (Fig. 21C). In this respect, contrary to *eya2*, *eya4* resembles the zebrafish *eya1* gene, which is reported to be expressed in the somites during early development until around 26-28 hpf [SAHLY, 1999]. The period of *eya4* expression in the pectoral fin seems to be limited to a time window ranges from 48 hpf until

approximately 60 (Fig. 21G). As a result of preparation processing, the pectoral fin often is missing in flatmounts, therefore earlier expression of *eya4* in the pectoral fin could not be detected. However observations in the whole-mount may assume that a week expression of *eya4* in the pectoral fin already becomes visible at 36 hpf.

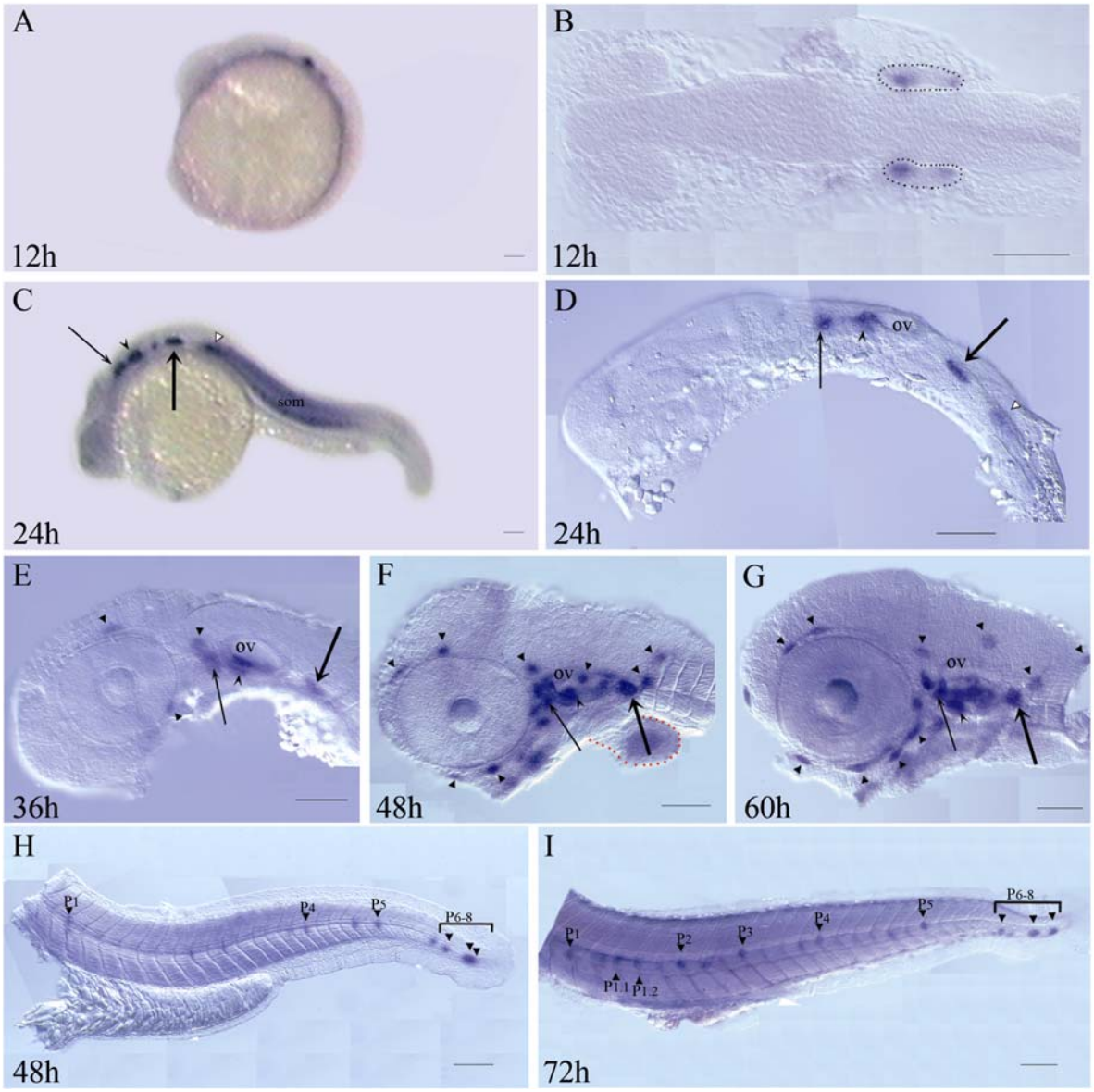

Figure 21 Expression pattern of *eya4* during the first 3 days of development. (A, C) Whole mounted and (B, D-I) dissected embryos hybridised *in situ* with *eya4* antisense riboprobe are shown in lateral views with anterior to the left and dorsal to the top (A, C-I), B shows a dorsal view with anterior left. The stages are indicated in hours post fertilization (h) on each panel. *Short arrows* indicate the various placodal regions, with *closed arrowheads* denoting trigeminal placodes, *thin open arrowheads* pointing to the anterior lateral line placodes and *thick open arrowheads* indicating posterior lateral line placodes. Longer arrows of the respective version indicate the cranial ganglia deriving from these placodes. The otic placode is outlined with a *black dotted line* (B), the statoacoustic ganglia are indicated by an *open arrowhead*. *Short thick arrows with closed arrowheads* indicate olfactory placodes. *Black arrowheads* point to lateral line neuromasts, $P_{(1-8),}$ primary neuromasts; $P_{1.1}$, first secondary neuromast; *white arrowheads* to lateral line primordia. The pectoral fin bud is outlined with a *red dotted line* (F); ov, otic vesicle. Scale bar, 100µm.

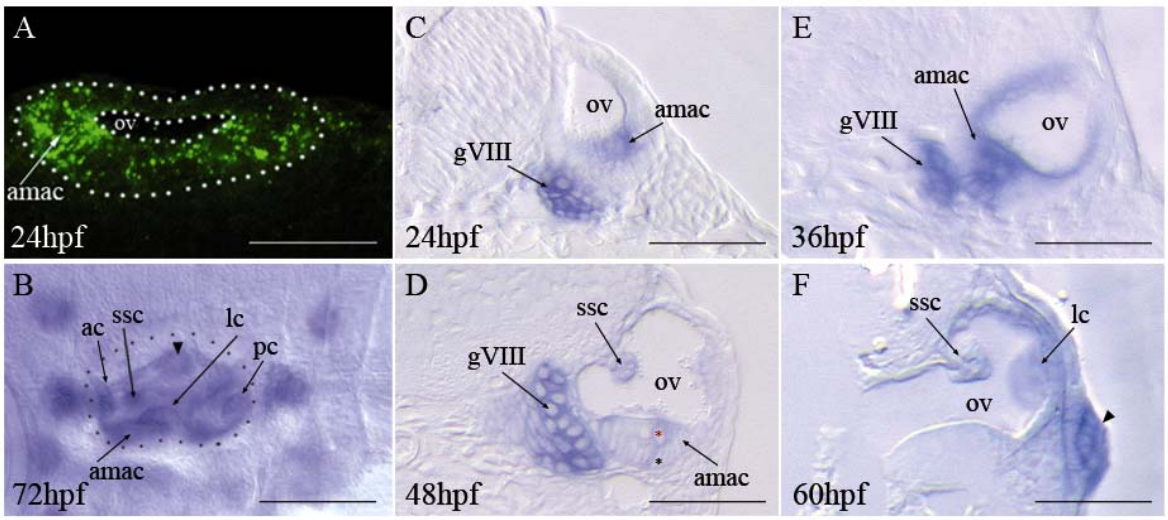

Figure 22 *eya4* expression in the developing otic vesicle. Shown are (A) Whole mounted embryo (anterior to the left, dorsal to the top), (B) dissected (anterior to the left, dorsal to the top) and (C-F) cross-sectional (dorsal to the top) views of *eya4* antisense riboprobe *in situ* hybridised embryos. The stages are indicated in hours post fertilization (h) on each panel. ac, anterior crista; amac, anterior macula; gVIII, statoacoustic ganglion; lc, lateral crista; ov, otic vesicle; pc, posterior crista; ssc, semicircular canal; * hair cells; * supporting cells; arrowheads, neuromast. Scale bar, (A, B) 100µm; (C-F) 25µm.

3.2.3 Expression of *eya2* and *eya4* in ectodermal placodes and cranial ganglia

During the period of segmentation, three distinct placodally derived sensory ganglia are formed in the preotic region: the ganglia of the trigeminal nerve, the anterior lateral line, and the vestibuloacoustic nerve. The sensory neurons in these ganglia express the HNK-1 antigen, which is detected by the zn12 antibody, starting at 14 hpf in trigeminal sensory neurons [METCALFE, 1990; TERVARROW, 1990]. At 12 hpf, *eya2* expression is found next to the neural keel, extending around the posterior end of the mid-hindbrain boundary to the anterior margin of rhombomere 3, which is consistent with the expression site of the trigeminal placode. Previous studies reported, about *eya2* homologues in mouse and chicken, which are expressed in the trigeminal placode/ganglion [DUNCAN, 1997; XU, 1997; MISHIMA, 1998], indeed no trigeminal *eya* expression could be detected in the zebrafish so far. To make sure that the observed expression of *eya2* actually marks the area of the trigeminal placode, triple *in situ* hybridisations were undertaken, using the gene markers *pax2.1* and *krox20* in addition to *eya2*. The paired-box containing *pax2.1* gene encodes a putative transcription factor, which is among others expressed in the mid-hindbrain boundary during embryonic development [KRAUSS, 1991]. *Krox20* encodes a zinc finger protein transcription factor, whose expression is restricted to rhombomere 3 and 5 [SCHNEIDER-MAUNOURY, 1993; SEITANIDOU, 1997; WILKINSON, 1998]. With *eya2/pax2.1/krox20* hybridised embryos have shown that *eya2* expression ranges from the *pax2.1* labelled mid-hindbrain boundary to the *krox20* labelled rhombomere 3 (Fig. 23A,C,E), consistent with the trigeminal expression site. In order to distinguish between expression in placodes and in the respective ganglia, cross-sections of *in situ* hybridised and immunolabeled embryos were performed (Fig. 23B,D,F). In cross-section, this expression domain does not show the typical appearance of a placode as a cell-layer of thickened epithelial cells. Instead, the expression extends over several cell diameters at 12 hpf (23C; 24C). By 14 hpf, the first zn12 positive trigeminal neurons are found at a position, which

appears to have expressed *eya2* at 12 hpf. However, these immunolabeled sensory neurons do no longer express *eya2*. Instead, *eya2* mRNA can be clearly detected in an overlying region of embryonic ectoderm, the presumed trigeminal placode. While the size of the trigeminal ganglion increases during the next hours of development, at around 17/18 hpf *eya2* expression in the trigeminal placode decreases gradually (Fig. 23E; 24E). At the stage of 14 hpf, a second placodal domain expressing *eya2* arises from the anterior margin of the otic placode (Fig. 23C; 24C), extending anteriorly, overlying the posterior part of the nascent trigeminal ganglion by 17 hpf (Fig. 23F; Fig. 24E). This placode gives rise to sensory neurons, which are first recognized by zn12 immunolabeling around 18 hpf [METCALFE, 1990], and neuromasts of the anterior lateral line (Fig. 25E,F). In contrast to *eya2*, *eya4* expression could not be detected in trigeminal placodes or ganglia between 12 hpf and 17 hpf (Fig. 24B,D,F).

At 24 hpf, *eya2* expression is absent from the trigeminal ganglion and the overlying ectoderm (Fig. 25A,C). In contrast to *eya2*, *eya4* expression can be detected in a subset of statoacoustic sensory neurons (Fig. 25G,H). At the level of the anterior lateral line ganglion, strong expression of both genes can be found in the overlying neuromasts of lateral line. However in the ganglion itself expression of both genes differs, while *eya4* is strongly expressed in the ganglion, in comparison *eya2* expression greatly apperes weaker (Fig. 25A,B,E,F) In the postotic region, *eya2* and *eya4* transcripts can be detected in the posterior lateral line ganglion but are absent from the overlying ectoderm (Fig. 25A,B,I,J).

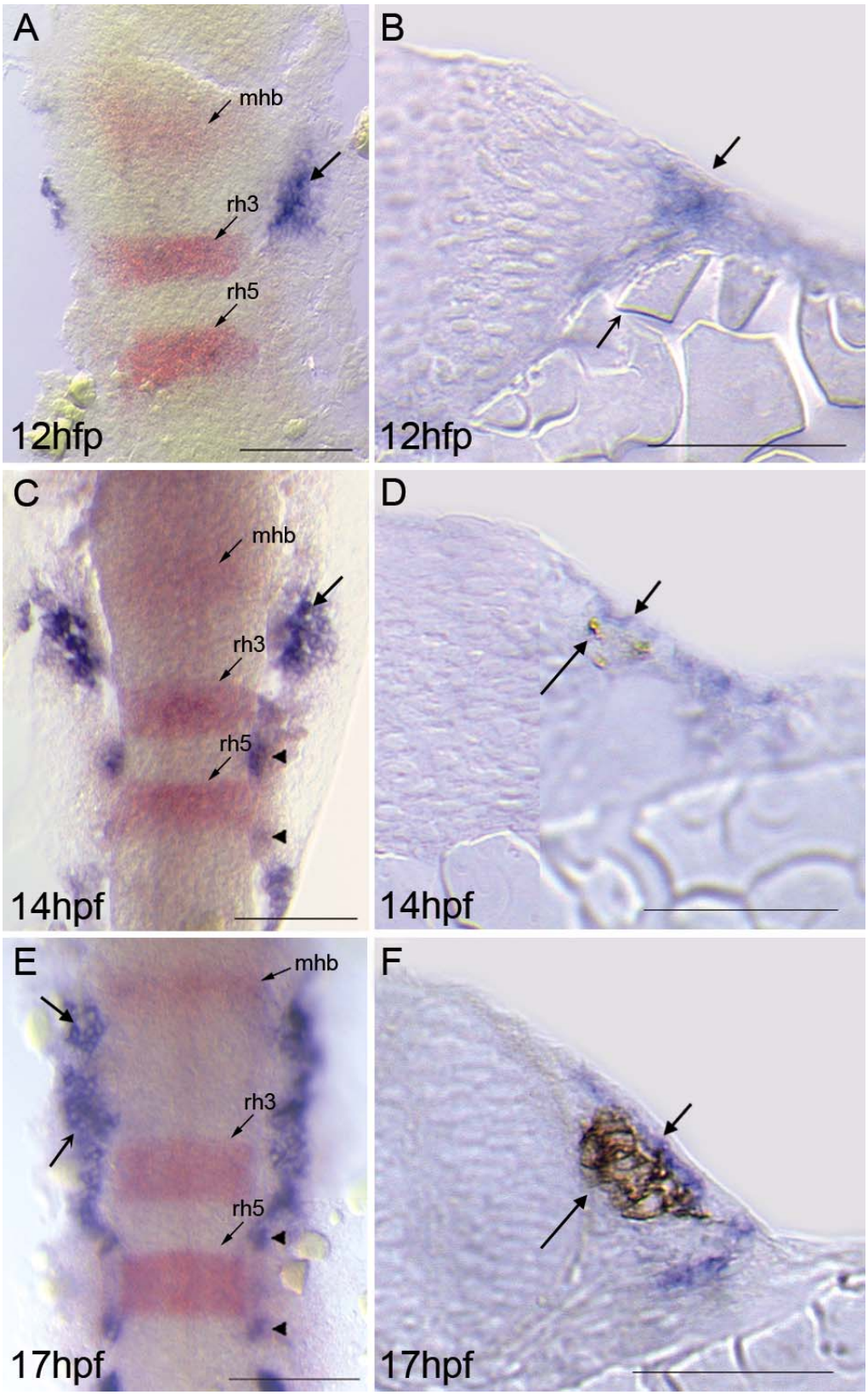

Figure 23 Expression of *eya2* in the trigeminal placodal region during early segmentation stage. Embryos in panels A, C, and E were hybridised *in situ* with *eya2* probe (blue), fluorescein-labeled *pax2.1* and *krx20* probes (red) as iondicated, are shown flatmounted in dorsal view, anterior to the top. Embryos in panels B, D, and F hybridised *in situ* with *eya2* were also immunolabeled with zn12 antibody, shown as cross sections through the region of the developing trigeminal ganglion. The stages are indicated in hours post fertilization (hpf) on each panel. *Short arrows with closed arrowheads* indicate the trigeminal placode, while *longer arrows with closed arrowheads* point to the trigeminal ganglion. Short arrows with open arrowheads indicate the anterior lateral line placode. *Black arrowheads* point to small clusters of *eya2* expressing cells in the developing otic placode. mhb, midbrain-hindbrain boundary; rh3; rhombomere 3; rh5, rhombomere 5. Scale bars, A, C, E 50µm; B, D, F 25µm.

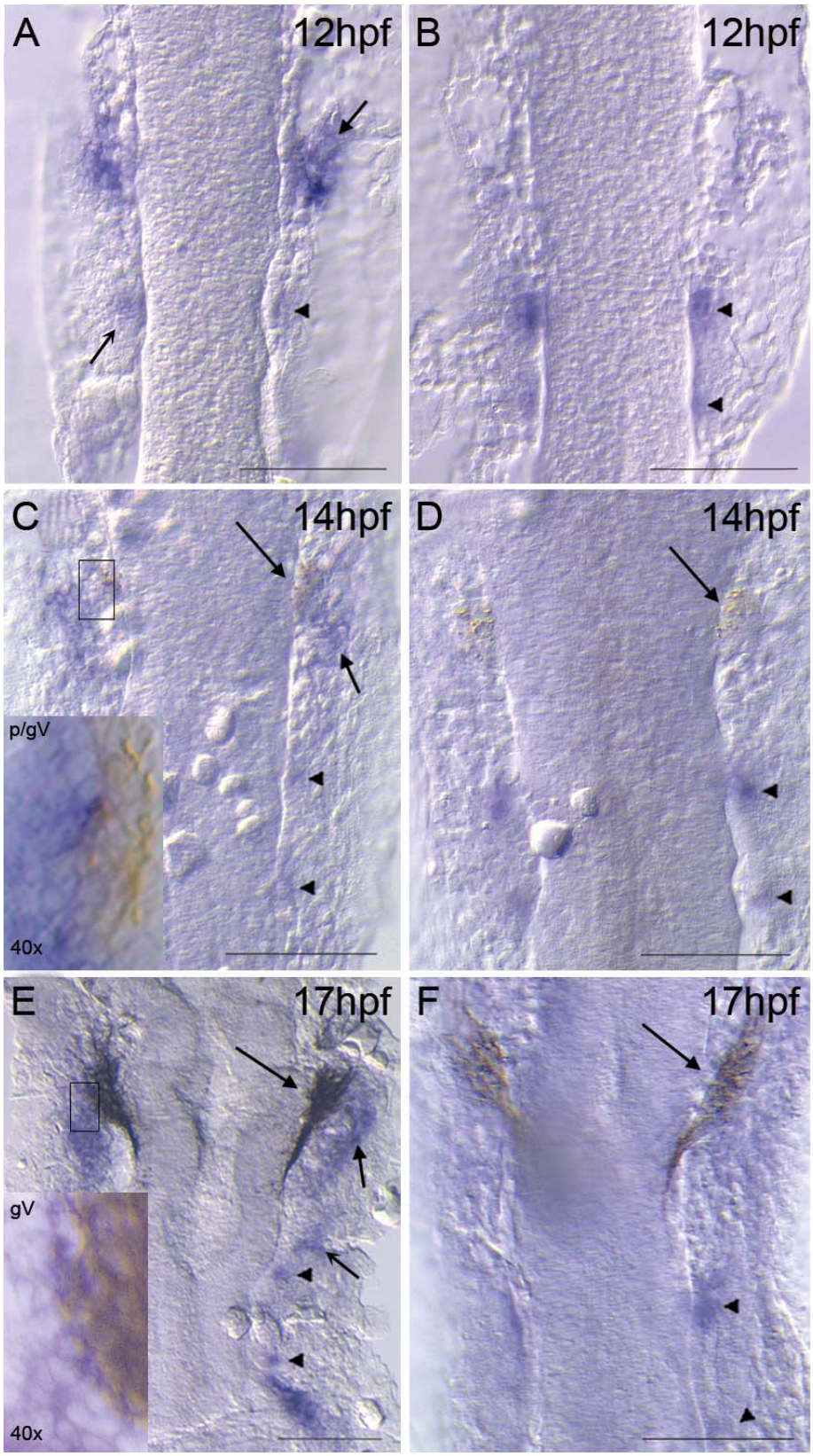

Figure 24 Comparison of *eya2* and *eya4* expression in the preotic placodal region during early segmentation stage. All embryos, hybridised *in situ* with *eya2* or *eya4* probe (blue) and immunolabeled with zn12 antibody as indicate, are shown flatmounted in dorsal view, anterior to the top. In panels C and E the trigeminal placode respectively ganglion (frame) is also shown 40-times magnified (on the bottom, left corner in each panel) revealing single neuronal cells underlying still *eya2* expressing trigeminal placodal cells. The stages are indicated in hours post fertilization (hpf) on each panel. *Short arrows with closed arrowheads* indicate the trigeminal placode, while *longer arrows with closed arrowheads* point to the trigeminal ganglion. Short arrows with open arrowheads indicate the anterior lateral line placode. *Black arrowheads* point to small clusters of *eya* expressing cells in the developing otic placode. gp, trigeminal placode; gV, trigeminal ganglion. Scale bars, 50µm.

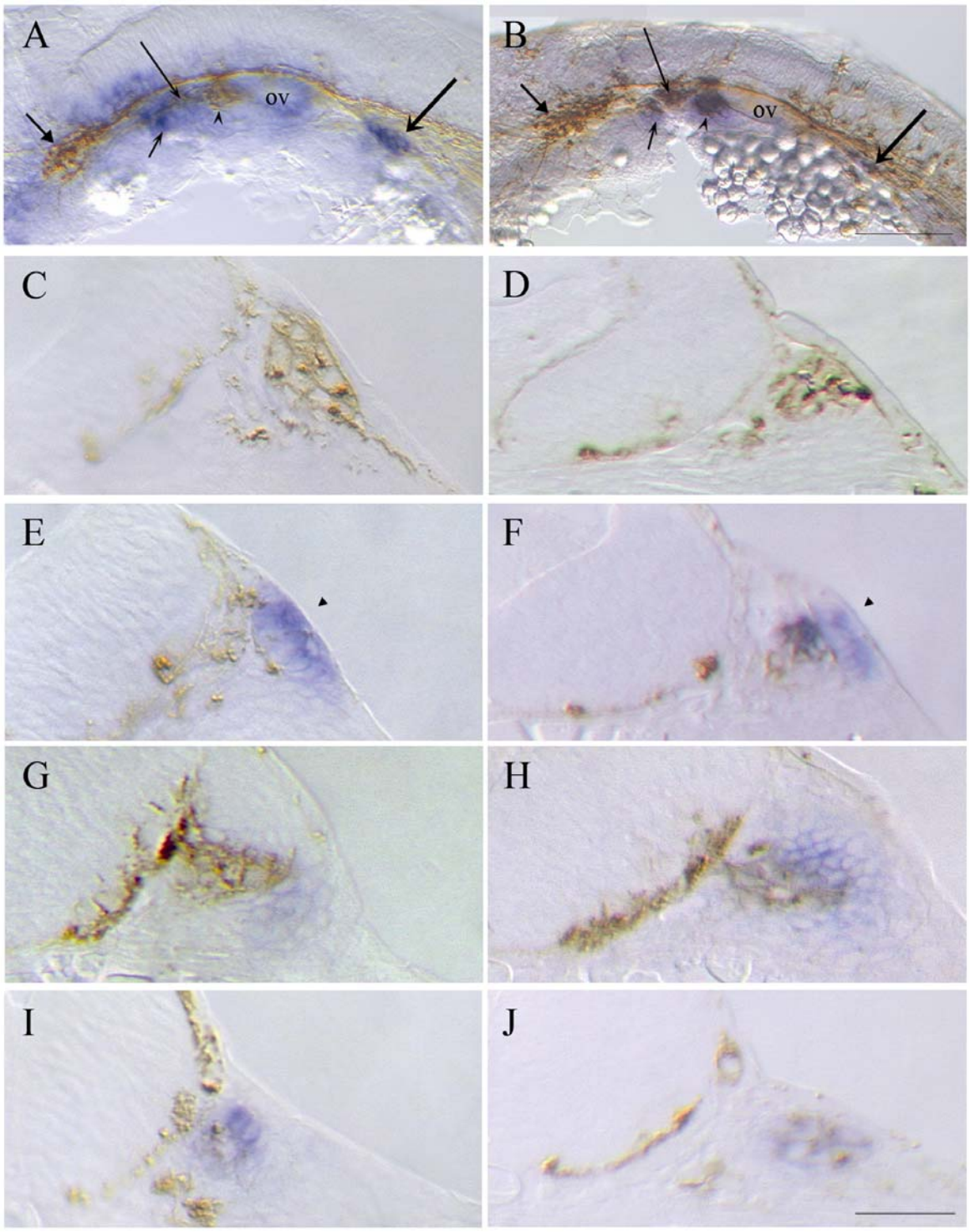

Figure 25 Comparison of *eya2* (A, C, E, G, I) and *eya4* (B, D, F, H, J) expression in cranial ganglia at 24 hpf. Embryos, *in situ* hybridised (blue) and immunolabeled with zn12 antibody as indicated, are shown in cross-sections, except for A and B, which are dissected views with anterior to the left and dorsal up. C, D: trigeminal ganglion. E, F: anterior lateral line ganglion. G, H: statoacoustic ganglion. I, J: posterior lateral line ganglion. Arrows with closed arrowheads denote trigeminal ganglia, long thin arrows with open arrowheads indicate anterior lateral line ganglia, long thick arrows with open arrowheads point to posterior lateral line ganglia. Open arrowheads indicate statoacoustic ganglia and closed arrowheads point to developing neuromasts of the anterior lateral line. *ov*, otic vesicle. Scale bar (A, B), 100µm; (C-J), 25µm.

3.2.4 Summary of *eya* expression sites in the early zebrafish

Table 4 Expression domains of *eya1*, *eya2* and *eya4* during the first three days of development. *eya1* expression is based on Sahly et al. (1999) and Peter Andermann (personal communication). Only the presence (+) or absence (-) of transcripts has been noted. ? indicates uncertain expression due to limitations of the whole mount in situ hybridization technique.

	Segmentation period								
	10hpf			12/13hpf			17/18hpf		
	eya1	*eya2*	*eya4*	*eya1*	*eya2*	*eya4*	*eya1*	*eya2*	*eya4*
pre-placodal field	+	-	-	-	-	-	-	-	-
adenohypophyseal placode	-	-	-	+	-	-	+	-	-
olfactory placode	-	-	-	+	+	-	+	+	-
trigeminal placode	-	-	-	-	+	-	-	+	-
trigeminal ganglion	-	-	-	-	-	-	-	+	-
otic placode/vesicle	-	-	-	+	+	+	+	+	+
statoacoustic ganglion	-	-	-	-	-	-	+	-	+
ant. lateral line placode	-	-	-	+	+	-	+	+	-
ant. lateral line ganglion	-	-	-	-	-	-	+	+	+
pos. lateral line placode	-	-	-	+	+	-	+	+	-
pos. lateral line ganglion	-	-	-	-	-	-	+	+	+
Lateral line primordia	-	-	-	-	-	-	+	+	+
somites	-	-	-	+	-	-	+	-	+

	Second day of embryonic development								
	24hpf			36hpf			48hpf		
	eya1	*eya2*	*eya4*	*eya1*	*eya2*	*eya4*	*eya1*	*eya2*	*eya4*
adenohypophysis	+	-	-	+	-	-	+	-	-
olfactory organ	+	+	-	+	+	-	+	+	-
otic vesicle	+	+	+	+	+	+	+	+	+
statoacoustic ganglion	+	-	+	+	-	+	+	-	+
ant. lateral line placode	+	+	-	+	+	-	+	+	-
ant. lateral line ganglion	+	+	+	+	+	+	+	+	+
pos. lateral line placode	+	+	-	+	+	-	+	+	-
pos. lateral line ganglion	+	+	+	+	+	+	+	+	+
primordia	+	+	+	+	+	+	+	+	+
neuromasts	-	-	-	+	+	+	+	+	+
branchial arches	+	+	-	+	+	-	+	+	-
somites	+	-	+	+	-	-	-	-	-
pectoral fin	-	-	-	+	+	?	+	+	+

	Third day of embryonic development					
	60hpf			72hpf		
	eya1	*eya2*	*eya4*	*eya1*	*eya2*	*eya4*
olfactory organ	-	+	-	-	+	-
otic vesicle	+	-	+	+	-	+
statoacoustic ganglion	-	-	+	-	-	+
ant. lateral line ganglion	+	-	+	?	-	+
pos. lateral line ganglion	+	-	+	?	-	+
neuromasts	+	+	+	+	+	+
branchial arches	+	-	-	+	-	-

3 Results – Part II

Besides the identification, sequence and expression pattern analysis of a gene, its functional activity is of significant interest. The function of *eya* gene family members in zebrafish is not well known yet. Therefore, loss- and gain-of-function effects were investigated by Morpholino-antisense oligonucleotide and *in vitro* synthesised mRNA injection methods in the zebrafish embryo.

3.3 Loss-of-function of *eya2* and *eya4*

3.3.1 Targeting genes of interest

To understand the molecular function of *eya* genes within sensory organ development and disease, the zebrafish *eya1/dog-eared* (*dog*) mutation, was cloned and characterized by WHITFIELD (1996). Further sequence analysis revealed three single point mutations, which were located in the splice donor sequence of putative exon[4]10. On the basis of morpholino oligonucleotid (MO) injections, complementary to the primary RNA, the *eya1* gene could be identified as being responsible for the *dog-eared* phenotype [KOZLOWSKI, 2005].

This study also shows, that *eya1* mRNA start-site morpholinos, which inhibit the translation of the whole eya protein, do not show any detectable effects in the manipulated embryos. In contrast, microinjection of *eya1* mRNA correctly spliced at the exon10-intron[5]10 splice junction phenocopies the *dog-eared* mutation. This splice junction is located immediately upstream of the eya homology region, resulting in a truncated eya protein, which only lacks the highly conserved eya domain. Based on these findings *eya2* and *eya4* splice-site morpholinos were designed for the following “knock-down” experiments.

To target the gene of interest with splice-site blocking MO, it is necessary to determine the exon/intron structure.Then, a 25-mer MO complementary to the corresponding splice donor site can be designed. The exon/intron structure of *eya2* has been determined by comparing the obtained cDNA sequence with the respective genomic DNA sequence deposited in Gene bank (accession number BX005392). Subsequently, an *eya*2 antisense MO (5’-TTGGTTGTTTTCTACCTGTGTGTG-3’) complementary to the exon4/intron4 splice donor site was designed (Fig. 26), as well as a corresponding control oligonucleotide containing 5 mismatches. Based on comparison of the *eya4* cDNA sequence with the genomic DNA sequence for zebrafish *eya4*, deposited inGeneBank (CR759830), the exon11/intron11 splice donor site was chosen to design an *eya4* antisense MO (5’-CCATCCGAACATACCTCAAGGTCAC-3’) (Fig. 27) and the corresponding mismatch control MO. Following KOZLOWSKI (2005), who obtained detectable results by injecting 20ng of MO*eya1*, approximately 20 ng were injected in 1-16 cell stage wildtype embryos.

[4] Coding regions of a gene.
[5] Noncoding regions of a gene (intervening regions)

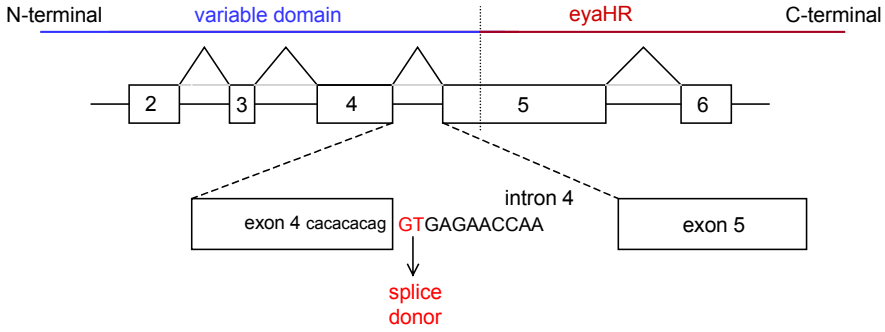

Figure 26 Schematic representation of the splicing pattern for the *eya2* gene.

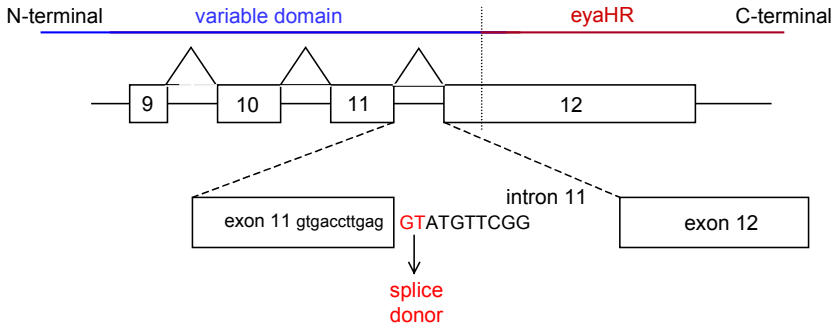

Figure 27 Schematic representation of the splicing pattern for the *eya4* gene.

3.3.2 *In situ* detection of apoptotic cells by TUNEL assay in loss-of-function embryos

KOZLOWSKIS' study (2005) has also shown an increased, apoptosis-mediated level of cell death in the developing otic vesicle of *dog-eared* embryos, detected by the terminal deoxynucleotidyl transferase-mediated nick end labelling (TUNEL) assay. To investigate whether a higher quantity of apoptotic cells can also be observed in *eya2* and/or *eya4* "knock-down" zebrafish, with MO*eya2* and MO*eya4* injected embryos were detected by using the TUNEL assay.

Within normal zebrafish development, the first apoptotic cells in sensory structures appear during the second day of development. Most sensory tissues show a specific period of intense apoptosis throughout a limited time frame (Fig. 28). Although the amount of apoptotic cells varies among individuals of the same age, the location, pattern and timing of apoptotic cells are consistent. Additionally there can be huge differences between batches of offsprings obtained from each breading event.

To unravel any effects on apoptotic cell behaviour in the manipulated embryos, TUNEL-positive cells were counted in *eya2* and/or *eya4* expressing sensory structures at the time these structures undergo normal programmed cell death in the wildtype embryo. Therefore TUNEL-positive cells were counted in the olfactory organ, the trigeminal and anterior lateral line ganglion and the otic vesicle at 27 hpf. To detect effects on sensory structures, which are not yet developed at 27 hpf, like the neuromasts of the

anterior and posterior lateral line, TUNEL-positive cells were also counted at a later stage of development, at 54 hpf. Additionally, apoptotic cells were counted in the olfactory organ and the otic vesicle where programmed cell death still occurs at this stage (Fig. 28).

Cells were counted for each sensory structure of 40 injected embryos, which were obtained from two separate experiments. Data are presented as mean value profile counts and +/- standard deviation. As internal control uninjected wildtype embryos as well as mismatch morpholino injected embryos were also detected by the TUNEL assay to exclude the possibility of non-specific labelling. To determine if or which sensory structures were affected, double staining with TUNEL assay and the monoclonal antibody zn-12 were performed.

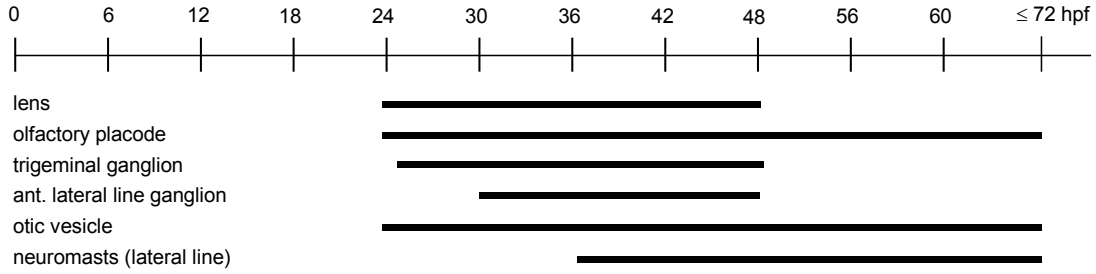

Figure 28 Time frame of apoptosis in sensory organs. Earliest apoptosis events happen at around 24 hpf within the lens, olfactory placode, the trigeminal ganglion and the otic vesicle. The first apoptotic cells in the anterior lateral line ganglion are detectable at around 30 hpf, in the neuromasts at around 36 hpf. At first apoptosis stops in the lens, trigeminal and anterior lateral line ganglion at around 48 hpf. In the olfactory organ, the otic vesicle and the neuromasts apoptosis can still be observed after 72 hpf [ZAKERI, 1993; COLE & ROSS, 2001; own observations]

3.3.2.1 Effects of *eya2* "knock-down" on the sensory structures

In the *eya2*MO injected embryos, initial phenotypic characterisations have not shown any morphological defects or differences from the wildtype siblings. Subsequently, apoptotic cell death was examined at 27 hpf and 54 hpf. At the stage of 27 hpf knock-down embryos show an increased number of TUNEL-positive cells, which is restricted to the region of the trigeminal ganglion and the anterior lateral line ganglion (Fig. 30 A,B,C,D). Quantitative analysis reveals an increase of 41% of TUNEL-positive cells in the trigeminal ganglion and 62,5% in the anterior lateral line ganglion (Fig. 29 A,C). In contrast, no differences between knock-down and control embryos could be detected in the olfactory placode or in the otic vesicle. At this stage neuromast development has just started, so no apoptotic cells could be distinguished in neuromasts at all. The occurrence of cell death events has changed at 54 hpf. Apoptosis arises in the olfactory placode, otic vesicle and neuromasts of the anterior and the posterior lateral line. Exclusively in the olfactory organ, an enhancement of apoptotic cells can be identified. An increase of 100% was detected (Fig. 29B,D; Fig. 30E,F).

A

	Olfactory organ	Trigeminal ganglion	Anterior lateral line ganglion	Otic vesicle
MO*eya2*	6,0 ± 0,5	23 ± 1,0	20,8 ± 2,2	5,3 ± 0.6
mMO*eya2*	7,1 ± 1,0	15,3 ± 0,8	11,9 ± 1,3	5,3 ± 0,4
WT sibling	7,2 ± 0.8	16,2 ± 1,2	12,8 ± 2,5	5,5 ± 0,8

B

	Olfactory organ	Otic vesicle	Neuromasts ant.lateral line	Neuromasts pos.lateral line
MO*eya2*	24,5 ± 4,9	11,2 ± 1,1	4,1 ± 2,7	3,3 ± 2,6
mMO*eya2*	11,1 ± 2,2	10,8 ± 0,8	4,0 ± 0.9	3,1 ± 1,3
WT sibling	12,2 ± 1,6	12,7 ± 2,2	2,8 ± 1,7	2,8 ± 1,6

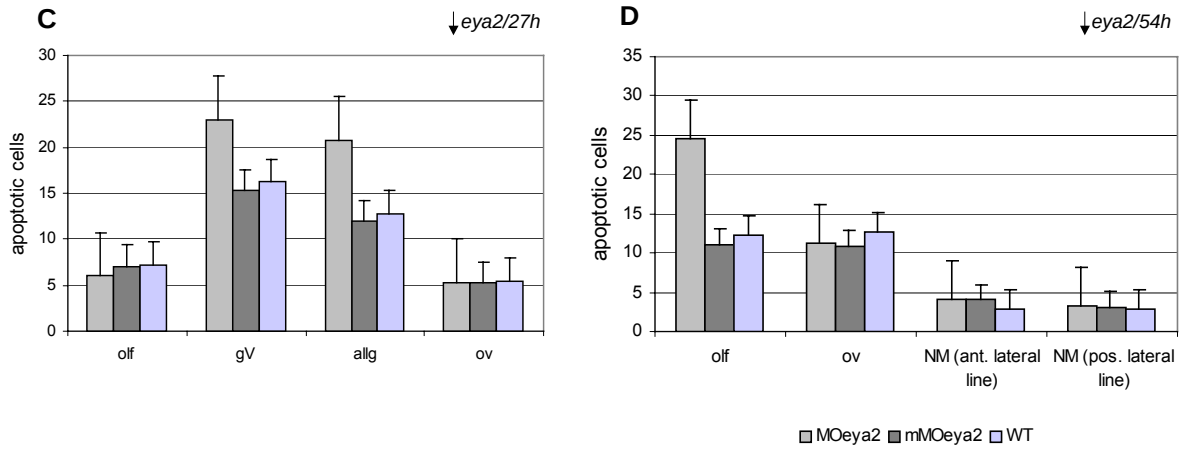

Figure 29 Apoptosis in the sensory organs at 27 hpf (A, C) and 54hpf (B, D) in *eya2* MO injected embryos. Number of apoptotic cells is the mean followed by the standard deviation. Graphs showing the numbers of apoptotic cells in the different sensory structures of *eya2*MO injected embryos, *eya2*mMO injected embryos and wildtype siblings. allg, anterior lateral line ganglion; gV, trigeminal ganglion; NM, neuromast; olf, olfactory organ; ov, otic vesicle.

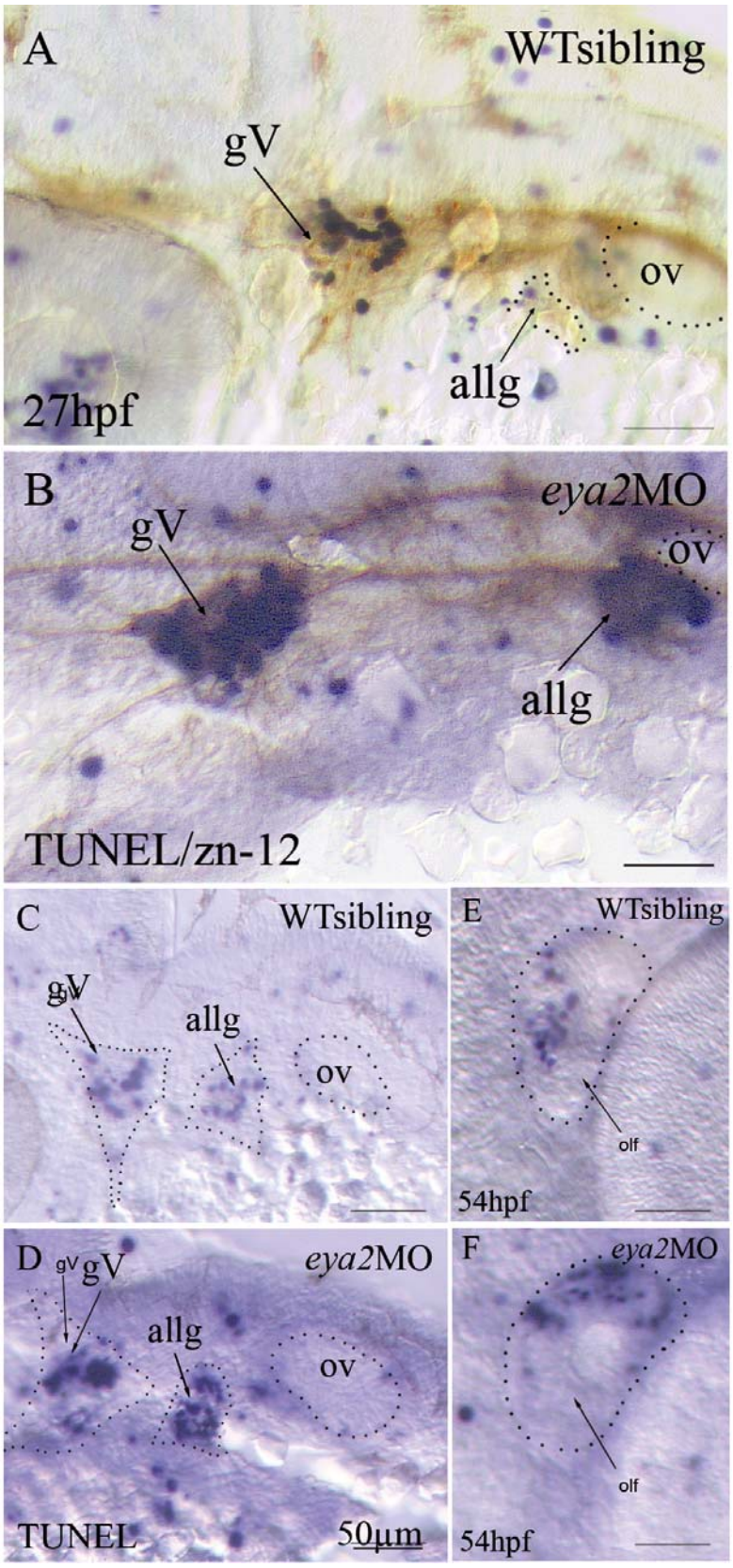

Figure 30 Increased apoptotic cell death in *eya2* loss-of-function embryos. Whole-mount *in situ* detection of TUNEL-positive cells (blue) in wildtype siblings (A, C, E) and in *eya2*MO injected embryos (B, D, F). (A, B) Wildtype sibling and *eya2*MO embryos additionally stained with the monoclonal zn12 antibody. Dissected embryos are shown anterior left, dorsal to the top. The stages are indicated in hours post fertilization (hpf) in each panel. Scale bar: A, B 100µm, C-F 50µm.

3.3.2.2 Effects of *eya4* "knock-down" on the sensory structures

The TUNEL assay of *eya*4MO injected embryos reveals an exceeding amount of apoptotic cells in the anterior lateral line ganglion at 27 hpf (Fig. 32) Counts of apoptotic cells in this sensory structure have verified an increase of 130% in the anterior lateral line ganglion. At this stage of development, no intensification of apoptosis could be detected in the olfactory placode, the trigeminal ganglion or the otic vesicle (Fig, 31A,C). At 54 *eya*4MO injected embryos do not show any alterations in the sensory structures, except in the neuromasts of the anterior lateral line, where the number of detected TUNEL-positive cells is increased by 143% (Fig. 31B,D). To confirm this observation, 96 hours old embryos were examined by DASPEI staining, revealing that neuromasts seem to be smaller (have fewer haircells) than normal, particularly in the neuromasts MI1 and D1, while it appears that the neuromast OC1 lacks completely (Fig. 33).

A

	Olfactory organ	Trigeminal ganglion	Anterior lateral line ganglion	Otic vesicle
MO*eya4*	4,4 ± 0,8	14,9 ± 2,3	19,2 ± 2,8	5,5 ± 0,5
mMO*eya4*	4,4 ± 0,5	12,2 ± 2,5	7,8 ± 0,3	4,6 ± 0,7
WT sibling	4,2 ± 0,7	14,1 ± 1,6	8,3 ± 1,6	4,4 ± 0,4

B

	Olfactory organ	Otic vesicle	Neuromasts ant.lateral line	Neuromasts pos.lateral line
MO*eya4*	12,2 ± 1,6	9,0 ± 1,3	7,3 ± 2,1	2,9 ± 1,4
mMO*eya4*	10,8 ± 1,1	9,2 ± 0,9	3,0 ± 1,2	3,1 ± 1,1
WT sibling	11,5 ± 0,7	9,5 ± 1,25	2,9 ± 1,4	3,0 ± 1,6

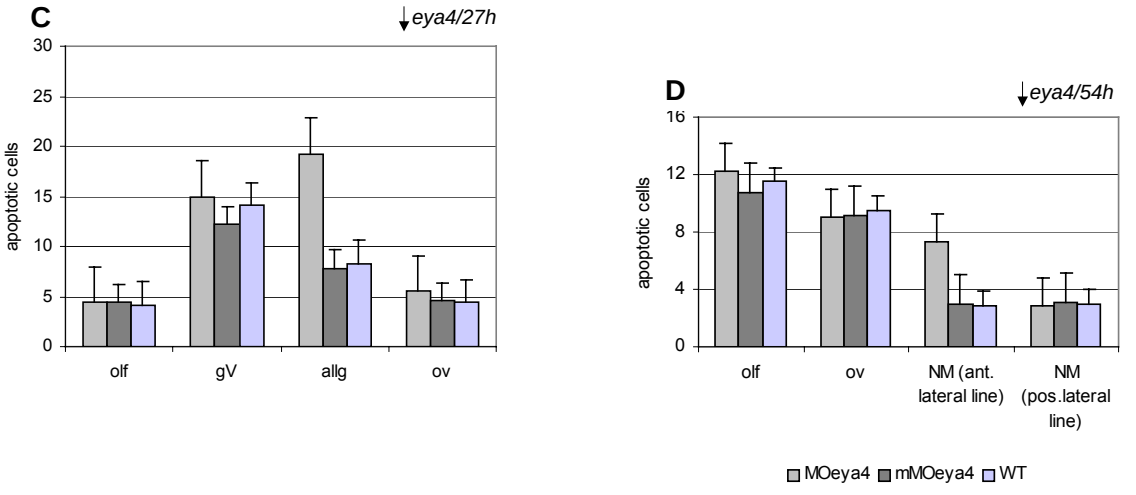

Figure 31 Apoptosis in the sensory organs at 27 hpf (A, C) and 54hpf (C, D) in *eya4* MO injected embryos. Number of apoptotic cells is the mean followed by the standard deviation. Graphs showing the numbers of apoptotic cells in the different sensory structures of *eya4*MO injected embryos, *eya4*mMO injected embryos and wildtype siblings. allg, anterior lateral line ganglion; gV, trigeminal ganglion; NM, neuromast; olf, olfactory organ; ov, otic vesicle.

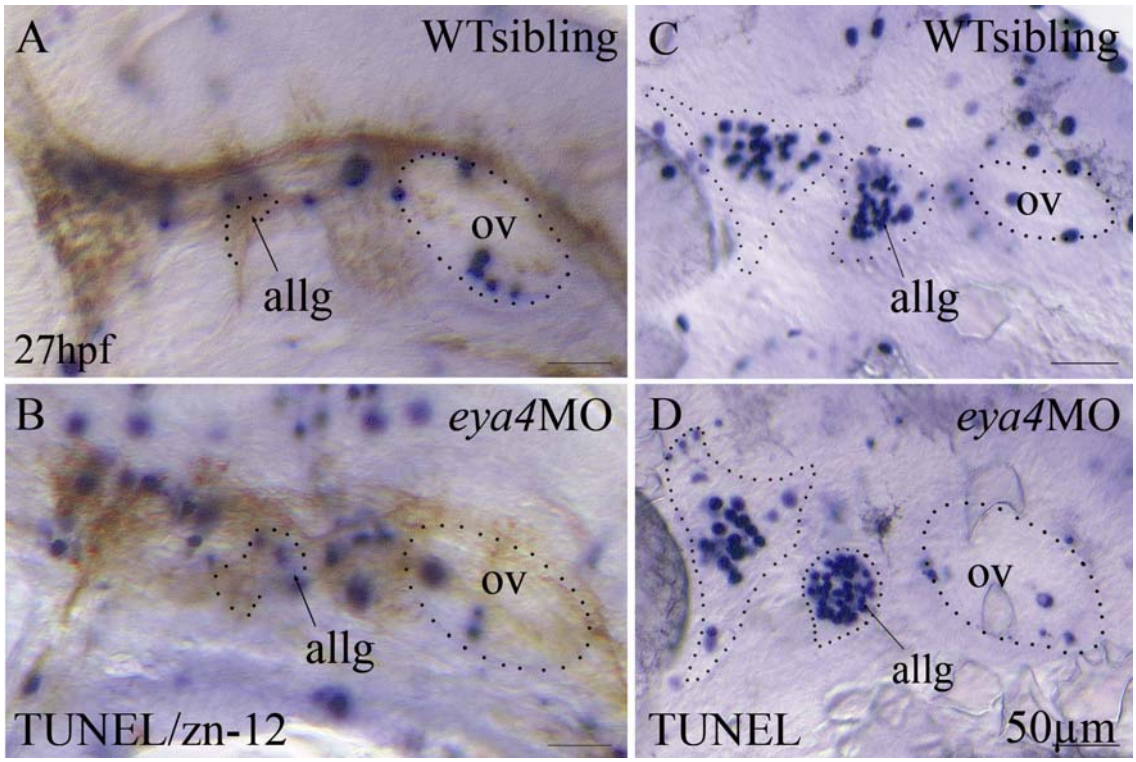

Figure 32 Increased apoptotic cell death in *eya4* loss-of-function embryos. (A-D) Whole-mount *in situ* detection of TUNEL-positive cells (blue) in wildtype siblings (A, C) and in *eya4*MO injected embryos (B, D). (C, D) Wildtype sibling and *eya2*MO embryos additionally stained with the monoclonal zn12 antibody. Dissected embryos are shown anterior left, dorsal to the top. The stages are indicated in hours post fertilization (hpf). Scale bar: A, B 50µm, C, D 100µm.

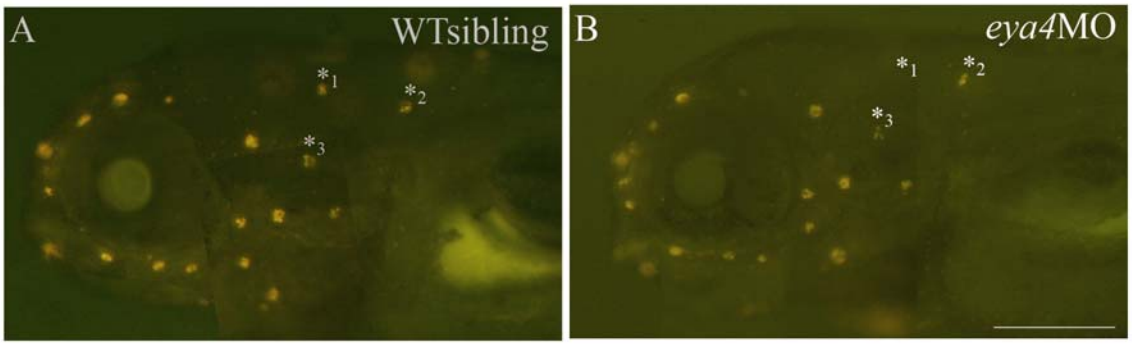

Figure 33 The andterior lateral line in *eya4* knock-down embryos. Confocal images of live embryos stained with the vital dye DASPEI showing hair cells in the neuromasts of the anterior lateral line (yellow dots). In *eya4*MO injected embryos the neuromasts have fewer hair cells than normal, strongly reduced are the haircells of the neuromasts MI1 (*3) and D1 (*2), the neuromast OC1 (*1) is completely missing. Scale bar: 200µm.

3.4 Gain-of-function of *eya1, eya2* and *eya4*

3.4.1 Effects of ectopic *eya1, eya2 and eya4* detected by the TUNEL assay

To obtain further information about the function of *eya* and its importance within the process of apoptosis in normal development, overexpression experiments were conducted. If the loss of *eya* function is responsible for an increased level of apoptosis, possibly the gain of *eya* function can reduce programmed cell death. Studies in *Drosophila* have shown, that the overexpression of *eyes absent* causes the development of ectopic eyes.

Based on these findings *in vitro* synthesised *eya1*, *eya2* or *eya4* mRNA was injected into 1-16 cell stage wildtype zebrafish embryos as described before. As internal control *in vitro* synthesised mRNA encoding green fluorescent protein (GFP) was coinjected, which allows to observe the distribution of the injected mRNA by fluorescence microscopy (488nm). Approximately 0,15ng of *eya* mRNA and 0,5 ng of GFP mRNA was injected.

To observe effects of ectopic *eya* expression, TUNEL-positive cells were counted in the lens, a sensory structure normally is not expressing any of the *eya* genes. To determine If ectopic *eya* expression actually influences apoptotic behaviour, the number of apoptotic cells should be reduced in the lens after overexpression of *eya* genes. Numbers of TUNEL-positive cells were counted in 27 hpf old embryos for two reasons. Apoptosis in the zebrafish lens starts to be active at around 20 hpf, peaks between 24 hpf and 30 hpf. At this point in time the process of programmed cell death can be manipulated. Furthermore *in vitro* synthesised mRNA stability is limited to the early stages of development. Within the embryonic development the firstly injected mRNA concentration weakens with every cell division event, therefore to obtain reliable results investigated embryos should not be older than 30 hpf. Cell were counted for each lens of 60 injected embryos, which were obtained from three separate experiments. Data are presented as mean value profile counts and +/- standard deviation.

Neither of the investigated embryos, which were injected with *eya1*, *eya2* or *eya4* have shown any morphological distinct features. Whereas the TUNEL assay of each, *eya1*, *eya2* and *eya4* reveals a reduced number of TUNEL-positive cells in the lens (Fig. 35A-F). In ectopic *eya1* expressing embryos apoptosis in the lens was reduced by 17%. Gain of function of *eya2* reveals a reduction of 28% and ectopic expressed *eya4* shows a 35% reduction (Fig. 34). Besides the decrease in the lens, no other effect on apoptopic-mediated cell death was observed.

A

	eya1	*eya2*	*eya4*
syn.mRNA	6,9 ± 2,5	9,9 ± 1,5	6,1 ± 1,2
WT sibling	8,3 ± 1,9	13,7 ± 2,5	9,3 ± 1,4

B

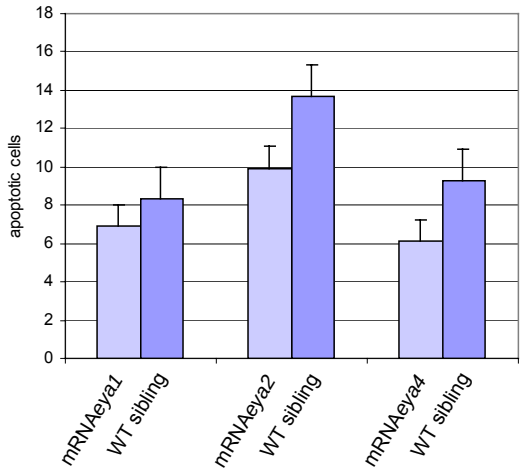

Figure 34 Ectopic *eya1*, *eya2* and *eya4* expression reduces TUNEL-positive cells in the lens at 27hpf. (A) Number of the apoptotic cells is the mean followed by the standard deviation. (B) Graphs showing the numbers of apoptotic cells in the lens for each ectopically expressed *eya gene* and wildtype sibling controls.

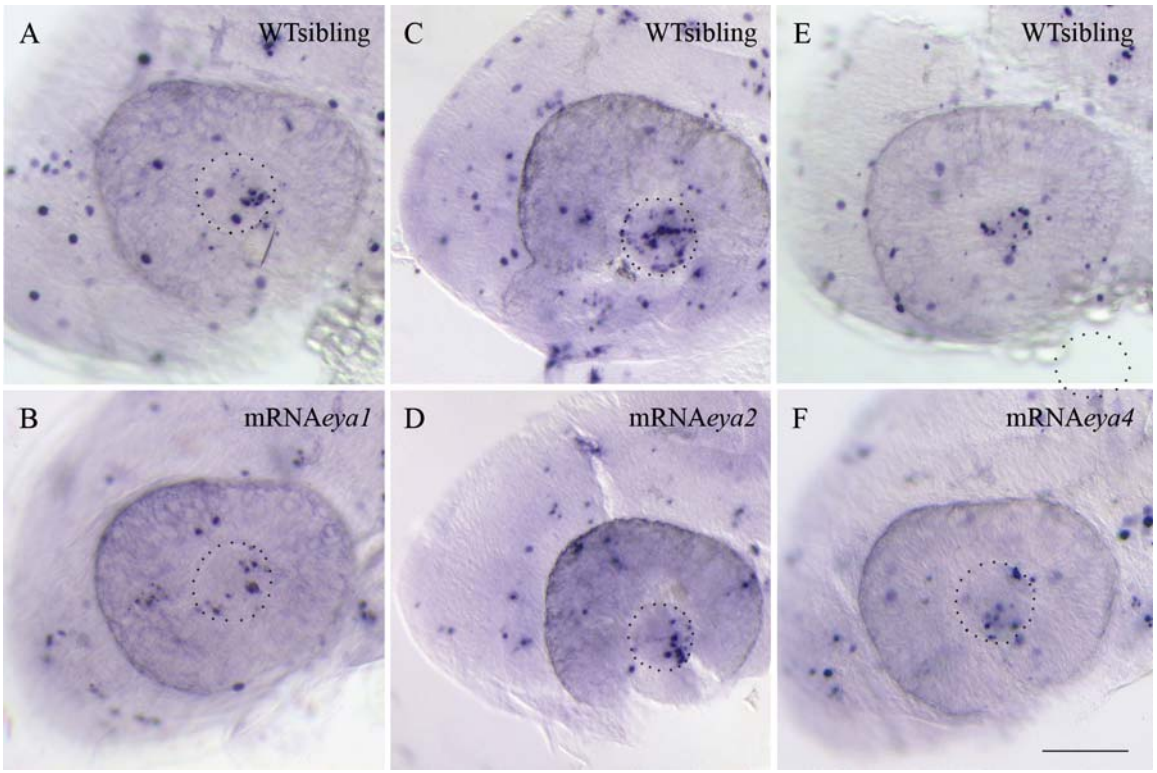

Figure 35 Decreased apoptotic cell death in ectopic *eya1*, *eya2* and *eya4* expressing embryos at 27 hpf. Whole-mount *in situ* detection of TUNEL-positive cells. Dissected embryos are shown anterior to the left, dorsal up. The lens is outlined with a black dotted line. Scale bar, 50µm.

4 Discussion – Part I

4.1 Conservation of *eya2*, *eya3* and *eya4* sequences in vertebrates

The present results indicate that the zebrafish *eya2*, *eya3*, and *eya4* are homologues of the *Drosophila eyes absent* gene and moderately conserved proteins within the vertebrates. Sequence analysis indicated with *Eya4* as the strongest conserved member of the e*ya* gene family, while *Eya3* revealed the lowest level of identity.

Comparison of the predicted amino acid sequences of the zebrafish *eya* genes and the corresponding mammalian Eya proteins revealed the eya-typical, highly conserved C-terminal domain and the variable N-terminal domain with, an overall identity of 64%(mouse) / 62%(human) for the eya2 protein, 48%/58% for the eya3 protein and 74%/73% for the eya4 protein. The characteristical, in the C-terminal located eya homology region (eyaHR) shows an identity of 79-90% between the zebrafish and the mammalian proteins. A second, but shorter homology region (ED2) was found in the N-terminal, although it is less identical between zebrafish and mammalian than the eyaHR (35%/eya3; 48/40%/eya2; 72%/eya4)

The N-terminal region of the predicted protein of all three eya proteins in zebrafish is proline-serine-threonine-rich, as demonstrated previously for the mammalian Eya1-3 proteins by XU 1997). Furthermore contain the eyaHRs of all zebrafish eya proteins two signature motifs characteristic of the haloacid dehalogenase (HAD) hydrolase, which are responsible for the enzymatic activity of Eya proteins [TOOTLE, 2003]. While both motifs in the eya3 protein are 100% identical between zebrafish and mammalian, motif III in eya2 and eya4 differs among the Eya proteins because of the amino acid substitutions.

4.2 Alternatively spliced transcript variants

Amino acid alignments of the deduced zebrafish *eya* cDNAs lead to the identification of *eya2* and *eya4* as alternatively spliced transcript variants. Alternative gene splicing is a post-transcriptional modification in which a single gene can code for multiple proteins. Gene splicing enables a single gene to increase its coding capability, allowing the synthesis of protein isoforms that are structurally and functionally distinct. Thus, it is an important reason for protein diversity. The most common known gene splicing mechanism occurs in exon-intron borders of the pre-mRNA, mostly in the N-terminal region. Thereby including or excluding exon(s) from the final gene transcript leading to extended or shortened mRNA variants [BRETT, 2001; BLACK, 2003]. Alternatively spliced transcripts have been found in the *Drosophila eya absent* [BONINI, 1993; BONINI, 1998], in the human *Eya1* [ABDELHAK, 1997], and in the human *Eya4* [BORSANI, 1999]. Specific splice variants may causes diseases, disorders, or pathological conditions.

However not any insertion or gap can be assumed to be an exon, which in general spans multiple amino acids. Additions or substitutions of only an insignificant number of amino acids can be assumed as results of the alignment program, determine the highest analogy between compared amino acids.

An alternative selection of promoters is another method of splicing in the 5'UTR produces an alternative N-terminus domain in proteins. The zebrafish *eya2* clone can be assumed to be a splice variant containing an alternative promoter. Comparison with mammalian Eya2 proteins revealed that the translated zebrafish eya2 protein lacks the first 70 amino acids. That is a splicing event in the 5'UTR generated an isoform with alternative ATG start codon. Indeed, a similar splice variant was found in another murine eya2 transcript [GeneBank accession number U81603; ZIMMERMANN, 1997], confirming this assumption.
Amino acid alignments of zebrafish *eya4* cDNA clone revealed a gap of 28 amino acids in the N-terminal region in the zebrafish protein. However, in two of four compared mammalian Eya4 transcripts, in the murine Eya4 protein and in the human Eya4 protein isoform II, a similar lack of amino acids was found. Additionally in the zebrafish this gap is located at the exon4-intron4 border of the pre-mRNA. For those reasons it can be assumed, that the zebrafish *eya4* cDNA clone is an alternatively spliced transcript.
The N-terminal region of the zebrafish *eya3* cDNA clone contains 12 insertions; four of those span ten or more amino acids, suggesting these insertions are exons. Corresponding transcripts were not found in mammalian homologues, therefore it is difficult to decide if this zebrafish *eya3* cDNA clone is a definite splice variant. The *eya3* cDNA clone may also be a mutation or inappropriate splicing event, resulting in a genetic dysfunction. The physiological activity of splice variant products and the original protein may be the same, completely different, or even absent. When a variant and the original sequence have the same or opposite activity, they may differ in various properties not directly connected to biological activity, such as temporal pattern of expression and up or down regulation mechanisms [BRETT, 2001; BLACK, 2003]. This thesis has shown that no expression of the *eya3* gene can be found in the zebrafish at all. The function of the eya3 protein in zebrafish may be overtaken by another gene or utterly dispensable. Eventually the zebrafish *eya3* gene is about a pseudo-gene, a gene without any activity, at least in the teleosts.

4.3 Comparison of *Eya2* and *Eya4* expression during early vertebrate development

Similar overlapping and unique expression sites of *Eya* genes are found in different vertebrates like the zebrafish, *Xenopus* [DAVID, 2001; KRIEBEL, 2007], chicken [MISHIMA, 1998] and mouse [ABDELHAK, 1997; DUNCAN, 1997; XU, 1997; ZIMMERMANN, 1997; BORSANI, 1999] (Tab. 6).

4.3.1 *Eya2* and *Eya4* expression in the cranial placodes and their derivates

Although progress has been made in recent years to identify the molecular players that mediate placode specification, induction and patterning, the processes that initiate placode development are still not well understood. A defining feature for *eya2* and *eya4* is their combined expression in many ectodermal cranial placodes and placode derivates. *Eya2* is expressed in various ectodermal placodes like the trigeminal, lateral line as well as otic placodes, and their derivates. Early placodal *eya4* expression could only be found in the otic placode. Though *eya2* is expressed in the otic placode as well as in the delaminating cells forming the statoacoustic ganglion, no expression could be found in differentiated neurons of the ganglion itself. Instead the statoacoustic ganglion reveals an abundant expression of *eya4*. Thus, while *eya2* is both placodal and neuronal expressed, *eya4* expression is, apart from the otic placode, restricted to fully differentiated cells.

Comparison of the two novel zebrafish *eya* genes with the zebrafish *eya1* gene [SAHLY, 1999] reveal overlapping expression of two or all *eya* genes in various sensory structures. However *eya1* expression occurs already in the pre-placodal field, consequently earlier than *eya2* and *eya4* during the embryonic development. Therefore it has to be assumed, that *eya1* is upstream of *eya2* and *eya4*. Similar expression of *eya2* and *eya1* is shown in different cranial placodes, like the olfactory, branchial and otic placodes. However, either of them has a unique expression site, *eya2* is exclusively expressed in the trigeminal placode, *eya1* in the adenohypophyseal placode. Apart from the trigeminal ganglion, in all diffenetiated cranial structures *eya2* and/or *eya4* are coexpresse with *eya1* (Tab. 5).

Murine *Eya2* expression is found in various ectodermal cranial placodes and ganglia, among others in the trigeminal placode and ganglion. Therefore it can be assumed that the unique expression site of *Eya2* in the trigeminal placode and ganglion is conserved between zebrafish and mice. No murine *Eya2* expression is described for the otic placode or the differentiated otic vesicle. That is while *eya2* is expressed in the otic placode and its derivates, even though for a short period, this expression site got lost completely in higher vertebrates. Similar to the zebrafish *eya4* gene, the murine *Eya4* is, except of the nasal placod, restricted to differentiated cells. However, both the zebrafish and the murine *Eya4* gene has one placodal expression site, the otic placode and the nasal placode respectively. After differentiating events the murine *Eya4* is expressed in the nasal pit and the otic vesicle. The nasal expression of *Eya4* is a new expression feature of the murine *Eya4* homologue.

The early expression of *Eya2* in chicken is almost identical with the zebrafish. *Eya2* can be detected in the nasal pit, the epibranchial placodes and ganglia and the trigeminal ganglia. Like the murine and zebrafish *Eya2* gene, chicken *Eya2* is neither expressed in the early lens placode nor in the optic

vesicle. Although partial sequences for chicken *Eya1*, *Eya3 Eya4* genes are known, there is no information about any expression domains reported yet.

These results suggest that cranial *Eya2* expression sites ar highly conserved within the vertebrates and that it is a specific gene marker for the trigeminal placode and ganglion in zebrafish, mouse and chicken. One exception presents the *Xenopus Eya1* homoloug, which is expressed in the the trigeminal ganglion. The *Eya1* expression in the cranial placodes of *Xenopus* is widespread and corresponds to the combined zebrafish *eya1* and *eya2* as well as the combined murine *Eya1* and *Eya2* expression sites. This suggests a complementary evolutionary loss of expression domains in the two different lineages [FORCE, 1999; DAVID, 2001]. In both zebrafish and mice the expression of *Eya4* is strongly limited within the cranial placodes, but furthermore restricted to differentiated cells.

In *Drosophila eyes absent* is known as being essential for proper eye development. Apart from the mammalian *Eya1* gene, no vertebrate *Eya1*, *Eya2* or *Eya4* gene is expressed in the developing eye. However, *eyes absent* gene expression in the optic placode as well as in the optic vesicle has been described for the *Xenopus* and murine *Eya3* gene (Tab. 6).

4.3.2 *Eya2* and *Eya4* expression in the inner ear and lateral line

The development of the zebrafish inner ear commences during somitogenesis with the formation of the otic placode. The otic placode is an expression site of *eya2* as well as *eya4*, although their expression is less prominent than the expression of *eya1*, which is abundant in the whole placodal tissue. However, expression of each zebrafish *eya* gene in the otic placode starts at the same time around 12/13 hpf. After formation of the otic vesicle all three zebrafish *eya* genes are expressed in the ventral wall, although *eya2* expression is limited to the posterior ventral edge. While at these early stages of development *eya4* expression is restricted to the anterior ventral part of the otic vesicle, during further formation it extends within the inner ear. The ventral wall of the otic vesicle gives rise to the neurons of the maculae and the statoacoustic ganglion. In contrast, neither of the zebrafish *eya* genes are expressed in the dorsal part of the otocyst, where the walls of the semicircular canal system and cristea rises from. While *eya4* is expressed in four of the five otic sensory structures, the anterior macula and the anterior, posterior and lateral cristea, after differentiation of the otocyst until at least 72 hpf. Contrary *eya2* expression is restricted to the area of the posterior macula. Furthermore is the expression of *eya2* temporary limited, ending at 48 hpf. This results reveal the otocyst as a major expression site of *eya4* and *eya1*, whereas *eya2* expression is less prominent (Tab. 7). A similar restriction of *Eya2* expression in the otic vesicle is described in mice embryos, where expression is concentrated on the ventromedial wall of the otocyst. However, contrary to the zebrafish *eya2* gene murine *Eya2* expression is also visible in the adjacent statoacoustic ganglion. [XU, 1997]. Like the murine *Eya4*, the murine *Eya2* gene reveals an additional expression site (Tab. 6).

The lateral line sensory system, which is an exclusive structure of fishes and amphibians, is a major expression site of zebrafish *eya2*, *eya4* as well as *eya1*. In the pre- and postotic lateral line placodes *eya2* and *eya1* expression occurs at early stages around 12 hpf, followed by expression of *eya4* in the differentiated neuronal cells and their compaction into lateral line ganglia around 17/18 hpf.

Expression of *eya2* and *eya4* as well as *eya1* continues in both migrating primordia and neuromasts, whereas it is almost identically in intension as well as duration.
In Xenopus *Eya1* is known to be expressed in the lateral line, although its expression sites are not described in detail yet [DAVID, R, 2001]

4.3.3 *Eya2* and *Eya4* expression in the somites and the pectoral fin

No *eya2* expression was found in the somites at all, whereas *eya4* can be detected transiently between 20 hpf and 26 hpf. For this period it is coexpressed with *eya1*, which is abundantly expressed in the somites between 12 hpf and 28 hpf. At this time the somites have already formed, they but off from the cranial end of presomitic mesoderm at 10 hpf [BORYCKI & EMERSON, 2000]. Therefore it can be assumed that no *eya* gene is part of the initial process of condensation and epithelialisation of somite precursor cells. By 24 hpf expression of both *eya4* and *eya1* becomes restricted to the cells of the ventrolateral side of the four somites, which are migrating to the forming pectoral fin buds from 24 hpf until 36 hpf. Therefore *eya* expression in the somites rather can be linked to specified but undifferentiated myognetic precursor cells. The pectoral fin itself expresses *eya2*, *eya4* as well as *eya1* mRNA transcripts between 36 hpf and 48 hpf.
Contrary to the zebrafish *eya* genes, whose expression follows somitogenesis, in avian (*Eya2*) and mamalian *(Eya1*, *Eya2, Eya4*) embryos *Eya* gene expression is also reported for the presomitic mesoderm. This expression continues during further development and can be observed in the developing wing/limb including the dermomyotome, migrating muscle precursors and tendons.

Table 5 Zebrafish *eya* gene family members with unique and identical expression during early embryonic development.

eya genes with unique expression in sensory organ development

→ Adenohypophysis (*eya1*)

→ Trigiminal placode (V) (*eya2*)

eya genes with overlapping expression in sensory organ development

→ Branchial arches (*eya1, eya2*)

→ Olfactory placode (*eya1*, *eya2*

→ Lateral line placode (*eya1*, *eya2*)

→ Lateral line ganglia (*eya1*, *eya2, eya4*)

→ Statoacoustic ganglion (VIII) (*eya1*, *eya4*)

→ Otic placode(*eya1*, *eya2, eya4*)

→ Lateral line primordia (*eya1*, *eya2, eya4*)

→ Neuromasts (*eya1*, *eya2, eya4*)

→ Somites (*eya1*, *eya4*)

→ Pectoral fin bud (*eya1*, *eya2, eya4*)

Expression sites		zfeya2	zfeya4	Xeya1	meya1	meya2	meya3	meya4	ceya2
PNS*	adenohypophyseal	-	-	+	+	-	-	-	-
	lens	-	-	-	+	-	+	-	+
	epibranchial	+	-	-	+	+	-	+	+
	olfactory	+	-	+	+	+	-	+	+
	trigeminal (gV)	+	-	+	-	+	-	-	+
	lateral line anterior**	+	+	+	-	-	-	-	-
	lateral line posterior**	+	+	+	-	-	-	-	-
	statoacoustic (gVIII)	-	+	+	+	+	-	+	+
	otic	+	+	+	+	-	-	+	+
	primordia**	+	+	+	-	-	-	-	-
	neuromasts**	+	+	-	-	-	-	-	-
Non-neural	somites	+	+	+	+	+	-	+	-
	pectoral fin**	+	+	-	-	-	-	-	-
	limb***	-	-	-	+	+	+	+	+
	wing***	-	-	-	-	-	-	-	+

Table 6 Comparison of eya expression domains of genes from Xenopus (*Xeya1; Xeya3*) [DAVID, 2001; KRIEBEL, 2007], mouse (*mEya1; mEya2; mEya3; mEya4*) [DUNCAN, 1997; XU, 1997, ZIMMERMANN, 1997; BORSANI, 1999] and chicken (*cEya2*) [MISHIMA, 1998] and zebrafish. * cranial ganglia; (+) Presence/ (-) absent of transcripts in the described structures.

** Structures exclusively developed fish and amphibians.

*** Mammalian and avian structures respectively.

4.4 Evolution of Eya

A phylogenetic similarity tree, based on eyaHRs of in this thesis compared *Eya* homologues, discloses the relatedness within the *Eya* gene family. According to this, two gene duplications (exact copies of a gene) happened within vertebrate evolution, in which the vertebrate *Eya1* and *Eya3* genes duplicated at first at about the time of the fly/vertebrate divergence. At this time other *Drosophila* genes related in sequence to *eyes absent* have not been identified. It seems that no duplicated genes exist in *Drosophila* and that the divergence observed in vertebrates occurred subsequent to the fly/vertebrate division [LYNCH & CONERY, 2000]. So far the murine *Eya1* and *Eya3* gene are the only *Eya* genes, that are expressed in the eye anlage combined with the sequence analysis have been performed in this work may verify the closest relationship between the *Drosophila eyes absent* and the vertebrate *Eya1* and *Eya3* gene. Phylogenetic analysis indicates that the vertebrate *Eya1* gene was duplicated to the *Eya4* gene as well as the *Eya3* gene was duplicated to *Eya2.* Duplicated genes can have overlapping expression and redundant function or undergo a period of changes that enables functional diversification to create two different genes. For this reason, highly conserved and redundant as well as unique expression sites are found along all vertebrate *Eya* genes. There is a high rate of gene duplication along evolution that is accompanied by a high rate of gene loss in a relatively short period after gene duplication [LYNCH & CONERY, 2000]. This may be the case within the zebrafish *eya3* cDNA clone analysed in this thesis.

4.5 *Eya* genes – important player in evolutionary conserved gene networks

The conservation of sequences and expression patterns across species is highly suggestive of functional conservation. Therefore, expression analysis and comparison in different model organisms can help to identify gene functions.
In the zebrafish otic placode and its derivates a various number of genes of different gene families have been found, including the two novel genes *eya2* and *eya4*. For further understanding of the character of these two zebrafish genes, it is useful to compare their expression patterns with potential antagonists in the otic vesicle at different stages of development. Candidates, that were chosen for comparison were *eya1* [SAHLY, 1999], *six1* [BESSARAD, 2004], *six4.1*, *six4.2* [KOBAYASHI, 2000], *dachA*, *dachB* and *dachC* [HAMMOND, 2002], based on previous studies, which revealed that these genes have distinct and partially overlapping expressions in the zebrafish inner ear (Tab. 7).

The transcriptional coactivator and tyrosine phosphatase *eyes absent* is vital for eye development in *Drosophila*. Furthermore, vertebrate homologues were identified in mouse and human, which are also expressed in the developing eye (*Eya1*). This led to the assumption, that *eya* gene homologues may function in aspects of vertebrate eye development like they do in flies, even though these visual organs are morphologically distinct, the molecular mechanisms that underlie their development are remarkably conserved. [QUIRING, 1994; ZUKER, 1994]. Earlier molecular evidences suggest that placode induction is a multi-step process, in which each individual placode is induced at different times by a different combination of genes and tissues, often as part of a signalling network. Signalling networks

have increased in complexity during evolution as a result of gene duplication events and the incorporation of redundant or compensatory signalling events. Many proteins in these networks have modular and conserved protein interaction domains that are quite vague in biochemical assays. It is well documented, that eya proteins do not bind to DNA, but they are characterised by a highly conserved protein/protein-binding domain.

In *Drosophila*, the Eya domain participates in protein/protein-binding with the Six protein to form a transcriptional complex in which Eya provides the transactivation function while Six provides the DNA binding activity. This transcriptional interaction is essential for *eya* nuclear translocation [OLIVER, 1995; OTHO, 1998; OTHO, 1999; ESTEVE & BOVOLENTA, 1999; RELAIX & BUCKINGHAM, 1999; KOBAYASHI, 2000; KAWAKAMI, 2000; IKEDA, 2002]. All *six* gene family members are characterised by two conserved domains, the SIX domain, which mediates protein-protein interactions, and a homeobox DNA-binding domain [SEO, 1999; KAWAKAMI, 2000]. The *Six1* gene has been described as being crucial for the development of many tissues and plays an important part in regulating cell proliferation [CHEYETTE, 1994; DOZIER, 2001; CARL, 2002; OZAKI, 2004]. In addition, studies in mice have revealed that the *Six1* transcription factor operates as both activator and repressor, depending upon their specific cofactors [LI, 2003].

However, Eya can also bind to other proteins than Six. Recent protein interaction studies in *Drosophila* identified Dach proteins as potential Eya-binding partners [KAWAKAMI, 1996; KAWAKAMI, 2000; HAMMOND, 2002; GIOT, 2003]. Analysis in *Drosophila* have positioned *Dach* genes downstream of *Six* and *Eya* genes. Additionally, *Dach* genes have also been shown to have discrete protein-protein interactions with *Eya* as well as *Six* during development of various organs. In *Drosophila dach* synergises with *eya* to increase the size of ectopic eyes when both are expressed together, suggesting *dach* may recruit the transcriptional activatior activity of *eya* to promote target genes. A repressor complex between *six1* and *dach* has also been described that might switch from being a repressor to an activator trough the functaion of Eya protein phosphatase [LI, 2003].

The interactions among these genes have been worked out in most detail for Drosophila eye development, in which their homologues, *eyeless (Pax)*, *sine oculis (Six)*, *eyes absent (Eya)* and *dachshund (Dach)*, are critical for eye development. As a regulatory network of genes, *eyeless* binds directly to the *eyes absent* promoter region and regulates *sine oculis*, while both activate or suppress *dachshund* expression, including positive feedback regulation of each others expression [CHEN, 1997, HALDER, 1998, PIGNONI, 1997; NIIMI, 1999; WAWERSIK & MAAS, 2000]. Similar gene networks among these gene families have also been found to function in vertebrate organ development like in the cranial ganglia, otic vesicle, kidney and limb, though this network is more complex in vertebrates, which have multiple orthologs of each fly gene [OLIVER, 1995; XU, 1997; CAUBIT, 1999; DAVIS, 1999]. Therefore, when their respective homologous genes were found to be expressed in overlapping patterns in vertebrates, it might be suggested that these factors might operate in a similar regulatory network.

Table 7 Comparison of *eya1*, *eya2*, and *eya4* zebrafish genes with several other marker genes showing overlapping expression sites in the developing ear. [1] SAHLY et al. (1999), PETER ANDERMANN (personal communication); [2] BESSARAB et al. (2004); [3] KOBAYASCHI et al. (2000); [4] HAMMOND et al. (2002); [a], additional expression sites described by Marcus Eich (unpublished); [b], additional expression sites described by Denis Denter (unpublished).

	Expression sites in the inner ear									
Gene of expression	ventral domain	medial domain	dorsal domain	ant. macula	pos. macula	ant. crista	lat. crista	pos. crista	ssc	**Timewindowof expression (hpf)**
eya1[1]	+	-	-	+	+	-	-	-	-	24 – 72
eya2	+	-	-	-	+	-	-	-	-	24 – 48
eya4	+	-	-	+	-	+	+	+	+	24 – 72
six1[2]	+	-	-	+	+	+	+	+	+	24 – 96
six4.1[3]	+	-	-	+[a]	-	-	+[a]	-	+	24 – 60
six4.2[3]	+	-	-	+	-	-	-	-	+[a]	24 – 60
dachA[4]	-	+	+	+	+	-	-	-	+	24 – 72
dachB[4]	-	-	-	+	+	+	+	+	-	24 – 72
dachC[4]	+	+[b]	+[b]	-	-	-	-	-	+	24 – 60

At the stage of 24 hpf all three *eya* genes, all *six* genes and all member of the *dach* gene family are expressed in the otic vesicle, in unique and overlapping sites. Transcripts of all three *eya* genes were found in the ventral wall of the otic vesicle, although the expression of *eya1* is widely spread along the whole ventral site, while *eya2* and *eya4* are restricted to the anterior and posterior maculae respectively. A similar situation was found in *six* gene expression, where *six1* is expressed in the complete ventral wall, while *six4.1* and *six4.2* expression could only be detected at the anterior ventral edge. Contrary to *eya and six*, expression of *dachA* was described to be in the dorsal and medial wall of the otic vesicle, extending to regions of the anterior and posterior maculae. While the expression of *dachB* is distinct in both maculae, *dachC* expression can be detected through the whole otic vesicle, at the ventral, medial as well as dorsal wall. With the exception of *dachC*, all compared genes are expressed in the maculae, although *eya2* expression exclusively occurs in the posterior macula. Furthermore the posterior macula does not express *six4.1* and *six4.2*. In the other sensory patches, the cristae, the gene expression is more limited. *Eya4*, *six1* and *dachB* show overlapping expression in anterior, lateral and posterior cristae. S*ix4.1* is only expressed in the lateral crista.

The semicircular canal primordia express all three members of the *six* gene family, *dachA* and *dachB* as well as *eya1* and *eya4*.

The comparison exposed distinct overlapping expression patterns in the otic vesicle of various members the *eya*, *six* and *dach* transcription factor gene families, including the two novel *eya* genes, *eya2* and *eya4.* These findings assume that the Pax-Six-Eya-Dach signaling network may also be responsible to regulate otic development in zebrafish. However, the regulatory relationship among these genes seems to be different in the various sensory patches of the ear. Except of *eya2* and *dachC* all genes may act together during anterior macula formation (Fig. 34A), while just *six1*, *eya1* and *eya2* as well as *dachA* and *dachB* could cooperate in the development of the posterior macula (Fig. 34B). *Six1* and *six4.1*, *eya4* and *dachB* seem to interact in regulating the development of the cristae (Fig. 34C), while the formation of the semicircular canals appears to be regulated by the three *six* genes, *eya1*, *eya4*, *dachA* and *dachC* (Fig. 34D). The three zebrafish *eya* genes have both discrete and overlapping expression patterns in the otic vesicle, suggesting that their functions may not be fully redundant, although detailed studies of knockout combinations remain to be performed.

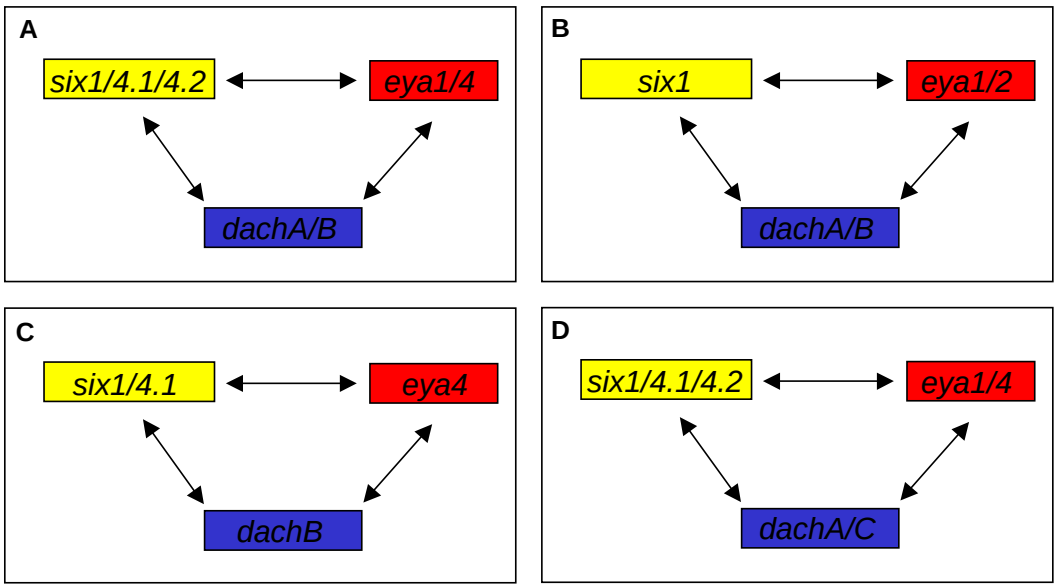

Figure 36 Model of possible regulation and feedback regulation between *eya*, *six* and *dach* genes in different sensory structures of the developing vertebrate otic vesicle based on *in situ* hybridised expression patterns. Shown are the (A) anterior macula, (B) posteriori macula, (C) cristae and (D) semicircular canals.

Discussion – Part II

In *Drosophila* a mutation in any of the compared genes leads to the absence or reduction of the eye, while ectopic expression of *eya* along with either *sine oculis* or *dachshund* is capable of inducing ectopic eyes [BONINI, 1993; BONINI, 1997; CHEN, 1997; MARDON, 1994; PIGNONI, 1997] Previous genetic studies of *Drosophila eyes absent* and of its vertebrate homologues *Eya1-Eya4* have revealed important roles for these genes in cell survival and differentiation, particularly during tissue specification [BONINI, 1993; BONINI, 1998; XU, 1997; XU 1999]. Furthermore, the partial or complete loss of the compound eye in the *Drosophila eyes absent* loss-of-function mutant is associated with inappropriate apoptosis.

In the zebrafish *eya1*$^{-/-}$ (*dog-eared*) mutants morphological defects of the otic vesicle becomes faintly visible at around 48 hpf. During further development the *dog-eared* phenotype turns out to be more obvious. At 72hpf the otic vesicle is significantly smaller. Sensory structures deriving from the pre- and postotic placodes are similarly affected. The size and number of lateral line neuromasts are reduced in zebrafish *dog-eared* mutants [WHITFIELD, 1996; KOZLOWSKI, 2005]. In addition to the morphological anomalies, *eya* $^{-/-}$ zebrafish embryos reveal an increased level of apoptosis, which firstly can be observed at around 24 hpf in the migrating primordia of the posterior lateral line as well as in the ventral region of the developing otocyst. This is 24 hours before first aberrations in the phenotype become visible [KOZLOWSKI, 2005].

4.5 The loss of *eya* promotes apoptosis

While the *dog-eared* phenotype shows distinct anomalies, morphological differences are barely or not visible in *eya2* and *eya4* loss-of-function zebrafish embryos. No phenotypic alterations can be detected in the MO*eya2* phenotype, while at 96 hpf the anterior lateral line neuromasts in MO*eya4* embryos are slightly smaller and the neuromast OC1 is absent. Based on findings of increased levels of cells undergoing programmed cell death in *dog-eared* mutations [KOZLOWSKI, 2005], *eya2* and *eya4* knock-down embryos were analysed with the TUNEL assay to unravel if these genes have a similar effect on apoptotic cell behaviour in the sensory anlagen of the embryo.

At 27 hpf TUNEL-positive cells were counted in the otic vesicle, olfactory organ, the trigeminal and anterior lateral line ganglion in MO and mismatchMO embryos as well as in wildtype siblings. COLE and ROSS (2001) have shown that all listed structures are undergoing the process of programmed cell death at this stage except for the trigeminal ganglion (Fig. 28). In their study, they investigated embryos at the stage of 24 hpf and 30 hpf. At 24 hpf they could not detect any apoptotic cells in the trigeminal ganglion, while at 30 hpf TUNEL-positive cells were found in this structure. However, in this work apoptotic cells in the trigeminal ganglion could be detected already at 27 hpf. Presumably the process of programmed cell death in the trigeminal ganglion starts between 24 hpf and 27 hpf.

MO*eya2* embryos reveal an increased level of apoptotic cells in the trigeminal ganglion (41%) and in the anterior lateral line ganglion (62,5 %), which are distinct expression sites of *eya2*. No differences have been seen in the olfactory organ and the otic vesicle. Because the trigeminal ganglion is an exclusive expression site of *eya2*, the increase of TUNEL-positive cells in this structure has to be viewed as a direct consequence of the loss of *eya2* function. Although *eya2* is expressed in the otic vesicle, even though weakly, no effect on apoptotic behaviour could be observed in the ear. The loss of *eya2* function do not seem vitally important. Another explanation could be the presumption that *eya* genes are highly redundant and can compensate each others functions. The otic vesicle is a highly distinct expression site of *eya1*, which potentially can cover the loss of *eya2* function. This assumed redundancy of *eya1* and *eya2* would also explain why no differences could be detected in the olfactory organ, where both genes are expressed at this stage of development. Although both genes are expressed in the anterior lateral line ganglion, it seems that the loss of *eya2* function can not be rescued by *eya1*. On the other hand WHITFIELD et al. (1996) have shown that in the *dog-eared* mutant the anterior lateral ganglion does not show an increased number of TUNEL-positive cells. This is confirmed by the observation, that the homeobox gene and neuronal marker *tlxA* is properly expressed in the ganglion and does not reveal any size reductions [KOZLOWSKI, 2005]. Possibly, *eya2* can compensate the loss of *eya1* in the anterior lateral line ganglion. However the anterior lateral line is also an expression site of *eya4*. Therefore it has to be assumed that either *eya2* or *eya4* or both save the loss of *eya1* function.

Like the loss of *eya2*, the loss of *eya4* function causes a highly increased level of apoptosis (130%) in the anterior lateral line ganglion at 27 hpf. Based on the assumption of a high redundancy among *eya2*, *eya4* and *eya1* in zebrafish, it can be anticipated *eya2* and/or *eya4* can rescue *eya1*, but they can not compensate each others function. Beside in the anterior lateral ganglion no other effects on apoptotic cell behaviour was seen in *eya4* loss of function embryos. In the otic vesicle it may be a similar situation like in the loss of *eya2*. Either *eya4* function is not vitally important or its function can be covered by another *eya* gene, in this case *eya1*. *Eya4* is neither expressed in the olfactory organ nor the trigeminal ganglion, therefore an effect on programmed cell death was not expected.

At 54 hpf apoptosis was investigated in the otic vesicle, olfactory organ, and the neuromasts of the anterior and posterior lateral line in MO and mismatchMO embryos as well as in wildtype siblings. At this stage, all these structures undergo programmed cell death in wildtype embryos (Fig. 28) [COLE & ROSS, 2001].

Except for the olfactory organ, no differences could be detected within the sensory structures in *eya2* knock-down embryos and wildtype siblings. Because *eya2* is no longer expressed in the otic vesicle at this point of time, the loss of function does not affect programmed cell death in the inner ear. In contrast, *eya2* is expressed in the neuromasts of both the anterior and posterior lateral line. Nevertheless, the loss of *eya2* function does not have any effect on apoptotic activity in here. The neuromasts are also major expression sites of *eya4* as well as of *eya1*. It appears that *eya1* and/or *eya4* can compensate the loss of *eya2* in the anterior and posterior neuromasts. The olfactory organ revealed an increased number of TUNEL-positive cells (100%). It is uncertain if *eya1* is expressed in

the olfactory organ at this stage. Distinct expression can be seen at 48 hpf, but it is absent at 60 hpf. In addition, KOZLOWSKI et al. (2005) have shown that the apoptotic activity in *dog-eared* embryos does not have any effects in this sensory structure. This suggests two possible interpretations: either the olfactory organ is a distinct expression site of *eya2* at this stage of embryonic development, consequently the loss could not be compensated by another *eya* gene, or both, *eya1* and *eya2* are expressed in overlapping patterns but *eya1* can not rescue the loss of *eya2* function.

MO*eya4* injected embryos do not show any increase of apoptotic activity in olfactory organ or the otic vesicle. In contrast to the loss of *eya2*, the loss of *eya4* function leads to an increased level of apoptosis in the anterior neuromasts (143%), but not in those of the posterior lateral line. DASPEI staining has shown that the neuromasts are smaller, one neuromasts is even absent. In *dog- eared* mutants DASPEI staining reveals a similar situation. The anterior neuromasts are consistently smaller, and some of them are absent. Contrary to the loss observed in *eya4* "knock-downs", in *dog-eared* the neuromasts of the posterior lateral line are mostly absent [WHITFIELD, 1996]. It can be supposed, that both *eya1* and *eya4* are vitally important for proper development of the lateral line neuromasts, therefore the deficit of one of them can not be compensated by the other *eya* gene.

Eya4 is not expressed in the olfactory organ, which explains why no differences in apoptotic behaviour could be observed. Indeed the otic vesicle is a major expression site of *eya4*, although only in differentiated sensory structures at later stages. The inner ear in *dog-eared* mutants show both an increased level of apoptosis throughout the whole otic vesicle as well as morphological defects. While the apoptosis can be detected already at 24 hpf, defects in the phenotype emerge at later stages around 48 hpf and more distinct at 72 hpf. Most *dog-eared* embryos reveal absent hair cells in the three cristae, in rare cases 2-3 hair cells in one of the three cristea could be detected. For that reason *eya1* does not seem to be required to differentiate hair cells, but rather for maintenance or survival of the hair cells [KOZLOWSKI, 2005]. Contrary, neither *eya2* nor *eya4* reveal any morphological aberrations or increased apoptotic activity in the inner ear. *Eya1* seems to be capable to compensate the deficit of both genes. Consequently, each gene for itself does not seem to be vitally important during ear development. However, *eya4* expression in the ear lasts at least until 72 hpf. Therefore it's possible that the loss of *eya4* function may have consequences at later stages of development.

These findings in MO*eya2* as well as MO*eya4* injected embryos show, that the loss of a single *eya* gene triggers apoptosis-mediated cell death. More precisely the loss of the eyaHR is responsible for the inappropriate programmed cell death. The used splice-site morpholinos truncated the protein immediately upstream of the eya domain, therefore just the highly conserved eya region is missing in the MO injected embryos, instead of the whole gene sequence. The loss of the eyaHR, the protein/protein binding domain, prevents eya from interacting with six or dach and being transported into the nuclei. These findings of inappropriate cell death support the leading hypothesis proposes that eya represses programmed cell death. It is assumed that the loss of eya proteins exerts a dominant-negative effect. Dominant-negative mutations have an altered gene product that acts negatively to the wild-type allele. This usually occurs when the truncated protein product still interacts with the same elements as the wild-type product, but is lacking some aspects of its functions. These mutations are characterised by a dominant or semi-dominant phenotype. Dominant negative mutations often result in autosomal dominant diseases. The fact that Branchio-Oto-Renal syndrome is an autosomal dominant

disease caused by a mutation in the human Eya1 protein supports the view that a dominant negative mechanism is responsible for the eya mutant phenotype.

The loss of *eya* function in zebrafish is less severe than the loss of *eyes absent* in *Drosophila*. This is due to the fact that gene duplications in vertebrates subdivided ancestral functions amongst two or more redundant homologous genes. Nevertheless, even though the three zebrafish *eya* genes have many overlapping expression sites they can not save each others function without any exceptions. The functional redundancy seems to be limited and variable among genes as well as structures. Therefore, double and triple knock-down experiments of *eya1*, *eya2* and *eya4* would be of interest, to obtain further information of the role and importance of eya genes in vertebrates.

4.6 The gain of eya function repress apoptosis

The *Drosophila eyeless (ey)* was the first gene shown to be capable of directing ectopic eye formation [HALDER, 1995]. *Drosophila eyeless* derives its name from the “eyeless” phenotype that is caused by the loss of function of the *ey* gene. *Ey* is a homologue of the vertebrate *Pax6* transcription factor, which contains two DNA-binding motifs: a paired box and homeobox [QUIRING, 1994]. *Ey* function is required for the expression of downstream genes, like *eya*, *six* and *dach*. This “transcriptional hierarchy” is not absolute, ectopic expression of downstream members of the network can also induce ectopic eye tissue and the expression of the upstream gene eyeless via regulatory feedback loops [BONINI, 1997, SHEN & MARDON, 1997]. Both *eya* and *dach* were shown to be capable of directing ectopic eye formation by themselves. However, *eya* combined with *ey*, *dach* or *six* were more effective, generating larger and more frequent ectopic eyes in *Drosophila* [BONINI 1997, CHEN, 1997, PIGNONI, 1997].

In contrast to the fly, it is not known yet, if ectopic expression of *eya* genes have a similar effect in the zebrafish. Therefore, gain-of-function experiments were performed, by injecting embryos with in vitro synthesised *eya1*, *eya2* or *eya4* mRNA. According to the knock-down experiments, programmed cell death in *eya1*, *eya2* or *eya4* overexpressing embryos were detected with the TUNEL assay. Gain of function effects can be detected in structures that are not expressing the respective gene in the wildtype. Therefore, the lens, as a non-*eya* expressing sensory structure, provides an appropriated tissue to unravel if ectopic expression of *eya* genes affects apoptotic cell behaviour in the sensory anlagen.

Unlike in *Drosophila*, ectopic *eya1*, *eya2*, or *eya4* expression in zebrafish embryos reveals no phenotypic anomalies at 27 hpf. However detection of apoptotic cells has shown reduced numbers of TUNEL-positive cells in the lens of *eya1* (17%), *eya2* (28%) as well as *eya4* (35%) mRNA injected embryos. These findings reveal that the overexpression of a single *eya* gene can reduce naturally occurring programmed cell death in ectopically *eya* expressing structures. However it is not capable of inducing the development of ectopic sensory structures usually expressing *eya*. This could be for the same reason that the loss of a single *eya* gene has not the same severe effect in zebrafish like in *Drosophila*. By the duplication of genes, functions, which are essential for the development of ectopic structures or tissues, were separated. Furthermore studies in *Drosophila* have shown that overexpression experiments of *eya* are more effective in combination with other transcription factors

like *six* or *dach* [BONINI 1997, CHEN, 1997, PIGNONI, 1997]. Therefore, as in loss of function studies, combined overexpression experiments of all three *eya* genes and *eya* combined with *six* or *dach* could be helpful for a better understanding of *eya* genes and their function during zebrafish development.

4.7 Eya regulates programmed cell death

The results of the present study demonstrate that *eyes absent* genes influence the process of programmed cell death in both directions. The numbers of cells undergoing apoptosis are higher in *eya2* and *eya4* loss-of-function embryos than in wild-type siblings. Contrary, gain of *eya1*, *eya2* or *eya4* function results in a reduced amount of apoptosis-mediated dead cells. These outcomes are in partial agreement with the before reported loss-of-*eya1* functional studies in *Drosophila* and mouse, where increased apoptosis was detected in various organs during embryonic development. Additionally, the present study has shown successfully that *eyes absent* is not just able to promote apoptosis, but also to reduce apoptotic cellular death. KRIEBEL et al. identified a vertebrate member of the *Eya* family in *Xenopus*, *Xeya3*, which is expressed in the anterior neural plate, including the eye field. Overexpression of *Xeya3* creates immense enlargements of brain and retinal tissues, mainly caused by overproliferation of neural precursor cells. On the other hand, suppression of *Xeya3* function induces local apoptosis within the sensorial layer of the anterior neuroectoderm. These data also reveal an active role of the *eya* genes in controlling apoptosis.

Apoptosis is a major factor in organ and tissue development, it is highly conserved and follows morphologically distinct patterns. These highly stereotyped morphological changes seem to be under the strict control of a strictly regulated cellular program. While cellular programs, which control apoptosis are well investigated, the signalling pathways triggering apoptosis are less clear yet. Genes of the cell death pathway encode for proteins functioning in three different ways, as regulators, adapters, or effectors to repress or support apoptosis [VAUX & KORSMEYER, 1999]. The functional signification of these findings is that e*ya* genes seem to act as such regulators. Both *eya1*, *eya2* and *eya4* loss-of-function embryos reveal an enhanced apoptosis, while the gain-of-function in these genes reduces levels of apoptosis. These results support the concept that inappropriate changes in the steady state levels of Eya proteins regulate programmed cell death during development by activating or repressing apoptosis. However the precise role of these developmental regulators in controlling programmed cell death is still unresolved.

Gene duplication is a prominent mechanism generating redundant genes. Redundancy provides a protective effect against deleterious mutations, therefore natural selection might be involved in generating and maintaining partial redundancy. Expression pattern analysis of the zebrafish *eya2* and *eya4* genes as well as comparisons with zebrafish *eya1* [SAHLY, 1999] have shown widely overlapping embryonic expression of all three genes. Therefore it can be assumed, that the specific morphological changes in the *dog-eared embryos*, in contrast to the widespread expression of *eya1*, are the consequence of functional redundancy between these three *eya* gene family members.

5 Conclusions and Perspectives

Combining these findings with *Xenopus* [DAVID, 2001; KRIEBEL, 2007], chicken [MISHIMA, 1998], mouse [XU, 1997; BORSANI, 1999] and human [ABDELHAK, 1997; ZIMMERMANN, 1997], it has become clear that the *Eya* genes are highly conserved among vertebrates. Sequence analysis have revealed a prominent level of amin acid identity, whereas expression pattern comparison demonstrated both overlapping as well as redundant expression of all three genes among all model organisms.

Within the early zebrafish inner ear development eya2 and eya4 proteins are part of the regulatory Pax-Six-Eya-Dach gene network. However the regulation of these genes depending on their binding activity with other transcription factors of this network reminds unclear yet.

Consistent with the published observations of an increased level of apoptosis mediated cell death in zebrafish *eya1* (*dog-eared*) mutations, an increase level of apoptosis was also found in zebrafish embryos with loss of *eya2* or *eya4* function. However the by loss of function affected region are not identical, but differ from each other depending on the respective expression sites. Though only the sensory structures are pretentious by a higher rate of cell death in the embryos with loss of eya function. Furthermore ectopically expressed eya proteins reduce the number of cells undergo programmed cell death.

The zebrafish *eya* genes are a useful marker to study placodal and neuronal development of cranial sensory structures in the developing zebrafish embryo. Further work addressing the relationship between the different *eya* gene family members as well as its role within the regulatory Pax-Six-Eya-Dach gene network will contribute substantially to understand the early sensory organ and the inner ear in particular development.

6 Summary

Developmental biology addresses how cells are organised into functional structures. Therefore it is crucial to understand the molecular basis for processes in development by studying the expression and function of relevant genes and their relationship to each other. A gene function can be studied by expression pattern analysis and comparison, creating a loss-of-function situation, in which the change in developmental processes is examined in the absence of a functional gene product, or in gain-of-function studies, where a gene product is ectopically upregulated. This thesis describes the characterisation of three novel members of the *Eya* gene family in zebrafish *(Danio rerio)*, *eya2*, *eya3* and *eya4*. A detailed analysis of expression pattern and missfunction studies in zebrafish embryos provides information about possible functions of these genes.

Sequence analysis of the zebrafish eya2, eya3 and eya4 proteins have revealed two highly conserved domains; the eya homology region (eyaHR) and eya domain 2 (ED2). Moreover all three eya proteins contain sequence motifs equivalent to the haloacid dehalogenase (HAD) superfamily of phosphohydrolases, recently described for mammalian Eya proteins by LI (2003); RAYAPUREDDI (2003) and TOOTLE (2003). Therefore zebrafish eya 2-4 proteins function as transcriptional co-factors which possess protein phosphatase activity. Alignments of the deduced amino acid sequences revealed a high conservation of both its phosphatase and transcription factor activity and identified significant homologies with their mammalian counterparts, as well with the *Drosophila* eya protein.

As a first step towards a functional analysis of the *eya* gene family during sensory organ development, with focus on the inner ear, the expression patterns of the three zebrafish *eya* genes were analysed and compared. Expression pattern analysis was carried out by RNA *in situ* hybridisation. While no *eya3* transcripts are detected in the early embryo, both *eya2* and *eya4* are expressed in distinct patches within the cranial placodes and their derivates, otic vesicle, and in primordia and neuromasts of the lateral line system. *Eya2* expression is observed in the olfactory and trigeminal placodes and the placodes of several cranial ganglia. *Eya4* transcripts are found in some of the corresponding cranial ganglia and in developing somites.

Eya proteins are part of an evolutionary conserved network of interacting proteins which also include Six (*sine oculis*) and Dach (*dachshund*) proteins. This network functions in various vertebrate organ development processes, among others the otic vesicle. They form transcriptional complexes that either activate or repress target genes, depending on the context in which they act. The intrinsic protein phosphatase activity of Eya is capable of switching the function of Six-Dach complexes from repression to activation, thereby regulating genes encoding growth control and signalling molecules required for precursor cell proliferation. For more detailed analysis of the *eya* gene during inner ear development, expression patterns of three zebrafish *eya (1,2,4)* genes, three *six (1,4.1,4.2)* genes, and three *dach (A,B,C)* genes during otic development in zebrafish embryos were compared. The data obtained indicates that the various members of the three gene families investigated subdivide the otic vesicle in regions with characteristic patterns of co-expression, indeed unique expression sites were also detected. Therefore a high level of functional redundancy among these genes can be assumed, although exclusive gene expression sites suggest that the functions are not completely redundant.

The significance and biological relevance of this observation is tested by overexpression experiments and the analysis of gene knock-down experiments by using in vitro synthesised *eya1*, *eya2*, and *eya4* mRNA as well as antisense *eya2* and *eya4* Morpholino oligonucleotides respectively injected into zebrafish embryos. Ectopically upregulated function of *eya1*, *eya2* and *eya4* revealed a reduced level of apoptosis-mediated cell death, while the loss-of-function of *eya2* and *eya4* triggers programmed cell death. These results maintain the idea of apoptosis affective activity, which was described for the loss-of-function for *eyes absent* in *Drosophila*, zebrafish (*eya1/dor-eared*) and mouse($Eya^{-/-}$), as a general function of *eya* gene relatives.

7 Methods

7.1 Zebrafish maintenance

Zebrafish were maintained under standard laboratory conditions WESTERFIELD (1993). From pair wise mating embryos were collected and staged by hours post fertilisation (hpf). Embryos were kept in 1x Embryomedium (EM) at 28,5°C. For microinjection experiments development was delayed by incubating the embryos at RT immediately after fertilization. When embryos were allowed to develop beyond 20 hpf, 0,003% phenylthiourea (PTU) was added to 1x EM to prevent melanisation. After 24 hpf embryos were dechorionated and fixed at desired stage for at least 4 h at RT or o/n at 4°C in 4% PFA. For dehydration and permeabilisation they were transferred to 100% methanol for 2 h at –20°C.

7.2 Molecular biological methods and Immunohistochemistry

If not otherwise stated, all methods were performed according to SAMBROOK and RUSSELL (2001). DNA/RNA concentration and purity was verified through agarose gelelectrophoresis and photometric quantification. Used concentrations and amounts of all preparations are shown below. Amounts of restriction enzyme used depended on the specific units/µl of each enzyme and should amount to 1-2 units per µg plasmid DNA.

7.2.1 Preparation of Plasmid DNA

7.2.1.1 Transformation

To obtain probes for *in situ* hybridisation or synthetic mRNA for microinjections sufficient template DNA had to be generated by transforming bacteria (*E. coli* DH-5α competent cells) with the respective plasmids. Therefore competent cells (stored at –80°C) were thawed on ice. 20ng/µl plasmid DNA were added to the bacteria and incubated on ice for 10min. Subsequently, cells were incubated at 42°C for 2min. This “heat shock” causes the bacterial cells to open their membranes and insert the plasmid. Transformed cells were added to LB-media (1:10) and incubated at 37°C while rocking at 250rpm on a shaker. Afterwards the cell culture was plated on LB-agar dishes and incubated o/n at 37°C. Because the plasmids carry resistance to the antibiotic ampicillin, LB-agar plates were supplied with ampicillin (1:1000), to make sure that just transformed bacteria grow.

7.2.1.2 Mini-Preparation

After transformation, DNA was isolated by Mini-Preparation using alkaline lysis. Therefore, single bacteria colonies were picked and transferred into 5ml LB-media/ampicillin (1:1000) and incubated o/n at 37°C/250rpm. To harvest bacteria cells, the overnight cell cultures were centrifuged for 5min at 4°C/14.000rpm. DNA preparation was carried out as follows. The obtained pellets were resuspended in 150µl SI. 2 volumes SII were added to the samples, inverted and incubated for 2min on ice. Another 1½ volume SIII was added, inverted and incubated for 5min on ice. Subsequently, the samples were

centrifuged for 7min at 4°C/ 14.000rpm and the supernatants transferred. The DNA was purified by phenol-chloroform-extraction (1volume phenol-chloroform-isoamylalkohol (25:24:1)) and precipitated by using 100% isopropanol. The obtained pellets was washed with 70% ethanol and resuspended in 50µl RNase-free H_2O.

7.2.2 Sequencing

To confirm that the provided clones are indeed three different homologs of the *Drosophila eyes absent* gene, the purified plasmid DNA was commercially sequenced by Sequence Laboratories, Göttingen. Using *Advantage Read* affords the reading of around 900 base pairs. If required, appropriate primer oligonucleotides were identified (designed by biomers.net and Roth, Karlsruhe) to run further *Advantage Reads* to obtain the whole DNA sequence. All sequences were sequenced from their 5'- and 3'- ends.

7.2.3 Subcloning

7.2.3.1 Dephosphorylisation pCS2+/ EcoRI

Vector DNA	0,5µg
Antarctic-phosphatase buffer	1µl
Antarctic-phosphatase	1µl
RNase-free H_2O	to a final volume of 10µl
37°C 20 min	
heat inactivation 65°C 5 min	

7.2.3.2 Ligation of Eya4/EcoRI; pCS2+/EcoRI

Linearised template pCS2+	100ng
Linearised template eya4	200ng
T4-DNA-ligase buffer	1µl
T4-DNA-Ligase	1µl
RNase-free H_2O	to a final volume of 10µl
RT 10 min	
Heat inactivation 65°C 10 min	

7.2.4 In vitro Transcription

7.2.4.1 Linearisation of plasmid DNA

Plasmid DNA	10µg
appropriate 10x buffer	3µl
(depending on the buffer 10x BSA	3µl)
specific restriction enzyme (20u/µl)	xµl
RNase-free H_2O	to a final volume of 30µl
37°C 2h	

Linearised DNA was purified by phenol-chloroform-extraction using Gel-Lock-Tubes (Eppendorf) and ethanol precipitation (1/10 volume 3M Na-acetate, pH 5.2.; 3 volume ice-cold 100% ethanol). Obtained DNA pellet was washed with ice-cold 70% ethanol and diluted in RNase-free H_2O to an optimal final concentration of 1µg/µl.

7.2.4.2 Synthesis of single-stranded RNA probes by In Vitro Transcription

Linearised template DNA	1µg
5x transcription buffer	4µl
100mM dithiothreitol DTT	2µl
RNase inhibitor (20u/µl)	2µl
10x NTP-DIG/FLU-Mix	2µl
DNA-dependent RNA polymerase (~ 10u/µl)	xµl
RNase-free H_2O	to a final volume of 20µl

37°C 2h
add 2µl DNase for 15min at 37°C
RNA precipitation: ½ volume 7.5M NH_4-acetate; ice-cold 100% ethanol.
Obtained RNA pellet was washed with ice-cold 70% ethanol and diluted in Hyb^+ to an optimal final concentration of 5ng/µl.

7.2.4.3 Synthesis of Capped RNA by In Vitro Transcription

To synthesize *in vitro* capped mRNA the Ambion mMessage mMachine kit (Ambion) SP6 and the RNeasy Cleanup Mini kit (Qiagen) were used.

Linearised template DNA	1-1,5µg
10x transcription buffer	2µl
2x ribonucleotide Mix	10µl
10x Enzyme Mix	2µl
RNase-free H_2O	to a final volume of 20µl

7.2.5 Whole-Mount *in situ* Hybridisation (ISH)

ISH is a convenient technique to detect the localisation of target mRNA in tissue or embryo by visualizing the transcription of the gene of interest. This method allows very sensitive detection of RNA transcripts and an excellent spatial resolution [STREIT & STERN 2001]. In Zebrafish it is, in most cases, applied on whole-mount embryos, using digoxigenin-labeled antisense RNA probes and the alkaline phosphatase (AP) detection method [WILKINSON 1998]. Patterns of gene expression can then be compared by microscope images, providing two-dimensional information; high-quality results has been shown by THISSE et al. (1993) *In situ* hybridisation was carried out as described by WESTERFIELD (1993) with slightly modifications.

For permeabilisation fixed embryos were rehydrated in 75%, 50%, 25% Methanol/PBS and washed 4x 5 min in PBT. Embryos older then 24 hpf were digested with proteinase K (final concentration: 2,5µg/µl in PBT) according to age (24 hpf/5min; 48 hpf/10min; > 60 hpf/20min) and refixed in 4% PFA for 20 min at RT followed by further washing steps in PBT. For pre-hybridisation the embryos were transferred in prewarmed Hyb^+ at least 1 h at 65°C. After Hyb^+ was replaced by also prewarmed RNA-probe (~ 1,5µg) in 300 µl Hyb^+ the embryos were incubated o/n at 65°C. The probe was removed and embryos washed 1x 10 min in 50% Hyb^-/ 2x SSCT, in 25% Hyb^-/ 2x SSCT and in 2x SSCT and 2x 30 min in 0.2x SSCT at 65°C. Afterwards embryos were washed 1x 5 min in 0,15x SSCT/ 25% PBT, 0,1% SSCT/ 50% PBT, 0,05% SSCT/ 75% PBT and in PBT, blocked in PBT plus blocking reagent (2% serum, 2 mg/ml BSA) for 1-2 h at RT and incubated o/n at 4°C in α-DIG-AP (1:4000 dilution in PBT + 2% FCS, 2 mg/ml BSA). Embryos were rinsed 5x 15 min in PBT and equilibrated 3x 15 min in alkaline phosphatase (AP) buffer. For detection embryos were stained with BM Purple substrate. Reaction was stopped by several washings with PBT. Subsequently embryos were refixed in 4% PFA o/n and stored in PBT at 4°C.

7.2.6 Whole-Mount double *in situ* Hybridisation (DISH)

For double ISH, embryos were hybridised with probe mix (DIG-labelled and FLU-labelled RNA-probes) and processed as described above. After BM Purple staining embryos were rinsed in PBT, refixed in 4% PFA o/n at 4°C and washed in PBT again. Embryos were treated with 100mM glycin-Cl, pH 2,2 for 10 min at RT to remove the alkaline phospatase-coupled α-DIG antibody, washed 5x 5min in PBT, blocked for 1 h at RT and incubated o/n at 4°C in α-FLU-AP (1:2000 dilution in PBT + 2% FCS, 2 mg/ml BSA). Instead of using BM Purple for detection freshly prepared FastRed substrat was used. After staining embryos were treated like described before.

7.2.7 Flourescent Whole-Mount *in situ* Hybridisation (FISH)

FISH was carried out by using the Flourscent in situ hybridisation TSA (Tyramide Signal amplication) kit (Invitrogen). Until the antibody incubation step the protocol is similar to the one used for regular ISH was processed. Instead of the AP conjugate a α-DIG-POD antibody (1:50 dilution in PBT + 2% FCS, 2 mg/ml BS) was used. Embryos were incubated at 4°C o/n and washed the following day all day and over night in PBT with at least 8 changes. For fluorescent staining the embryos were transferred for 10-15 min to TSA staining buffer (1:100 tyramide in reaction buffer + peroxidase) and subsequently rinsed several times for a few hours in PBT.

7.2.8 Immunohistochemistry on *in situ* hybridised embryos

In some case, it's useful to combine the detection of a RNA transcript by in situ hybridisation with the detection of a particular antigen by using a specific antibody.

In situ hybridised and refixed embryos were washed 2x 5 min in PBT, 1x5 min in H2O, permeabilised in prechilled acetone for 7 min at –20°C, washed 1x5 min H2O, 2x5 min in PBT, blocked in 10% FCS in PBT for 1 h at RT. Antibody incubations were performed as follows: Primary monoclonal zn12 antibody incubation (1:250 dilution in 10% FCS-PBT) o/n at 4°C. Embryos were washed 4x 30 min in

10% FCS-PBT at RT, and incubated o/n at 4°C in preabsorbed secondary biotinylated α-mouse IgG antibody (diluted 1:10000 in 10% FCS-PBT). After several washes in 10% FCS-PBT immunohistochemical staining was carried out with preincubated AB complex (ABC Kit Vector Laboratories), DAB substrate, and hydrogen peroxide (Vector Laboratories). Reaction was stopped by several washes with PBT, embryos refixed in 4% PFA o/n, and stored in PBT at 4°C.

7.2.9 DASPEI

DASPEI (2-(4-(Dimethylaminostyryl)- 1 –methyl-pyridinium iodid; Fluka BioChemika) is an easy and fast method, to mark haircells of surface neuromasts. 96-hour old larvae were covered in 1mM DASPEI for about 15 min and washed carefully in EM several times. For observation under the compound scope embryos were anaesthetised in tricane [WESTERFIELD, 1993] and mounted in methylcellulose in a depression slide.

7.2.10 Detection of Apoptotic Cells in Whole Mounts

Apoptosis is a form of cell death that eliminates compromised or superfluous cells. The employed ApopTag® Peroxidase In Situ Apoptosis Detection Kit detects apoptotic cells in situ by labelling and detecting DNA strand breaks by the TUNEL (terminal deoxynucleotide transferase (TdT) -mediated dUTP end labelling) assay. The enzyme TdT catalyses a template-independent addition of nucleotide triphosphates to the 3'-OH ends of double-stranded or single-stranded DNA. These DNA fragments are typically localized in morphologically identifiable nuclei and apoptotic bodies. DNA fragments labelled with an α-DIG-AP antibody and have been detected by using BM purple substrate [ZAKERI, 1993; WILKINSON 1998].

To permeabilise fixed embryos they were rehydrated in a methanol/PBT series (75%, 50%, 25%) for 5 min each, washed 3x 5 min in PBT and incubated in proteinase K (final concentration: 10µg/ml in PBT) at RT according to age like described above. Then washed twice for a few seconds in PBT, postfixed in 4% PFA for 20 min at RT, washed 5x 5min in PBT, and postfixed for 10 min with prechilled ethanol/acetate (2:1) at –20°C followed by 3 further washes with PBT. For the terminal transferase reaction embryos were incubated for 1 h at RT in 75µl (1 drop) equilibration buffer. To prepare working strength TdT enzyme the reaction buffer was added to the TdT enzyme in a ratio of 2:1. Equilibration buffer was replaced by working strength solution and embryos incubated at 37°C o/n. Reaction was stopped by washing in stop/wash buffer (1 ml stop/wash buffer in 34 ml dH_2O) for 3-4 h at 37°C. For detection embryos were washed 3x 5 min in PBT at RT, blocked with 2mg/ml BSA/ 5% FCS/ PBT for 1 h at RT and incubated for 2 h at RT with α-DIG-AP in2mg/ml BSA/ 5% FCS/ PBT (1:2000). Subsequently embryos were washed all day and o/n with 2mg/ml BAS in PBT with at least 8 changes of blocking buffer. Embryos were equilibrated 3x 5 min in alkaline phosphatase (AP) buffer and stained with NBT/BCIP. Reaction was stopped by several washings with PBT. Embryos were refixed in 4% PFA o/n and stored in PBT at 4°C.

7.3 Embryological methods

7.3.1 Microinjection

Microinjections are used to investigate the role of a gene during development by overexpression or misexpression of the gene of interest. To obtain a gain-of-function phenotyp synthetic mRNA was injected. To knock down gene function by gene-specific inhibition of mRNA translation antisense morpholino oligonucleotides (MO) have been used. For injection experiments the embryos were transferred into injection dishes immediately after spawning at the 1-cell stage. Injection dishes were prepared with 1% agarose in EM filled in petri dishes. Furrows were formed by placing a mold on top of the agarose while it cooled down [KIMMEL ZebrafishBook]. To hold embryos in place for injection they were aligned along the furrows. Surplus medium was sucked off so that surface tension of the remaining medium kept the embryos in place in the furrows. During the 1cell up to the 8 cell stage RNA was injected through the chorion into the yolk or the embryonic cell. Although it is preferable to inject directly into the blastomeres, RNA injected into the yolk will move into the cytoplasm via cytoplasmatic streaming [MULLINS, 2005]. All injections were done using a Transjector 5246 (Eppendorf). The injected volume was usually 2 nl, adjusted by changing the pulse duration and/or strength.

7.3.1.1 Morpholino (MO)

Morpholino phosphorodiamidate oligonucleotides (mopholinos, MPs) have been used successfully in zebrafish [NASEVICIUS & EKKER, 2000] and Xenopus [HEASMAN, 2000] to knock down gene function by gene-specific inhabitation of mRNA translation [EKKER, 2000]. These are chemically modified oligonucleotides that bind to and block translation of mRNA *in vitro*, in tissue culture cells [SUMMERTON, 1999] and in vivo [HEASMAN, 2000]. In addition to their ability to block cytosolic processes, MO can enter the nucleus [PARTRIDGE, 1996]. They function through an Rnase-H- independent mechanism by obstructive translation initiation and their high mRNA affinity and specifity makes in vivo targeting highly predictable and reduces non-specific effects. MO can act in two ways. Those who are designed to the 5' UTR or early coding sequences function by blocking cytosolic processes. MO designed to overlap splice sides can modify pre-mRNA splicing in the nucleus [DRAPER et al. 2001].

Based on the *eya2* and *eya 4* exon/intron structure 25-mer antisense splice side MO were designed. For *eya2* a morpholino were designed complementary to the exon4/intron4 splice junction (*eya2*MO: 5'-TTGGTTGTTTTCTCACCTGTGTGTG-3') as well as a mismatch morpholino, a morpholino sequnce containing 5 mispaired nucleotide (*eya2*mMO: 5'-TTcGTTcTTTTgTCACCTcTGTcTG-3'). For *eya4* the exon11/intron11 splice junction were used to design a morpholino (*eya4*MO: 5'-CCATCCGAACATACCTCAAGGTCAC-3') just as the mismatch morpholino (*eya4*mMO: 5'-CgATCCcAAgATACCTgAAGGTgAC-3'). Morpholino oligonucleotides were dissolved in water at the concentration of 160 mg/ml. The resulting stock solution was diluted in Danieau solution and phenolred to working concentration of 10ng/nl, injected volume was approximately 2nl. All Morpholinos were obtained from Gene Tools, LLC.

7.3.1.2 synthetic mRNA

To synthesize *in vitro* capped mRNA of *eya1*, *eya2*, *eya4* and GFP was diluted in Danieau solution and phenolred to a final concentration of 120ng/µl for *eay1*, *eya2* and *eya4* RNA. For internal control 80 ng/µl of GFP mRNA was coinjected and visualised before fixation. Injected volume was approximately 2nl.

7.4 Sectioning and microscopy

7.4.1 Mounting

Embryos can be mounted in glycerol or dehydrated and mounted in DPX Mountant. Glycerol causes less shrinking, but is not as effective as clearing agent. Except for the TSA labelled embryos glycerol mounting was used for all performed stainings.

7.4.1.1 Glycerol mounting

For whole-mount photography fixed embryos were transferred from PBS into glycerol. For analysis at higher magnifications, embryos were de-yolked and mid-sagittally hand-sectioned using a razor blade sliver fitted into a needle holder. The embryos were transferred into a glycerol droplet on a microscope slide. A coverslip was placed on top and gently pressed down until the embryo is flattened but not squished (Flat-Mounts). Flat-mounted embryos were observed and photographed under differential interference contrast (DIC) optics using a Zeiss Axiophot. Imaging DASPEI examined embryos a 589nm filter were used.

7.4.1.2 DPX mounting

Deyolked embryos were dehydrated through an increasing ethanol/PBS series: 30%, 50%, 70% (10min each), 2x 100% (10min each) ethanol and cleared in in 66% benzyl alcohol/ 33% benzyl/ benzoate. For mounting the embryos were picked up and placed in a drop of DPX mountant (Fluka BioChemica) on a bridged coverslip (see below). A new coverslip was gently lowered on top and rolled until the embryo was in the desired position. For documentation of mounted embryos a Leica MZ FLIII, 488nm was used.

7.4.1.3 Araldite Sectioning

Embryos were embedded into araldite (Polyscience). To this end they were dehydrated through a ascending ethanol/PBS series: 25%, 50%, 75% (10min each), 100% (1x 15min and 1x 30min) and washed in acetone for 15 min. The acetone was replaced by fresh acetone and embryos were washed for another 30min. Subsequently embryos were incubated in a mixture of 50% araldite and 50% acetone for 48 h at RT. Embryos were carried over into small chambers, covered completely with 100% araldite, and polymerised for 24 h at 60°C. 10µm slices were sectioned using a microtom (Leica JUNG RM 2055). Small drops of water were set up on with ethanol precleaned slides. Each slice was transferred to a single drop of water on top of a precleaned microscope slide. After evaporation of the water slides were covered with 100% araldite and a coverslip was placed on top. For polymerisation

slides were incubated for 24 h at 60°C. Sections were analysed and photographed under differential interference contrast (DIC) optics using a Zeiss Axiophot.

8 References

ABDELHAK, S. et al. A human homologue of the *Drosophila eyes absent* gene underlies Branchio-Oto-Renal (BOR) syndrome and identifies a novel gene family. Nat. Genet. 15, 157-164 (1997)

ABDELHAK, S. et al. Clustering of mutations responsible for branchio-oto-renal (BOR) syndrome in the *eyes absent* homologous region (eyaHR) of EYA1. Hum. Mol. Genet. 6, 2247-2255 (1997)

AHMED, Z. M. et al. The molecular genetics of Usher syndrome. Clin. Genet. 63(3), 431-444 (2003)

AKIMENKO, M. A. et al. Combinatorial expression of three zebrafish genes related to Distal-less: part of a homeobox gene code for the head. J. Neurosci. 14, 3475-3486 (1994)

AZUMA, H. et al. Mutations in a human homologue of the *Drsophila eyes absent* (EYA1) detected in patients with cogenital cataracts and ocular anterior segment anomalies . HUM: Mol: Genet. 9, 363-366 (2000)

BAKER, C. V. H., BRONNER-FRASER, M. Vertebrate Cranial Placodes I. Embryonic Introduction. Dev. Biol. 232, 1-61 (2001)

BAKER, C. V. H. et al. Pax3-Expressing Trigeminal Placode Cells Can Localize to Trunk Neural Crest Sites but are Committed to a Cutaneous Sensory Neuron Fate. Dev. Biol. 249, 219-236 (2002)

BESSARAB, D. A. et al. Expression of Zebrafish *six1* During Sensory Organ Development and Myodenesis. Dev. Dyn. 230, 781-786 (2004)

BEVER, M., FEKETE, D. M. Atlas of Developing Inner Ear in Zebrafish. Dev. Dynamics 223, 536-543 (2002)

BHATTACHARYYA, S., BRONNER-FRASER, M. Hierarchy of regulatory events in sensory placode development. Current Opinion iin Genetics & Development 14, 520.526 (2004)

BISSONNETTE, J. P., FBREKETE, D. M. Standard atlas of the gross anatomy of the developing inner ear of the chicken. J. Comp. Neurol. 368, 620-630 (1996)

BLACK, D. L. Mechanisms of alternative pre-messengar RNA splicing. Annual Rev. Biochem. 72, 291-336 (2003)

BONINI, N. M. et al. The *eyes absent* Gene: Genetic Control of Cell Survival and Differentiation in the Developing *Drosophila* Eye. Cell 72, 379-395 (1993)

BONINI, N. M. et al. The *Drosophila* eyes absent gene directs ectopic eye formation in a pathway conserved between flies and vertebrates. Dev. 124, 4819-4826 (1997)

BONINI, N. M. et al. Multiple roles of the eyes absent gene in *Drosophila*. Dev. Biol. 196, 42-57 (1998)

BORSANI, G. et al. EYA4, a novel vertebrate gene related to *Drosophila eyes absent*. Hum. Mol. Genet. 8, 11-23 (1998)

BORYCKI, A. G., EMERSON, C. P. Mutiple tissue interactions and signal transduction pathways control somite myogenesis. Curr. Opin. Dev. Biol. 48, 165-224 (2000)

BRETT, D. et al. Alternative splicing and genom complexity. Nat. Genet. 30, 29-30 (2001)

BRODBECK, S., ENGLERT, C. Genetic determination of nephrogenesis: the Pax/Eya/Six gene network. Pediatr. Nephrol. 19, 249-255 (2004)

CARL, M. et al. Six3 inactivation reveals its essential role for formation and patterning of the vertebrate eye. Dev. 129, 4057-4063 (2002)

CLAY, H., RAMAKRISHNAN, L. Multiplex fluorescent *in situ* hybridisation in zebrafish embryos using tyramide signal amplification. Zebrafish, 2(2) (2005)

CAUBIT, X. et al. Mouse Dac, a novel nuclear factor with homology to *Drosophila* dachshund shows a dynamic expression in the neural crest, the eye, the neocortex, and the limb bud. Dev. Dyn. 214, 66-80 (1999)

CHEN, R. et al. Dachshund and Eyes absent proteins form a complex and function synergistically to induce ectopic eye development in *Drosophila*. Cell 91, 893-903 (1997)

CHEYETTE, B. N. et al. The *Drosophila* sine oculis locus encodes a homeodomain-containing protein required for the development of the entire visual system. Neuron 12, 977-996 (1994)

CHISHOLM, A. Cell Determination. Academic Press University of California (2001)

COLE, L. K., ROSS, L. S. Apoptosis in the developing zebrafish embryo. Dev. Biol. 250, 123-142 (2001)

COLLAZO, A. et al. A dual embryonic origin for vertebrate mechanoreceptors. Science, 264, 426-430 (1994)

CORDES, S, FRIEDMAN, N. Genetic hearing loss. Grand Rounds Presentation, UTMB, Dept. of Otolaryngology (2000)

DAVID, R. et al. Xenopus Eya1 demarcates all neurogenetic placodes as well as migrating hypaxial muscle precursors. Mec. Dev. 103, 189-192 (2001)

DRAPER, B. W., MORCOS, P. A., KIMMEL, C. B. Inhibition of Zebrafish fgf8 Pre-mRNA Splicing With Morpholino Oligos: A,Quantitative Method for Gene Knock-down. Genesis 30, 154-156 (2001)

DOZIER, C The Caenorhabditis elegans Six/sine oculis class homeobox gene ceh-32 is required for head morphogenesis. Dev. Biol. 236, 289-303 (2001)

DUNCAN, M. K. et al. *Eyes absent*: a gene family found in several metazoan phyla. Mammalian Genome 8, 479-485 (1997)

EKKER, S. C. Morphant: a new systematic vertebrate functional genomic approach. Yeast 17, 302-306 (2000)

ERNEST, S. et al. Mariner is defective in *myosin VIIA*: a zebrafish model for human hereditary deafness. Hum. Mol. Genet. 9(14), 2189-2196 (2000)

ESTEVE, P., BOVOLENTA, P. cSix4, a member of the six gene family of transcription factors, is expressed during placode and somite development. Mech. Dev. 85, 161-165 (1999)

FEKETE, D. M. Cell fate specification in the inner ear. Curr. Opin. Neurobiol. 6, 533-541 (1996)

FESUS, L. Apoptosis fashions T and B cell repertoire. Immunol. Lett. 30, 277-282 (1991)

FORCE, A. et al. Preservation of duplicate genes by complementary degenerative mutations. Genetics 151, 1531-1545 (1999)

FRASER, F. C. et al. Genetic aspects of the BOR-syndrome – branchial fistulas, ear pits, hearing loss and renal anomalies. Am. J. Med. Genet. 2, 425-442 (1978)

FRASER, F. C. et al. Frequency of the branchio-oto-renal (BOR) syndrome in children with profound hearing loss. Am. J. Med. Genet. 7, 341-349 (1980)

FRITZSCH, B. et al. Developmental evolution of the inner ear sensory epithelia and thier innervation. J. Neurobiol. 53, 143-156 (2002)

FRITZSCH, B. et al. Cells, molecules and morphogenesis: the making of the vertebrate ear. Brain Res. 1091, 186-199 (2006)

FRITZSCH, B. et al. Molecular evolution of the vertebrate mechanosensory cell and ear. Int. J. Dev. Biol. 51, 663-678 (2007)

GALLAGHER, B. C., GRAINGER, R. M. Inductive prosseses leading to inner ear formation during *Xenopus* development. Dev. Biol. 175, 95-.107 1996)

GARLAND, A. "Morgan, Thomas Hunt". American National Biography Online. Oxford University Press. (2000)

GIMSING, S., DYRMOSE, J. Branchio-Oto-Renal dysplasi in three families. Ann Otpl. Rhinol Laryngol 95, 421-426 (1986)

GIOT, L. et al. A protein interaction mal of Drosophila melanogaster. Science 302, 1727-1736 (2003)

GHYSEN, A., DAMBLY-CHAUDIÈRE, C. Development of the zebrafish lateral line. Current Opinion of Neurobiol. 14, 67-73 (2004)

GLÜCKSMANN, A. Cells deaths in normal vertebrate ontogeny. Biol. Rev. 26, 59-86 (1951).

GOMPEL, N. et al. Pattern formation in the lateral line of zebrafish. Mech. Of Dev. 105, 69-77 (2001)

GORLIN, R. J. et al. Hereditary hearing loss and its syndromes. Oxford: Oxford University Press (1995)

GRAINGER, R. M. Embryonic lens induction: shedding light on vertebtare tissue determination. Tends. Genet. 8, 957-971 (1992)

GRANATO, M. et al. Genes controllino and mediating locomotion behavior of the zebrafish embryo and larva. Dev. 123, 399-413 (1996)

HADDON, C., LEWIS, J. Early Ear Development in the Embryo of the Zebrafish, *Danio rerio*. J Comp. Neuro. 365, 113-128 (1996)

HAFFTER, P. et al. The identification of genes with unique and essential functions in the development of the zebrafish, Danio rerio. Dev. 123, 1-36 (1996)

HAFFTER, P., NÜSSLEIN-VOLHARD C. Large scale genetics in a small vertebrate, the zebrafish.Int. J. Dev. Biol. 40(1), 221-227 (1996)

HALDER, G. et al. Eyeless initiates the expression of both sine oculis and eyes absent during Drosophila compound eye development. Dev. 125, 2181-2191 (1998)

HAMBURGER, V, HAMILTON, H. A series of normal stages in the development of the chick embryo. J. Morphol. 88, 49-92 (1951)

HAMBURGER, V, LEVI-MONTALCINI, R. Proliferation, differentiation and degeneration in the spinal ganglia of the chicken embryo under normal and experimental conditions. J. Exp. Zool. 111, 457-502 (1949)

HAMMOND, K. L. et al. Isolation of three zebrafish *dachshund* homologues and their expression in sensory organs, the central nervous system and pectoral fin buds. Mech. Dev. 112, 183-189 (2002)

HARRIS, A. J. et al. Neomycin-induced hair cell death and rapid regeneration in the lateral line of zebrafish (Danio rerio). J. Assoc. Res. Otolaryngol. 4(2), 219-234 (2003)

HEANUE, T. A. et al. Synergistic regulation of vertebrate muscle development by *Dach2*, *Eya2* and *Six1*, homologues of genes required for *Drosophila* eye development. Genes Dev. 13, 3231-3243 (1999)

HEASMAN, J., KOFRON M., WYLIE C. β-catenin signalling activity dissected in the early *Xenopus* embryo: a novel antisense approach. Dev. Biol. 222, 124-134 (2000)

HILDEBRAND, M. S. et al. A nvel splice site mutation in *EYA4* causes DFNA10 hearing loss. Am. J. Med. Genet. 143(14), 1599-1604 (2007)

HUNTER, T. Signalling – 2000 and Beyond. Cell 100, 113-127 (2000)

IKEDA, K. et al. Molecular interaction and synergistic activation of a promoter by Six, Eya and Dach proteins mediated through CREB binding protein. Mol Cell Biol 22, 6759-6766 (2002)

JACOBSON, A. G. The determination and positioning of the nose, lens, and ear. III effects of reversing the antero-posterior axis of epidermis, neural plate and neural fold. J. Exp. Zool. 154, 293-303 (1963c)

JACOBSON, M. D., WEIL M., RAFF, M. C. Programmed cell death in animal development. Cell 88, 374-354 (1997)

JAYANAGENDRA, P. et al. Eyes absent represents a class of protein tyrosine phosphatases. Nature 426, 295-298 (2003)

JEMC, J., REBAY, I. The eyes absent family of phosphotyrosine phosphatases: properties and roles in developmental regulation of transcription. Annu. Rev. Biochem. 76, 513-538 (2005)

JEMC, J., REBAY, I. Identification of transcriptional targets of the dual-function transcription factor/phosphatase eyes absent. Dev. Biol. 310(2), 416-429 (2007)

JOHNSON, K. R. et al. Inner ear and kidney anomalies caused by IAP insertion in an intron of the Eya1 gene in mouse model of BOR syndrome. Hum. Mol. Genet. 8, 645-653 (1999)

KALATZIS, V. et al. *Eya1* expression in the developing ear and kidney:towards the understanding of the pathgenesisof Branchio-Oto-Renal (BOR) syndrome. Dev, Dyn, 213, 486-499 (1998)

KAWAKAMI, K. et al. Structur, functaion, and expression of a murin homeobox protein AREC3, a homologue of Drosophila sine oculis gene product, and implication in development. Nucleic acid Res 24, 303310 (1996)

KAWAKAMI, K. et al. Six family genes – structure and functaion as transcription factors and their roles in development. Bioessays 22, 616-626 (2000)

KEATS, B. J., COREY, D P. The usher syndrome. Am. J. Med. Genet. 89(3), 158-166 (1999)

KIMMEL, C. B. et al. Stages of Embryonic Development of the Zebrafish. Dev. Dynamics 203, 253-310 (1995)

KOBAYASHI, M. et al. Expression of three zebrafish *Six4* genes in the cranial sensory placodes and the developing somites. Mech. Dev. 98, 151-155 (2000)

KOHLER, R. E. Lords of the Fly: Drosophila Genetics and Experimental Life. University of Chicago Press. (1994)

KÖNIG, R. Branchio-Oto-Renal syndrome: variable expressivities in a five-generation pedigree. Eur. J. Pediatr. 153, 446-450 (1994)

KRAUSS, S. et al. Zebrafish *pax[zf-a]*: a paire box-containing gene expressed in the neural tube. The EMBO J. 10 (12), 3609-3619 (1991)

KRAUSS, S. et al. Expression of the zebrafish paired box gene *pax[zf-b]* during early neurogenesis. Dev. 113, 1193-1206 (1991)

KRIEBEL M et al. Xeya3 regulates survival and proliferation of neural progenitor cells within the anterior neural plate of Xenopus embryos. Dev. Dyn. 236, 1526-1534 (2007)

LACLEF, C.et al. Thymus, kidney and craniofacial abnormalities in Six1 deficient mice. Mech. Dev. 120, 669-679 (2003a)

LACLEF, C.et al. Altered myogenesis in Six1-deficient mice. Dev. 130, 2239-2252 (2003b)

LEDENT, V. Postembryonic development of the posterior lateral line in zebrafish. Dev. 129, 597-604 (2001)

LEUNG, A. K. C. et al. Association of preauricular sinuses and renal anomalies. Urology 40, 259-262 (1992)

LI, X. et al. Eya protein phosphatase activity regulates Six1-Dach-Eya transcriptional effects in mammalian organogenesis. Nat. 426, 247-254 (2003)

LYNCH, M., CONERY, J. C. The Evolutionary Fate and Consequences of Duplicate Genes. Science 290(10), 1151-1155 (2000)

MAZET, F., SHIMMELD, S. M. Molecular Evidence From Ascidians for the Evolutionary Origin of Vertebrate Cranial Sensory Placodes. J. of Exp. Zool. (Mol. Dev. Evol.) 304B, 340-346 (2005)

MELNICK, M. et al. A new addition to the branchial arch syndromes. Clin. Genet. 9, 25-34 (1976)

METCALFE, W. K. et al. Primary neurons that express the L2/HNK-1 carbohydrate during early development in the zebrafish. Dev. 110(2), 491-504 (1990)

MISHIMA, N., TOMARVE, S. Chicken *Eyes absent 2* gene: isolation and expression pattern during development. Int. J. Dev. Biol. 42, 1109-1115 (1998)

MOODY, S. A. Principles of Developmental Genetics. Elsevier, Am. Press (2007)

MORTON, N. E. Genetic epidemiology of hearing impairment. Ann. N. Y. Acad. Sci. 630, 16-31 (1991)

MÜLLER, W. A., HASSEL, M. Entwicklungsbiologie und Reproduktionsbiologie von Mensch und Tier. Springer 2006

MULLINS, M. C. et al. Large scale mutagenesis in the zebrafish: in search of genes controlling development in a vertebrate. Curr. Biol. 4(3), 189-202 (1994)

MULLINS, M. C. Zebrafish Course (2005)

NASEVIVIUS, A., EKKER, S. C. Effective targeted gene 'knock-down' in zebrafish. Nat. Genet. 26, 216-220 (2000)

NIEUWLOOP, P. D. et al Development of the cephalic placodes. Cambridge University Press, Cambridge, 203-214 (1985)

NIIMI, T. et al Direct regulatory interaction of the eyeless protein with an eye-specific enhancer in the sine oculis during eye induction in *Drisophila*. Dev. 126, 2253-2260 (1999)

NORAMLY, S., GRAINGER, R. M. Determination of the Embryonic Inner Ear. Inc. J. Neurobiol. 53, 100-128 (2002)

NORTHCUTT, R. G. et al. Development of lateral line organs in the axolot. J. Comp. Neurol. 340, 480-514 (1994)

OHTO, H. et al. Cooperation of *six* and *eya* in activation of their target genes through nuclear translocation of Eya. Mol. Cell. Biol. 19, 6815-6824 (1999)

OHTO, H. et al. Tissue and developmental distribution of Six family gene products. Int. J. Dev. Biol. 42, 141-148 (1998).

OLIVER, G. et al. Homeobox genes and connective tissue patterning. Dev. 121, 693-705 (1995)

OPPENHEIM, R. W. Cell death during development of the nervous system. Annu. Rev. Neurosci. 14, 453-501 (1991)

ORDAHL, C. P., LE DOUARIN, N. M. Two myogenetic lineages within the developing somite. Dev. 114, 339-353 (1992)

OZAKI, H. et al. Six1 controls patterning of the mouse otic vesicle. Dev. 131, 551-562 (2004)

PARTRIDGE, M. et al. A simple method for delivering morpholino antisense oligos into the cytoplasm of cells. Antisense Nuclei Acid Drug Dev 6, 169-175 (1996)

PETIT, C. Genes responsible for human hereditary deafness: Symphony of a thousand. Nat. Genet. 14, 385-391 (1996)

PFEFFER, P. L. et al. Characterization of three novel members of the zebrafish *Pax2/5/8* family: dependency of *Pax5* and *Pax8* expression on the *Pax2.1* (noi) function. Dev. 125, 3063-3074 (1998)

PFISTER, M. et al. A 4-bp insertion in the eya homologous region (eyaHR) of EYA4 causes hearing impairment in Hungarian family linked to DFNA10. Mol. Med. 8(10), 607-611 (2002)

PIGNONI, F. et al. The eye-specification proteins So and Eya form a complex and regulate multiple steps in *Drosophila* eye development. Cell 91, 881-891 (1997)

POPPER, A. N., FAY, R. R. Sound detection and processing by fish: critical review and major research questions. Brain, Behaviour and Ecol. 41, 14-38 (1993)

POURQUIÉ, O. Segmentation of the paraxial mesoderm and vertebrate somitogenesis. Curr. Top. Dev. Biol.47, 81-105 (2000)

QUIRING, R. et al. Organization of the lateral line system in embryonic zebrafish. J. Comp. Neurol. 421(2), 189-198 (2000)

RAIBLE, D. W., KRUSE, G. J. Organization of the lateral line system in embryonic zebrafish. J. Comp. Neurol. 421(2), 189-198 (2000)

RAYAPUREDDI, J. P. et al. Eyes absent represents a class of protein tyrosine phosphatases. Nat. Nov 20; 426 (6964), 295-298 (2003)

REBAY, I. et al. New vision from Eyes absent: transcription factor as enzymes. Trans. Genet. 21(3), 163-171 (2005)

RELAIX, F., BUCKINGHAM, M. From insect eye to vertebrate muscle: redeployment of a regulatory network. Genet. Dev. 13, 3171-3178 (1999)

RILEY, B. B. et al. The *deltaA* gene of zebrafish mediates lateral inhibition of hair cells in the inner ear and is regulated by *pax2.1*. Dev. 126, 5669-5678 (1999)

SAHLY, I. et al. The zebrafish *eya1* gene and its expression pattern during embryogenesis. Dev. Genes. Evol. 209, 399-410 (1999)

SAITOU, N., NEI M. The neighbour-joining method: a new method for reconstructing polygenetic trees. Mol. Biol. Evol. 4, 406-425 (1987)

SCHNEIDER-MAUNOURY, S. et al. Disruption of Krox-20 results in alteration of rhombomere 3 and 5 in developing hindbrain. Cell 75, 1199-1214 (1993)

SEITANIDOU, T. et al. Krox-20 is a key regulator of rhombomere-specific gene expression in the developing hindbrainancer. Mech Dev. 65 (1-2), 31-42 (1997)

SÖLLNER C, et al. Mutations in cadherine 23 affect tip links in zebrafsih sensory hair cells. Nature 29 (4), 955-959 (2004)

STERN, H. M., ZON L. I. Cancer genetics and drug discovery in the zebrafish. Nat Rev Cancer 3, 533-539 (2003)

STREIT, A. Origin of the vertebrate inner ear: evolution and induction of the otic placode. J. Anat. 199, 99-103 (2001)

STREIT, A. Extensive cell movements accompany formation of the otic placode. Dev. Biol. 249, 237-254 (2002)

STREIT, A. Early development of the cranial sensory nervous system: from a common field to individual placodes. Dev. Biol. 275, 1-15 (2004)

STREIT, A., STERN C. D. Whole-Mount in Situ Hybridisation and Immunohistochemistry in Avian Embryos. Department of Genetics and Development, Columbia University, New York, USA 2000

SUMMERTON, J. Morpholino antisense oligomers: the case for an Rnase-H-independent structural type. Biochim. Biophys. Acta 1489, 141-158 (1999)

THISSE, C. et al. Structure of the zebrafish *snail1* gene and it's expression in the wild-type, spadetail and no tail mutant embryos. Dev. 119, 1203-1215 (1993)

TOOTLE, T. L. et al. The transcription factor Eyes absent is a protein tyrosine phosphatase. Nat. 426, 299-302 (2003)

TORRES, M., GIRALDEZ, F. The development of the vertebrate inner ear. Mech. of Dev. 71, 5-21 (1998)

TREVARROW, B. et al. Organization of hindbrain segments in the zebrafish embryo. Neuron 4(5), 669-679 (1990)

TWYMAN, R. Model organism: Fish. The Human Genom (2002)

VAN CAMP, G., SMITH, R. J. H. *Hereditary hearing loss homepage*: webhost.ua.ac.be/hhh/ Accessed Fedbruary 6, 2007

VAN EEDEN, F. J. et al. Developmental mutant screens in the zebrafish. Meth. Cell Biol. 60, 21-41 (1999)

VAUX, C. L., KORSMEYER, S. J. Cell death in development. Cell 96, 245-254 (1999)

VINCENT, C. et al. BOR an BO syndromes are allelic defects in EYA1. Eur. J. Hum. Genet. (5)4, 242-246 (1997)

WAWERSIK, S., MAAS, R. L. Vertebrate eye development as modeled in Drosophila. Hum. Mol. Genet. 9, 917-925 (2000)

WEBB, J. F., SHIREY, J. Postembryonic Development of the Cranial Lateral Line Canals and Neuromasts in Zebrafish. Dev. Dynamics 228, 370-385 (2003)

WEBB, J. R., NODEN, D. M. Ectodermal placodes: contribution to the development of the vertebrate head. Am. Zool. 33,434-447 (1993)

WEBB, S. E., MILLER, A. L. CA^{2+} signalling and early embryonic patterning during zebrafish development. Australian physiologic society (2007)

WEVER, E. G. The evolution of vertebrate hearing. Handbook of Sensory Physiology, Springer, 432-454, (1974)

WHITFIELD, T. et al. Mutations affecting development of the zebrafish inner ear and lateral line. Dev. 123, 241-254 (1996)

WHITFIELD, T. et al. Development of the Zebrafish Inner Ear. Dev. Dynamics 223, 427-458 (2002)

WHITLOCK, K. E., WESTERFIELD, M. A transient population of neurons pioneers the olfactory pathway in the zebrafish. J. of Neurosci. 18, 8919-8927 (1998)

WILKINSON, D. G. In situ hybridisation, a practical approach. Oxford University press, Oxford, England, 1998

WILKINSON, D. G. et al Segment-specific expression of the zinc-finger gene in the developing nervouse system of the mouse. Nat. 337, 461-464 (1989)

WINKELBAUER, R. Development of the lateral line system in Xenopus. Prog. Neurobiol 32, 181-206 (1989)

XU, PX. et al. Mouse *Eya* genes are expressed during limb tendon development and encode a transcriptional activation function. Dev. Biol. 94, 11974-11979 (1997)

XU, PX. et al. Eya1-deficient mice lack ears and kidneys and show abnormal apoptosis of organ primordial. Nat. Genetics 23, 113-117 (1999)

XU, PX. et al. *Six1* is required for the early organgenesis of mammalian kidney. Dev. 130, 113-117 (2003)

ZAKERI, Z. F. et al. Delayed internucleosomal DNA fragmentation in programmed cell death. Faseb. J. 7(5), 479-478 (1993)

ZHENG, W. et al. The role of Six1 in mammalian auditory system development. Dev. 130, 3989-4000 (2003)

ZIMMERMANN, J. E. et al. Cloning and Characterisation of Two Vertebrate homologous of the *Drosophila eyes absent* Gene. Genome Research 7, 128-141 (1997)

ZOU, D. Eya1 and Six are essential for early steps of sensory neurogenesis in mammalian cranial placodes. Dev. 131, 5561-5572 (2004)

ZUKER, C. S. On the evolution of eyes: would you like it simple or compound? Science 265 (5173) 742-3 (1994)

9 Appendix

9.1 Abbreviations

SI units and symbols of standard multiples (m, µ, l, etc.) are not listed. Additional abbreviations are introduced and explained in the text.

ant.	anterior
AP	alkaline phosohatase
ATP	Adenosine-tri-phosphate
bp	base pairs
BOR	Branchio-Oto-Ranal syndrome
BSA	bovine serum albumin
dach	dachshund
DIC	differential interference contrast
DIG	digoxygenin
DISH	double *in situ* hybridisation
DNA	desoxyribonucleic acid
dpf	days post fertilisation
ED2	eya domain2
EM	embryomedium
eya	eyes absent
eyaHR	eya-homologous region
FCS	foetal calf serum
FISH	fluorescent *in situ* hybridisation
FLU	flourescein
GFP	green flourescent protein
HAD	haloacid dehalogenase superfamily
hpf	hours post fertilisation
$Hyb^{+/-}$	hybridisation buffer
ISH	*in situ* hybridisation
mMO	mispaired antisense morpholino oligonucleotid
MO	antisense morpholino oligonucleotides
o/n	over night
ORF	open reading frame
pax	paired box
PBS(T)	phosphate buffer saline (+ Tween 20)
PFA	paraformaldehyde
post.	posterior

RNA	ribonucleic acid
rpm	rotation per minute
RT	room temperature
six	sine oculis
som	somites
SSC(T)	sodiumchloride/sodiumcitrate buffer (+ Tween20)
UTR	untranslated region
WT	wildtyp

9.2 Equipment

Cameras	EHD kamPro 04* SVHS CCD-Camera
	Hamamatsu Digital Camera
	Leica DM RBE
	Q Imaging Retiga 1300i SCI Tech
	Canon Typ Powershot G5
Centrifuges	Eppendorf Centrifuge 5415D
	Hermeline Z233 MK-2
	Sigma lab centrifuge 3K10
	Thermo Electron Corporation RC5B
Injection	Bachhofer micromanipulator
	Eppendorf Sterile Femtotips II
	Eppendorf Transjector 5246
Microscopes	Flou TM
	Leica MZ FLIII
	Leica TCS SP
	Zeiss Axioskop
	Zeiss Axioskop 2 plus
	Stemi SV11 Apo
Microtom	Leica JUNG RM 2055
Photometer	Thermo Electron Corporation BioMate3
Speedvac	Bachhofer Vacuum concentrator

9.3 Material

9.3.1 Fish strains

Wildtyp-strains: Darmstadt inbred lines derived from pet store fish; longfin; leopard (Tübingen)

9.3.2 Bacterial strains

E. coli XL1-Blue; DH5α

9.3.3 Chemicals, Buffer, Media, Solutions

All chemicals were obtained from Boehringer (Mannheim), Fluka (Buchs), Merck (Darmstadt), Peqlab (Erlangen), Roche (Mannheim), Roth (Karlsruhe), Sigma (Deisenhofen).

AP	100mM Tris-HCL pH 9,5; 50mM MgCl2; 100mM NaCl; 0,2% Tween-20; 0,2% Triton-X 100; Levamisol
10x PBS	137mM NaCl; 27mM KCL; 83mM Na_2HPO4; 15mM KH_2PO_4 to pH 7,3
20x SSC	Stock solution: 3M NaCL; 0,3M Na-Citrat
Ampicillin	Stock solution: 100mg/ml dH_2O Dilution 1:1000
DASPEI	(2-(4-(Dimethylaminostyryl)-1-methyl-pyridinium iodid; Fluka BioChemika) in EM to saturated solution, final dilution 1:3 in EM
Hyb-	50-65 % formamid; 5x SSC; 0,1% Tween 20
Hyb+	Hyb- + citric acid to pH 6,0; heparin 50µg/ml; totula RNA 0,5mg/ml
LB-media	0,5 % yeast extract; 1% trypton; 200mM NaCL to pH 7,5
Methylcellulose	4% in EM
NBT/BCIP	3,5µl BCIP, 4,5ml NBT in 1ml AP
Nucleotid (NTP)-Mix	10mM ATP; 10mM CTP; 10mM GTP; 7,5mM UTP; 2,50mM dig-/flu-UTP
PBT	0,1% Tween-20 in PBS
PFA	4% Paraformaldehyde in 1x PBS
50x PTU	(Phenylthiocarbamide, 1-phenyl-2-thiourea) 0,15% in dH_2O
Tricaine	Stock solution: 400mg Ethyl 3-aminobenzoate methanesulfonic acid (sigma); 97,9ml dH2O ; 2,1ml 1M Tris (pH 9) to pH 7 Dilution 1:20 in EM
LB-agar	15g agar to 1000ml LB-medium, ampicillin
10x EM	5M NaCl; 1M KCL; 1M Na2HPO4; 1M KH2PO4; 1M CaCl2; 1M MgSO4; 1% HEPES; pH 7,7
1x EM	0,1% Methylenblue in 1x EM
Danieau solution	58mM NaCl, 0.7mM KCL, 0.4mM $MgSO_4$, 0.6mM $Ca(NO_3)_2$, 5.0mM HEPES pH 7.6

BCIP	50mg/ml in 100% DMF (Dimethylformamid)
Fish water	4% see salt in dH20 + NaHCO3 to adjust pH to 6.5 – 7.5
NBT	75mg/ml in 70% DMF (Dimethylformamide)
Phenolred	2% in dH2O
Proteinase K	Stock solution: 20mg/ml
	Dilution 1:4000 in PBT

9.3.4 "KITS" & dyes

All kits and dyes were obtained from Ambion (USA), Chemicon (UK), Invitrogen (Karlruhe), Polyscience (Switzerland), Qiagen (Hilden), Roche (Mannheim), Sigma (Deisenhofen), Vector Laboratories (USA).

Ambion mMESSAGE mMACHINE® SP6
ApopTag® Peroxidase In Situ Detection Kit
Flourescent *in situ* hybridisation using TSA
PeroxidaseVECTASTAIN Elite ABC-KIT (mouse IgG)
Poly/Bed 812/Araldite 502 mini kit
QIAquick® Gel Extraction Kit
RNeasy® Mini Kit

BM Purple AP Substrat, precipitating
Fast Red RTR/Naphthol AS-MX Tablets
NBT/BCIP Stock Solution
Diaminobenzidin, HRP-Staining Solution (DAB)

9.3.5 Antibodies

If not otherwise stated, all antibodies were obtained from Invitrogen (Karlruhe and Roche (Mannheim).

Anti-Digoxigenin-AP, Fab fragments (Sheep IgG) (Roche)
Anti-Fluorescein-AP, Fab fragments (Sheep IgG) (Roche)
Digoxigenin-11-UTP (Roche)
Fluorescein-12-UTP (Roche)
Zn-12 Isotope: Mab Zn-12 (IgGI, k) (provided by M. MARUSICH, University of Oregon, USA)

9.3.6 Enzymes

All enzymes (EcoRI; BamHI; HindIII; NotI; PstI; PvuII) were obtained from New England Biolabs (Schwalbach), RNA-Polymerases (T3; T4; T7) and DNase from Promega (Mannheim).

9.3.7 Plasmides

Insert/ size	Vector/ size	Resistance	antisense probe	Referenz
eya2 / 2,5kb	pCS2+ / 4,1kb	Ampicillin	NotI/T7	RAIBLE et al. unpublished
eya3 / 2,4kb	PCS2+ / 4,1kb	Ampicillin	NotI/T7	RAIBLE et al. unpublished
eya4 / 2,5kb	pBSK+ /- 2,9kb	Ampicillin	EcoRI/T7	RAIBLE et al. unpublished
eya4 / 2,5kb	pCS2+ / 4,1kb	Ampicillin	NotI/T7	RAIBLE et al. unpublished
krox20 / 1,9kb	pBKS+/- / 2,9kb	Ampicillin	TstI/T3	JOWETT et al., 1993
pax2.1[6] / 2,6kb	unknown	Ampicillin	HindIII/T7	KRAUSS et al., 1991
GFP / 2,9kb	pCS2+ / 4,1kb	Ampicillin	NotI/T7	none

* pCS2+ -construct generated in David Raible's Laboratory by Josette Ungos (University of Washington, Seattle, USA).

9.3.8 pCS2+ vector

Due to the fact that capped mRNAs generated from CS2+-vectors, which include the SV40 polyA site, are more stable than conventional capped mRNAs when injected into embryos, pCS2+ is the vector of choice for the generation of expression constructs. CS2+ is a multipurpose expression vector. It contains a strong enhancer/promoter (simian CMV IE94) followed by a polylinker and the SV40 late polyadenylation site. A SP6 promoter is present at the 5'-end of the polylinker I region, allowing in vitro synthesis of sequences cloned into this region. The CS2+ vector also includes a T7 promoter in revers direction between the polylinker and theSV40 polyA site for probe synthesis, as well as a second polylinker after the SV40 polyA site to provide several possible sites to linearise the vector for SP6 transcription. The vector backbone is derived from pBlueskript II KS+.

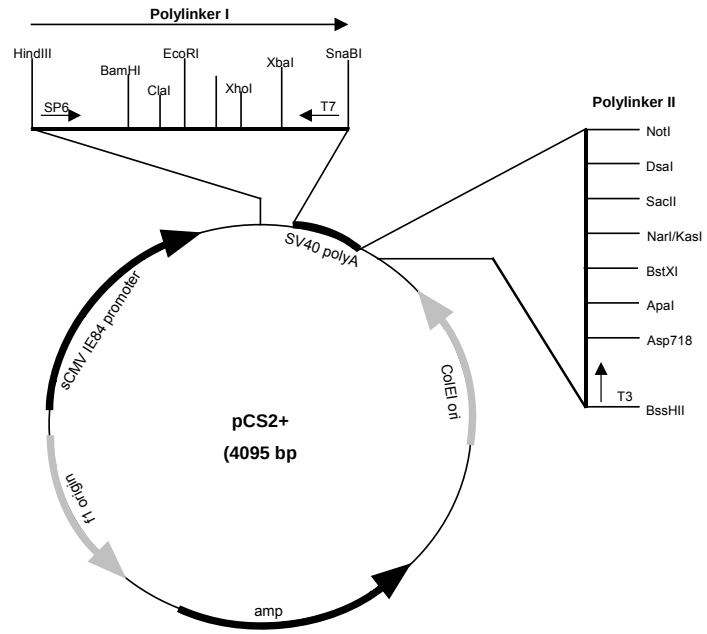

Figure 37 pCS2+ vector (DAVID RAIBLE Laboratory, University of Washington, USA).

[6] Synonym [zf-a]

9.3.9 Primer

All primer were obtained from biomers.net and Roth (Karlsruhe).

Primer (P)	Sequence	bp
P^{1st} *eya2* antisense	5' AGAGAAACAGCCTTCCCGGAGTCCTTGCCG 3'	30
P^{2nd} *eya2* antisense	5' TAATATTGTAGGACGTCATGCTGTATCCCC 3'	30
P^{1st} *eya2* sense	5' CGCAGTGCGGATGGGAAGCTGAGAGGCCGG 3'	30
P^{2nd} *eya2* sense	5' ATCTGTGGCTGACGCAGGCTCTCAAAGCCC 3'	30
P^{1st} *eya3* antisense	5' GCAAAAAGGGTAGCTCTTGTAGATGTTGCG 3'	30
P^{2nd} *eya3* antisense	5' GTTCTCGATGGGAAAAACGTCACCCAGGCC 3'	30
P^{1st} *eya3* sense	5' ACCTCACAGATCTACCAAGGAAGCATTATCCGG 3'	30
P^{2nd} *eya3* sense	5' GACGCTCCCAACCGGTGTGGCTCTGCCCGC 3'	30
P^{1st} *eya4* antisense	5' GACATTGTGAGCTGTGGACATATTATCCGG 3'	30
P^{2nd} *eya4* antisense	5' CTTGATGAAGGGCAAGCAGGTCAGAGTGGC 3'	30
P^{1st} *eya4* sense	5' CCGTGAGTTCAGCAGGAGACTCTGGGCTGG 3'	30
P^{2nd} *eya4* sense	5'>ATCAGCTGCAGGACCCCATCATGACAGGGC 3'	30

CURRICULUM VITAE

Full name: Isabel Formella

Date of Birth: 25th September 1977

Place of Birth: Lübeck, Germany

Education:

Schule Paul-Gerhardt, Lübeck (1984-1988)
(Grundschule)

Gymnasium am Mühlenberg, Bad Schwartau (1988-1997)

Study of Biology at Philipps-Universität Marburg (1997-2003)
Majors: Zoology/Evolution, Ecology, Geography

Diploma thesis: "Comparative morphology analysis of molluscs based on radulae"

PhD student at Technische Universität Darmstadt (2005-2008)
Departement of Development and Neurogenetics

PhD Thesis: "Sequence characterisation and functional analysis of three novel eya genes during early development of the otic organ and lateral line in zebrafish (Danio rerio)

Grants

2005 – 2008 – PhD Grand of the Deutsche Forschungs-Gemeinschaft (DFG)

2006 – Visit Reasearch Grand (DFG)

Additional training

Undergraduate Research Assistant

Zoologische Gesellschaft Frankfurt / Ascociatión ANAI Talamanca

Project: Sea Turtle and Marine Conservation / ZFG-Projekt 1219/97; (Gandoca Beach, Costa Rica, February/March 1999)

Undergraduate Research Assistant

Zoologischer Garten Köln / ALSCO-Naturschutzprojekt Köln

Project: "Mammals surveys in natural habitats and those affected by humans". Designing, planning, and organizing of the research concept; (Köln, Germany; Nyasoso Station, Cameroon, February to April 2001)

Undergraduate Teaching Assistant

Philipps Universität Marburg, Department of Zoology and Evolution; (Marburg, Germany, April to July 2001)

Undergraduate Research Assistant

Deutsches Primatenzentrum Göttingen, Department Ecology and Behaviour

Project: Analysis of social behaviour and vocalisation by lemurs; (Kirindy Forest station, Madagascar, September/October 2001)

Undergraduate Research Assistant

Zoologischer Garten Frankfurt, Department of Science

Project: Research experiences in animal care and population management within the EEP (Europäisches Erhaltungszuchtprogramm); (Frankfurt, Germany, February to April 2002)

Visiting Research

Victor Chang Cardiac Research Institute, Laboratory of Prof. Peter Currie; (Sydney, Australia, October 2006 to December 2006)

Employment Experience

Junior postdoctoral fellowship at the Peter Currie Laboratory, Victor Chang Cardiac Research Institute (Sydney, Australia,)

Meetings and Presentations

Summer Academy Deutsche Forschungsgemeinschaft (DFG) – Hirschegg, Austria

Oral presentation: Investigating the role of the e*ya/six/pax/dach* gene network during development of the zebrafish inner ear

International Zebrafish Meeting 2005 – Dresden, Deutschland

International Zebrafish Meeting 2006 – Madison, USA

Poster presentation: Characterization of *eya*/*pax*/*six* gene network during otic development

Visiting research in the Laboratory of Peter Currie, Victor Chang Institut – Sydney, Australien

Oral presentation: Comparison of Three *Eyes Absent* Genes and their Roles during Inner Ear Development in Zebrafish *Danio rerio*

Meeting of the Gesellschaft für Entwicklungsbiologie (GfE) 2007 – Marburg, Germany

Australia and New Zealand Society for Cell and Developmental Biology NSW meeting 2007 – Sydney, Australia

Oral presentation: *Eya2* and *eya4* proteins mediate programmed cell death in zebrafish

Publications

Formella, I., Ungos, J., Raible, D. and Andermann,P.; "Isolation and expression pattern of *eya2* and *eya4*, two novel members of the zebrafisch *eya* gene family". (In preparation)

Formella, I.*, Wunder, K.*, Hoppe, U. and Andermann, P.; "Expression analysis of the pax-eya-six-dach network during zebrafish inner ear development". (In preparation)

Eidesstattliche Erklärung

Hiermit erkläre ich an Eides statt, dass ich die vorliegende Dissertation selbstständig und nur unter Verwendung der angegebenen Hilfsmittel angefertigt habe.

Isabel Formella

Sydney, den 20.03.2008